Role of Rac1 in Neuronal Responses to Injury: Hypoxia and Deoxysphingolipid-Induced Neurotoxicity

---

Dissertation

zur

Erlangung der naturwissenschaftlichen Doktorwürde
(Dr. sc. nat.)

vorgelegt der

Mathematisch-naturwissenschaftlichen Fakultät

der

Universität Zürich

von

Tanja Marina Güntert

aus

Deutschland

Promotionskomittee:

Prof. Dr. Max Gassmann (Vorsitz)
Dr. Omolara O. Ogunshola (Leitung der Dissertation)
Prof. Dr. Jean-Marc Fritschy
Prof. Dr. Agnes Görlach

Zürich, 2014

Summary

This thesis work elaborated two main projects both investigating the cellular response of primary cortical neurons to a pathological stimulus. Both studies highlight the contribution of Rho GTPases, particularly of Rac1 and downstream signaling, to the cellular consequences.

The first stimulus of interest was hypoxia, a condition where oxygen demand exceeds oxygen availability. Neurons are very sensitive to hypoxia and disturbed brain oxygenation has been associated with a number of neuropathies and neurodegenerative diseases. When oxygen levels drop, cells induce the transcription factor hypoxia-inducible factor-1 (HIF-1) that stimulates expression of genes that enable adaptation to the stress stimuli.
The aim of the first study was to determine the contribution of the Rho GTPase Rac1 in the neuronal response to hypoxia. In particular we intended to investigate whether Rac1 regulates hypoxic induction of HIF-1 signaling and neuronal survival during hypoxia.

We show that Rac1 is rapidly activated by oxygen deprivation and is crucial for stabilization of HIF-1α, the oxygen-regulated subunit of HIF-1, since pharmacological inhibition of Rac1 completely abrogated hypoxic HIF-1α accumulation. This mechanism was independent of the age of neurons and of the duration of the hypoxic stimulus. During acute hypoxia neuronal survival was not impaired even when HIF-1α was blocked via Rac1 inhibition. Chronic

hypoxia induced significant cell death in mature neurons that was further amplified when Rac1 was absent. We identified the signaling kinases GSK3 and JNK as mediators of Rac1-driven HIF-1α stabilization and suggest a neuron-specific mechanism by which GSK3 contributes to HIF-1α induction. We conclude that Rac1 is critical for neuronal HIF-1α stabilization and that its impact on cell survival is dependent on the duration of the hypoxic insult.

The second investigated stress stimulus was the cellular accumulation of the atypical sphingolipid 1-deoxysphinganine (1-deoxySA). Sphingolipids (SL) are part of cellular membranes but are also involved in diverse signaling pathways. Disturbed SL synthesis can result in the accumulation of atypical deoxysphingolipids, including 1-deoxySA, that have been shown to induce toxicity and cytoskeletal alterations. Recently they were shown to be associated with neuropathies, however the mechanism by which those lipids induce neurodegeneration is unclear. This study aimed to explore mechanisms of 1-deoxySA-induced neuronal death and to assess whether deregulation of Rho GTPases is involved in cytoskeleton alterations triggered by 1-deoxySA-treatment.

Upon 1-deoxySA-treatment cytoskeletal breakdown indeed was observed together with reduced activity of mainly Rac1 and deregulation of the cytoskeleton-associated proteins Ezrin and IRSp53. We demonstrate that 1-deoxySA induced neuronal death in a time and concentration dependent manner. It was internalized and metabolized to deoxydihydroceramide species however inhibition of ceramide synthase protected neurons from 1-deoxySA-induced

death. In addition we found evidence for activation of NMDA receptor signaling and indeed blocking this receptor reversed parts of the 1-deoxySA-triggered effects on survival and cytoskeletal proteins. In summary, we suggest that inhibition glutamate receptors could be a therapeutic approach to prevent deoxysphingolipid-induced neurodegeneration.

Zusammenfassung

Die vorliegende Dissertation beschäftigt sich hauptsächlich mit zwei Studien bei denen jeweils die zelluläre Reaktion von primären kortikalen Neuronen auf einen pathologischen Stimulus im Vordergrund steht. Bei beiden Studien liegt der Schwerpunkt auf den Rho GTPasen und ihren nachgeschalteten Signaltransduktionsproteinen, um deren Einfluss auf die zellulären Folgen des Stressimpulses zu klären.

Der erste untersuchte Stress-Stimulus ist der Sauerstoffmangel (Hypoxie). Neuronen reagieren sehr sensibel auf Sauerstoffunterversorgung und eine gestörte Durchblutung des Gehirns steht in engem Zusammenhang mit neurodegenerativen Erkrankungen und Neuropathien. Sobald die Sauerstoffkonzentration sinkt akkumulieren Zellen den sogenannten Hypoxie-induzierbaren Faktor-1 (HIF-1), ein Protein, das die Expression von Genen einleitet, die die Anpassung an die Stresssituation ermöglichen.
Das Ziel der ersten Studie war es die Rolle der Rho GTPase Rac1 für die neuronale Reaktion auf Sauerstoffmangel zu bestimmen. Im Besonderen untersuchten wir ob Rac1 den HIF-1 Signalweg einleitet und das Überleben von Neuronen während einer Hypoxie beeinflusst.

Wir konnten zeigen, dass Rac1 bei Sauerstoffmangel zügig hochreguliert und aktiviert wird. Zudem ist Rac1 ausschlaggebend für die Stabilisierung der Sauerstoff-abhängigen α-Untereinheit von HIF-1, denn pharmakologische

Hemmung von Rac1 verhinderte die Ansammlung von HIF-1α. Dieser Mechanismus war unabhängig vom Alter der Neuronen und auch von der Dauer der Hypoxie. Interessanterweise wurde der Zustand der Neuronen während der akuten Hypoxie-Phase nicht beeinträchtigt, unabhängig von Rac1 und HIF-1α. Chronischer Sauerstoffmangel hingegen verursachte signifikanten Zelltod in reifen Neuronen, der in der Abwesenheit von Rac1 weiter verstärkt wurde. Desweiteren konnten wir die Proteine GSK3 und JNK als Signalüberträger der Rac1-induzierten Stabilisierung von HIF-1α identifizierten und wir schlagen einen Neuronen-spezifischen Mechanismus vor, bei dem GSK3 zur Ansammlung von HIF-1α beiträgt. Wir kommen zu dem Schluss, dass Rac1 für die neuronale Stabilisierung von HIF-1α entscheidend ist, sein Einfluss auf das Überleben der Neuronen ist allerdings von der Dauer der Hypoxie abhängig.

Der zweite untersuchte Stress-Stimulus ist die zelluläre Akkumulierung des atypsichen Shingholipids 1-Deoxysphinganin (1-deoxySA). Sphingolipide (SL) bilden Teile der Plasmamembran und sind zudem involviert in zahlreichen Signalprozessen. Störungen der SL-Synthese können in der Ansammlung von untypischen Deoxysphingolipiden resultieren. Eines dieser Lipide ist 1-deoxySA, das Zytoskelett-Veränderungen hervorruft und toxisch für verschiedenen Zelltypen ist. Kürzlich wurde gezeigt, dass Deoxysphingolipide eng mit bestimmten Neuropathien verknüpft sind, die zugrundeliegenden Mechanismen sind jedoch weiterhin unklar.

Unsere Studie hatte zum Ziel den molekularen Mechanismus hinter der 1-deoxySA-induzierten Neurotoxizität aufzuklären und festzustellen ob eine

Deregulierung von Rho GTPases mit den Zytoskelett-Veränderungen, die durch 1-deoxySA ausgelöst werden, in Verbindung steht.

Nach der Behandlung der isolierten Neuronen mit 1-deoxySA wurde tatsächlich ein Verfall des Zytoskeletts zusammen mit verminderter Rac1-Aktivität und Veränderungen der Zytoskelett-assoziierten Proteine Ezrin und IRSp53 beobachtet. 1-deoxySA verursachte, abhängig von Zeit und Konzentration, neuronales Zellsterben und wir konnten zeigen, dass 1-deoxySA von den Neuronen aufgenommen und dann zu Deoxydihydroceramiden umgewandelt wird. Interessanterweise konnte der Zelltod durch Hemmung der Ceramid-Synthese verhindert werden. Wie fanden zusätzlich Hinweise darauf, dass 1-deoxySA-Behandlung zu einer Aktivierung der NMDA-Rezeptoren führt. In der Tat konnte eine Blockade der Rezeptoren den 1-deoxySA-verursachten Zelltod und auch die Deregulierung der Zytoskelett-assoziierten Proteine teilweise unterbinden. Wir schlussfolgern, dass das Blockieren von Glutamat-Rezeptoren therapeutische Ansätze bilden könnten, um Deoxysphingolipid-verursachte Neurodegeneration zu verhindern.

List of Abbreviations

1-deoxySA: 1-deoxysphinganine

AD: Alzheimer`s disease

AKT: Synonym for protein kinase B

AMPA: α-amino-3-hydroxy-5-methyl-4-isoxazolepropionic acid

ARNT: aryl hydrocarbon receptor nuclear translocator

Baiap2: Brain-specific angiogenesis inhibitor 1-associated protein 2

BSA: Bovine serum albumin

C18SA: Sphinganine

C18SO: Spingosine

CerS: Ceramide synthase

CMTD: Charcot-Marie-tooth disease

CNS: Central nervous system

DES: Δ4dihydroceramide desaturase

CDK5: Cyclin-dependent kinase 5

DAPI: 4',6-diamidino-2-phenylindole

deoxyLCB: deoxy-long chain base

DIV: Days in vitro

DMSO: Dimethyl sulfoxide

DRG: Dorsal root ganglion

DSN: Diabetic sensory neuropathy

E: Embryonic day

ER: Endoplasmic reticulum

FB1: Fumonisine B1

GAP: GTPase-activating protein

GAPDH: Glyceraldehyde 3-phosphate dehydrogenase

GDI: guanine-nucleotide dissociation inhibitor

GDP: Guanosine diphosphate

GEF: guanine nucleotide exchange factor

GSK3: Glycogen synthase kinase 3

GLUT1: Glucose transporter 1

GTP: Guanosine triphosphate

HD: Huntington`s disease

HIF-1: Hypoxia-inducible factor 1

HSAN1: Hereditary sensory and autosomal neuropathy type 1

Hx: Hypoxia

HRE: Hypoxia responsive element

HSP: Heat shock protein

IRSp53: Insulin receptor substrate p53

JNK: C-Jun N-terminal kinase

KSR: 3-keto-sphinganine reductase

LDH: Lactate dehydrogenase

LiCl: Lithium chloride

MAP2: Microtubule-associated protein 2

NMDAR: N-methyl-D-aspartate receptor

NF-H: Neurofiament heavy

NF-L: Neurofiament light

Nx: Normoxia

ODDD: Oxygen-dependent degradation domain

PD: Parkinson`s disease

PHD: Prolyl hydroxylation domain

PI3K: Phosphatidylinositol 3-kinase

PSD-95: Postsynaptic density protein 95

Rac1: RAS-related C3 botulinum substrate 1

Rcf: Relative centrifugal force

RhoA: RAS homolog gene family member A

RT-PCR: Real-time PCR

S1P: Sphingosine 1-phosphate

SL: Sphingolipid

SphK: Sphingosine kinases

SPT: Serine palmitoyltransferase

VHL: Van Hippel-Lindau

PHD: Prolyl hydroxylase

VEGF: Vascular endothelial growth factor

WASP: wiskott-aldrich syndrome protein

WAVE: WASP-family verprolin-homologous protein

1. Introduction

1.1 Hypoxia

Most organisms found on earth have the ability to sense and respond to changes in oxygen (O_2) levels. In humans and other mammals an oxygen-dependent stimulus can result in an acute (rapidly induced, of short duration) and chronic (delayed effects, long-termed) responses. When oxygen concentrations exceed physiological levels we speak about hyperoxia whereas when oxygen demand is higher than supply we define the condition as hypoxic. Total lack of oxygen availability is termed anoxia. Notably within the human body the physiological oxygen concentration is very heterogeneous. Although the atmosphere contains 21% O_2, levels in the alveoli are already decreased to 14% and while the arterial blood contains 12 % O_2, only 5.3% is found in the venous system. Within tissues the average oxygen concentration is 5 % and in the brain around 1 to 5 %[1]. Thus in the physiological context hypoxia is a relative term. A drop of oxygen availability is usually an alarm signal for the organism and is associated with the pathology of many diseases however during development hypoxia is an important factor for morphogenesis and organogenesis (Krishnan 2008, Simon 2008).

Clearly, understanding the physiological mechanisms by which the body regulates oxygen homeostasis but also responses to altered oxygen levels associated with pathophysiology will be beneficial to develop new therapeutic strategies to counteract the huge socio-economic burden caused by hypoxia-associated diseases.

1.1.1 HIF-1 - Main regulator of cellular response to hypoxia

On the cellular level hypoxia-inducible factor 1 (HIF-1) is the master regulator for adaptation to reduced oxygen concentrations. HIF-1 is a heterodimeric transcription factor that induces expression of adaptive genes upon its activation. Both the alpha and the beta subunit are basic helix-loop-helix (bHLH) proteins and belong to the PAS family [2]. HIF-1β (also know as aryl hydrocarbon receptor nuclear translocator, ARNT) is constitutively expressed however the transcriptional activity of HIF-1 is dependent on dimerization of HIF-1β with the alpha-subunit that is oxygen-regulated [3,4]. Under physiological oxygen levels HIF-1α is rapidly degraded after *de novo* synthesis. It is hydroxylated at two residues within the oxygen-dependent degradation domain (ODDD) by proteins of a family of prolyl hydroxylases named PHD1-3 after their *p*rolyl *h*ydroxylation *d*omain [5–7]. This modification leads to the recognition of the alpha-subunit by Von Hippel-Lindau (VHL) that is part of an E3 ubiquitin ligase complex that targets HIF-1α for proteasomal degradation [8–11]. As soon as oxygen levels drop below physiological levels PHDs are blocked since their activity depends on oxygen and a fast stabilization and nuclear translocation of HIF-1α occurs. In the nucleus it dimerizes with HIF-1β and associates with the additional co-activators p300/CBP and Src-1 to promote target gene expression via binding to hypoxia-responsive elements (HRE) [10,12,13]. In addition, the factor inhibiting HIF-1 (FIH-1) hydroxylates HIF-1α at a specific asparaginyl residue within the ODDD thereby blocking its interaction with the transcriptional co-activator CBP/p300 and thus HIF-1 transcriptional activity is inhibited [14–16]. Similar to PHDs FIH-1 is dependent on oxygen and contributes to the blockade of HIF-1 signaling during

normoxic conditions [17]. The oxygen dependent regulation of HIF-1α is shown in figure 1.

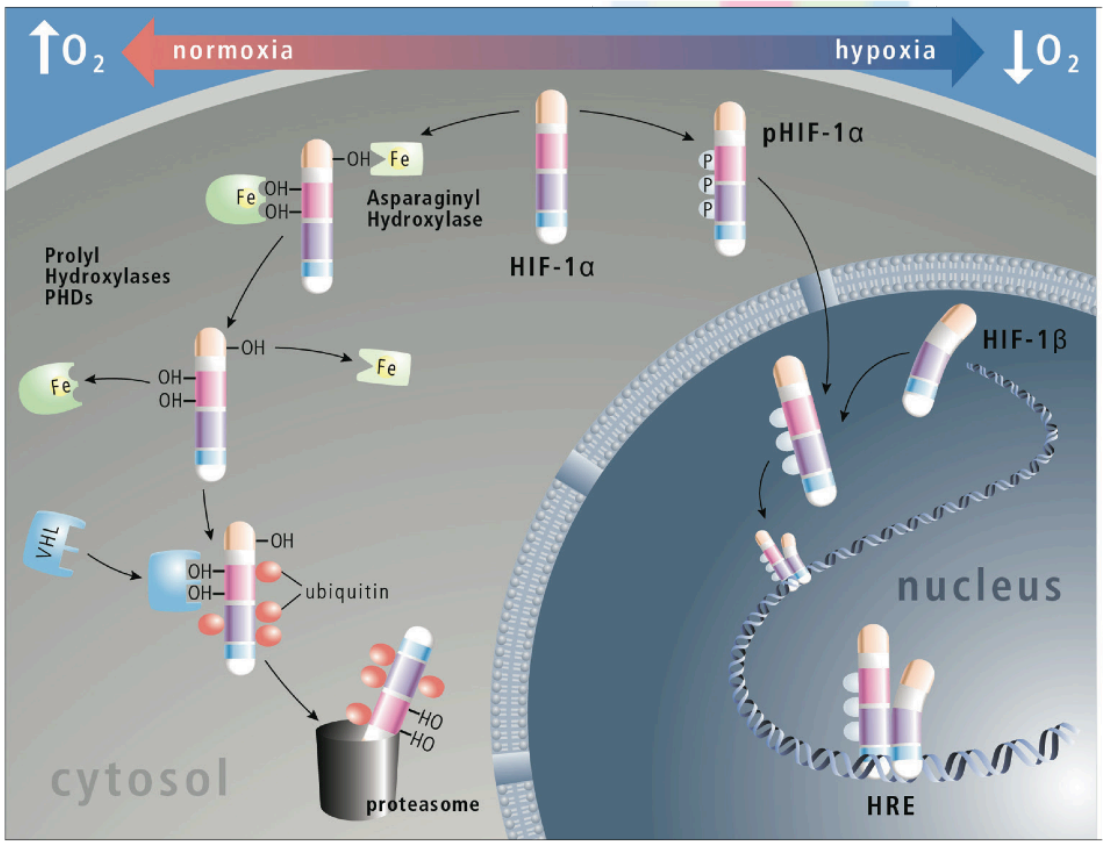

Figure 1: Oxygen dependent regulation if HIF-1α. The figure demonstrates the hydroxylation of HIF-1α by prolyl hydroxylases (PHDs), the subsequent binding of VHL and the proteasomal degradation under normoxia. Hydroxylation of HIF-1α by the asparaginyl hydroxylase FIH-1 suppresses HIF-1 transcriptional activity. When oxygen levels drop HIF-1α is stabilized and upon phosphorylation translocates in the nucleus. There is dimerizes with HIF-1β to bind hypoxia-responsive elements of its target genesand induce their expression. Adapted from Østergaard and Gassmann, 2011 [18].

As research on HIF-1 continued more and more regulators of HIF-1α have been discovered. Chaperons like HSP90 and HSP70 has been demonstrated to additionally regulate degradation of the alpha subunit [19–22]. The tumor suppressor p53 and its negative regulator mdm2 together with HIF-1α have

complex interactions to regulate their protein stability (for review see [23]). Furthermore several posttranslational modifications further participate in control of HIF-1 signaling and are summarized in table 1. Most of these modifications are located within the ODDD domain, the N-terminal and C-terminal transactivation domain (N-TAD/C-TAD) and in the region between the later two. The bHLH/PAS domain mediates dimerization and DNA binding [24]. An overview of the domain organization and the localization of modifications are shown in Figure 2.

Table1: Posttranslational modifications and their regulatory effect on HIF-1α. Adapted from Brahimi-Horn et al., 2005 [25]**.**

Modification	**Effect on HIF-1α**	**Regulators**	**Reference**
Prolyl hydroxylation	Recognition for polyubiquitinylation	Prolyl hydroxylases	10
Polyubiquitinylation	Proteasomal degradation	VHL, E3 ubiquitin ligase complex	8,10
Asparaginyl hydroxylation	Inhibition of transcriptional activity	FIH-1	14,15
Acetylation	Destabilization	ARD-1	26
Phosphorylation	Stimulation of transactivation and transcriptional activity	p42/44 MAPK, GSK3, PKA	11,27–29
SUMOylation	Suppression of translocation	evtl. E3 ligase RanBP2	25
S-nitrosation	Regulation of stability and transcriptional activity	NO	30

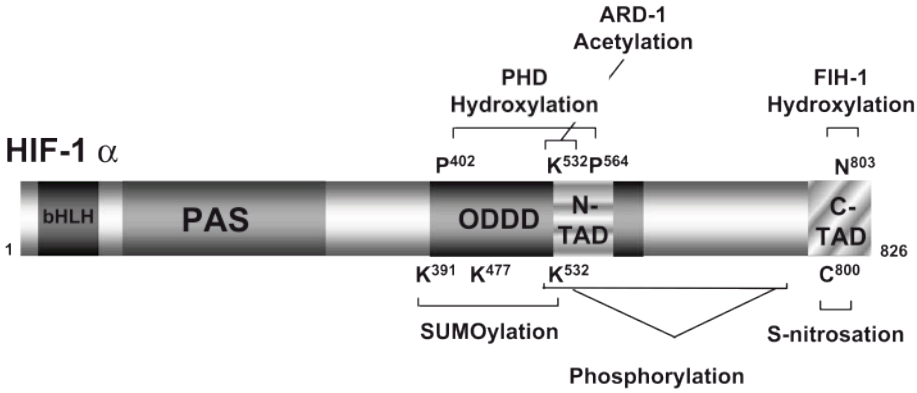

Figure 2: Structural domain organization of HIF-1α with the location of posttranslational modifications (modified from Brahimi-Horn et al., 2005 [25]). The bHLH (basic helix-loop-helix)/PAS domain confers dimerization and DNA binding. Residues within the ODDD (oxygen-dependent degradation domain), the N-TAD and the C-TAD (N-terminal/C-terminal transactivation domain) and within the region between the transactivation domains are modified.

Notably beside HIF-1α two additional isoforms, HIF-2α and HIF-3α, have been described. HIF-2α shows 48 % of amino acid sequence identity with HIF-1α and therefore has similar features like dimerization with HIF-1β and HRE binding [31–33]. HIF-2α is expressed in distinct cell types of different organs and is induced in the brain endothelium and in glia cells but not in neurons [33]. During intermittent hypoxia HIF-1α and 2α are differentially regulated [34] and seem to have different roles in hypoxic gene regulation since it has been shown in endothelial and epithelial cells HIF-1α but not HIF-2α induced glycolytic genes [35,36]. HIF-3α has been less studied but is also induced in various tissues. HIF-1α can induce HIF-3α expression that then seems to negatively regulate the hypoxic response [37,38]. In addition a splice variant of HIF-3α, IPAS (inhibitory PAS), has been identified

that can interact with HIF-1α and thereby prevent DNA binding [39]. Also it has been shown to be involved in a negative feedback loop for HIF-1 activity [40].

As mentioned before hypoxia is an important physiological stimulus in development and particularly HIF-1 is a critical player for developmental processes. A knockout mouse model demonstrated that loss of HIF-1α results in developmental arrest and embryonic lethality by E11. Those embryos developed neural tube defects and cardiovascular abnormalities [41,42]. Mice with a neuron-specific HIF-1α deletion exhibit hydrocephalus, loss of neural cells and impairment of spatial memory, demonstrating the crucial role for HIF-1 signaling for organogenesis [43]. Thus during development a loss of HIF-1 has detrimental consequences, however the general role of HIF-1 in cell survival remains under debate.

1.1.2 HIF-1 and its role for cell survival during hypoxia

The list of HIF-1 target genes is long, heterogeneous and constantly being expanded. Hypoxic induction of HIF-1 target genes is schematically presented in figure 3. While studying the various proteins that are controlled by HIF-1 one might already appreciate that its role in cell survival is a highly discussed issue. HIF-1 is believed to be protective since many of its numerous hypoxia-induced target proteins assist the single cell, organ and subsequently the whole organism to adapt to decreased oxygen levels. One of those major adaptive processes is a change in metabolism. When oxygen, the final electron acceptor of the mitochondrial respiratory chain[44] is limited the cell switches to anaerobic metabolism to produce ATP via glycolysis (see review [45]). Therefore HIF-1

induces proteins involved in glucose metabolism and transport like glucose transporter 1, hexokinase 1 & 2, aldolase and phosphoglycerate kinase 1 [46–48]. Another important adaptive process stimulated by HIF-1 is angiogenesis to ensure tissue oxygenation by the blood [49]. Proteins induced are therefore for example VEGF and endoglin [46]. Furthermore HIF-1 initiates expression of genes encoding proteins that directly promote survival (adrenomodullin, IGF2) and proliferation (TGF-3β) [50–52]. In contrast, evidence also exists for HIF-1 having a role in mediating cell death. In this context HIF-1 has been shown to drive gene expression of pro-apoptotic genes like BNIP3, NIP3, NOXA/NIX and RTP801 [53–55] as well as induce apoptosis via stabilization of the tumor suppressor p53 [46,56,57]. Moreover HIF-1α was reported to mediate caspase-3 induction in the ischemic mouse brain [58]. Similarly, deletion of HIF-1α in the nervous system showed contradictory results. On the one hand late-stage brain-specific loss of HIF-1α was reported to reduce hypoxic-ischemic damage [59]. On the other hand a neuron-specific loss of *Phd2* that increased HIF-1α protein level was shown to be beneficial after transient cerebral ischemia [60]. In agreement a neuron-specific knockout of HIF-1α was demonstrated to increase brain injury after focal cerebral ischemia [61]. Other studies suggest that the role of HIF-1 signaling for cellular survival seems to depend on experimental conditions, the kind of stimuli and the cell type [62–64]. Thus HIF-1α stabilization seems to be a double-edged sword regarding the outcome after injury.

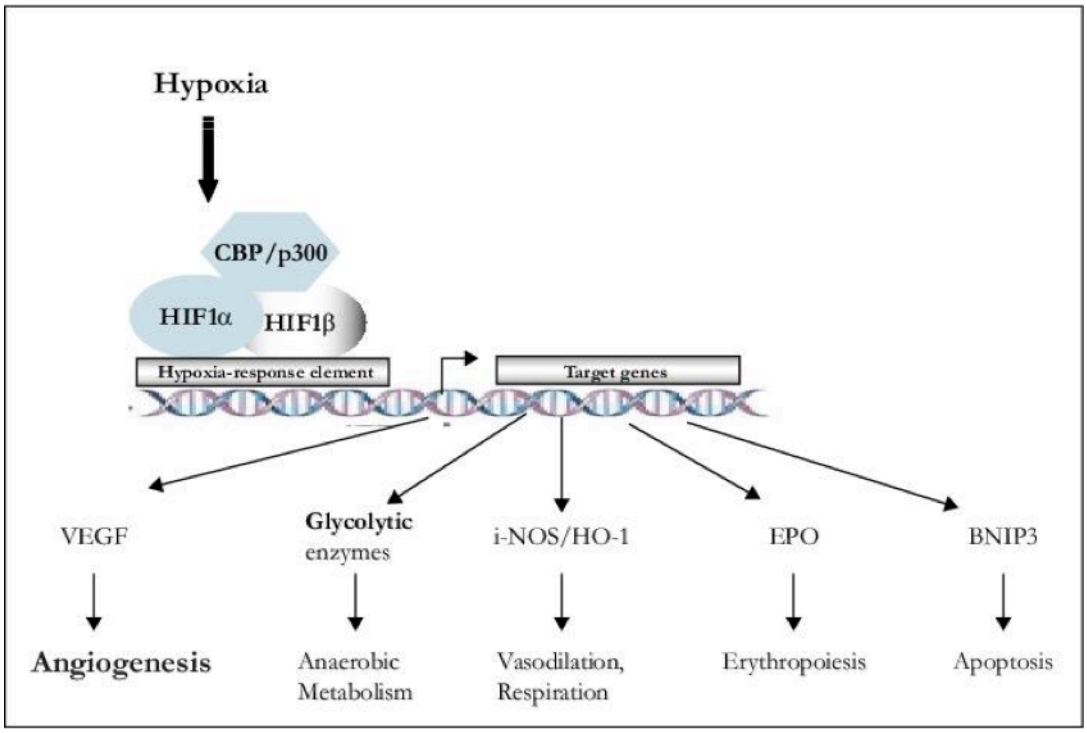

Figure 3: Hypoxic induction of HIF-1 target genes. Schematic shows dimerization of HIF-1α and HIF-1β upon hypoxic stimulus and binding to the hypoxia-responsive element of target genes together with the co-activators p300/CBP (CREB (cyclic-AMP-response element-binding protein) binding protein. Different target genes promote adaptation and survival, others impair cell survival during hypoxia. Adapted from Brahimi-Horn et al., 2006 [65].

1.1.3 The hypoxic brain and neurodegeneration

Since the brain controls whole body physiology it is no surprise that it is the main consumer of energy. Neurons are almost completely dependent on aerobic metabolism and therefore are especially sensitive to inadequate oxygen supply. In contrast other brain cells like oligodendrocytes, endothelial cells and especially astrocytes are more resistant to reduced oxygen levels than neurons [66–69]. Differences in hypoxic sensitivity are even observed within neuronal cells. Global brain ischemia induces death of CA1 hippocampal neurons already within

5 minutes, striatal neurons after 10 minutes while cortical neurons survive 15-20 minutes when normothermic and normoglycemic level were maintained [70–72]. Insufficient oxygen delivery to the brain can be due to a vessel occlusion or result from reduced blood supply caused by cardiovascular or respiratory disorders. Subsequent neuronal dysfunction and death contribute thereupon to irreversible brain damage and diseases that can cause periods of cerebral hypoxia are often associated with neurodegeneration (summarized in figure 4). Stroke victims for example may be up to tenfold more likely to develop Alzheimer´s disease (AD) in the subsequent years compared with an age-matched cohort [73]. Although the association of cerebral hypoxia and neurodegenerative disease is known we are just at the beginning of understanding the mechanisms behind this connection. Moreover since a few years HIF-1α is proposed to be a potential factor to counteract neurodegenerative processes due to its neuroprotective function (for review see [74]). It was demonstrated that HIF-1α levels were decreases in AD patients [75] and that forced HIF-1α stabilization protected cells *in vitro* against Aβ and inhibits AD progression in patients [76].

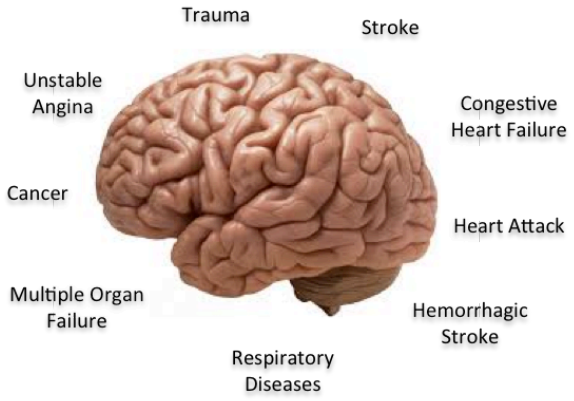

Figure 4: Summary of diseases that can cause cerebral hypoxia.

Both hypoxic and neurodegenerative disease are associated with cytoskeleton alterations. The neuronal cytoskeleton consists of microtubules, microfilaments (actin filaments) and neurofilaments (intermediate filaments). While hypoxia induces a breakdown of cytoskeleton structures [77–79] in neurodegenerative diseases abnormal accumulations or modulation of cytoskeleton components and associated proteins are observed [80,81]. Rho GTPases are key regulators of the cytoskeleton and indeed their deregulation is implicated in numerous neurodegenerative disorders and moreover they are involved in the adaptation to hypoxia.

1.2 Rho GTPases

1.2.1 Rho GTPases – Regulation and function

Rho GTPases are small (~21 kDa) monomeric G proteins belonging to the Ras superfamily and are master regulators of the cytoskeleton. In addition they are involved in diverse signaling processes often induced by extracellular stimuli. Rho GTPases are divided into 10 subgroups with Rac1, RhoA and Cdc42 being the best characterized members. Rho GTPases act as molecular switches and cycle between an active, GTP-bound, and an inactive, GDP-bound, state associated with conformational changes [82]. The state of activity is tightly regulated by three sets of proteins, the guanine nucleotide exchange factors (GEF), the GTPase-activating factors (GAP) and the guanine nucleotide-dissociation inhibitors (GDI). In the cytosol the GDIs bind to Rho GTPases, thereby keeping them in an inactive state [83]. Upon different stimuli specific GEFs are activated and bind the guanine nucleotide depleted Rho protein and allow

GTP-binding that is occurring rapidly due to high cytosolic GTP levels [84]. Active Rho GTPases are mostly bound to the plasma membrane via their farnesyl or geranylgeranyl anchors and transmit signals by binding to their effectors like protein and lipid kinases, phospholipases or scaffolding proteins [85–87]. To terminate Rho GTPase-mediated signals GAPs are activated and stimulate the intrinsic GTPases activity of Rho proteins thus GTP gets hydrolyzed and Rho GTPases switch back to their inactive state [88]. The activity of GAPs and GEFs is regulated as well by various signaling molecules hence Rho GTPase signaling is controlled by a very complex network and is schematically represented in figure 5. Furthermore crosstalk exits between the different Rho GTPases (see for review [89]). Importantly, Rac1 and Cdc42 often have complementary roles whereas RhoA signaling has an opposing outcome. An example is the regulation of actin dynamics during neuronal development where Rac1 and Cdc42 promote growth cone progression and neurite outgrowth whereas RhoA induces growth cone collapse and neurite retraction [90]. Beside the cytoskeleton regulation Rho GTPases are involved in the control of various intracellular processes like endo- and exocytosis, cell cycle, gene expression, motility and adhesion, growth control and mitogenesis, stress response and apoptosis [91]. Thus RhoGTPases represent multifunctional regulators that are critical for cell development and signaling during health and disease.

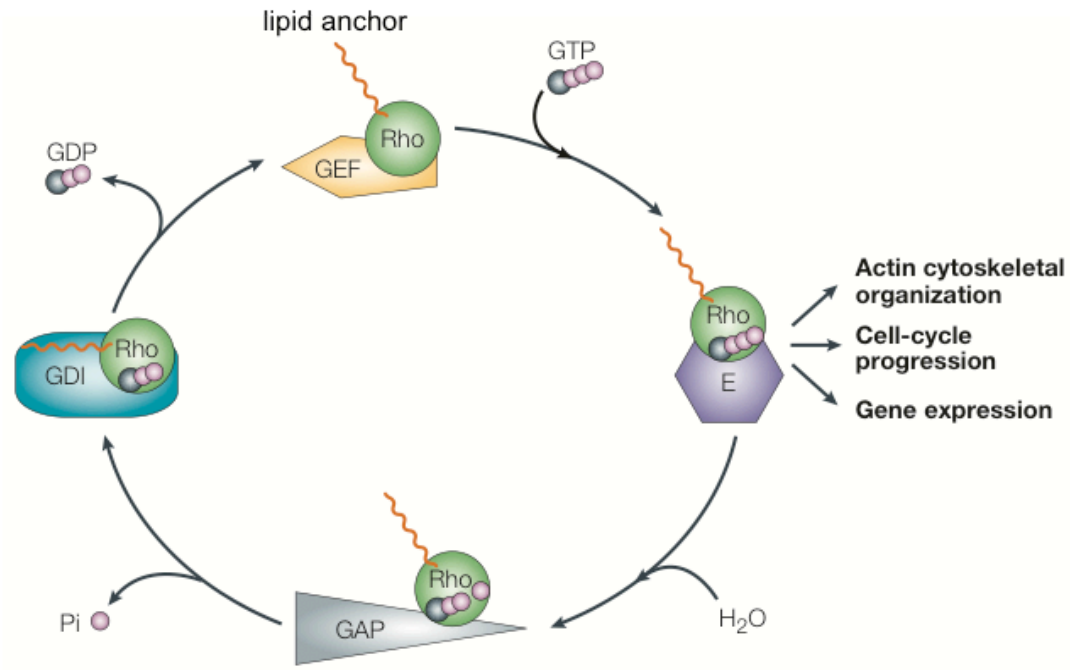

Figure 5: The regulation of Rho GTPases by guanine nucleotide exchange factors (GEF), GTPase-activating factors (GAP) and the guanine nucleotide-dissociation inhibitors (GDI). E: effector; Pi: inorganic phosphate. Modified from Rossman 2005 [91].

1.2.2 Rho GTPases in hypoxia

Increasing evidence for the involvement of Rho GTPases in responses to reduced oxygen concentrations has been presented using various *in vitro* and *in vivo* models. Both RhoA and RhoB have been demonstrated to be involved in neuronal death after ischemic injury. In mouse cerebral cortex RhoA was activated after occlusion of the middle cerebral artery [92] and RhoB was shown to be an early marker of neuronal death that contributes to neurodegeneration by triggering microfilament rearrangements in a murine stroke model [93]. For Rac1 it was reported that its inhibition protected against necrosis and apoptosis in a non-lethal ischemia/reperfusion mouse model [94]. In contrast another study

showed decreased Rac1 activity was associated with poor cell survival and recovery after global cerebral ischemia [95]. On the cellular level Rac1, Cdc42 and RhoA were rapidly upregulated when oxygen levels dropped [96]. In pulmonary artery endothelial cells opposing roles of Rac1 and RhoA were shown in a hypoxia/reperfusion model. Hypoxic Rac1 inhibition led to RhoA activation during hypoxia that promoted stress fiber formation, disruption of junctions and increased endothelial permeability. Subsequent reperfusion activated Rac1 that reinduced cortical localization of actin and VE-Cadherin [95].

Upon the discovery that Rac1 is activated by hypoxia and is crucial for HIF-1α stabilization in HEK293 cells [97] it has been demonstrated in other cancer cells and in epithelial cells that Rac1 is indeed critical for HIF-1 signaling [98–100]. More recently, Rac1-dependent HIF-1α accumulation has been associated with increased formation of reactive oxygen species since NADPH oxidase activity depends on Rac1 [101–103]. Furthermore NF-kappaB, ERK and PI3K have been proposed to be involved in Rac1-driven HIF-1α induction in different cell types [100,104–106]. In neurons however the involvement of Rac1 in HIF-1 regulation has so far been unexplored and is a main focus of the current thesis work.

1.2.3 Rho GTPases in neurodegeneration

In the last decade it became more and more evident that deregulation of Rho GTPases is implicated in neurodegenerative disorders. Some of these deregulations are associated with cytoskeletal alterations underlying the disease pathology. An overview is given in table 2. In Alzheimer`s disease (AD) RhoA activity was reduced and the protein co-localized with hyperphosphorylated tau

found in neurofibrillary tangles [107]. Similarly reduced Rac1 activity was associated with shortening of neurites in an *in vitro* AD model [108]. Accordingly the expression of Rac1 effectors PAK1 and PAK2, and their activity, is diminished in AD brains resulting in disturbed actin remodeling in dendritic spines [109]. Altered Rho GTPase regulation has also been associated with Huntington`s disease that is characterized by the aggregation of a protein named huntingtin (Htt). Inhibition of RhoA effector ROCK has been shown to reduce Htt accumulation in a Drosophila model [110]. Furthermore the Cdc42-interacting protein 4 (Cip4) a Cdc42 effector involved in cytoskeleton organization via WASP has been associated with Htt and overexpression of Cip4 resulted in neuronal death [111]. Deregulation of Rho GTPases, their effectors and regulators is similarly involved in the pathogenesis of Glaucoma, Parkinson`s disease (PD) and Charcot-Marie-tooth disease (CMTD), (see table 2). Thus clearly Rho GTPases can be associated with many different disorders and make significant impact on disease outcome. Moreover data from the current thesis work suggests an important link between Rac1 and neuropathology progression of hereditary sensory and autonomic neuropathy type 1 (HSAN1), (see below, chapter 1.3.3 and manuscript chapter 7.2).

Table 2: Summary of Rho GTPases and their regulators associated with neurodegenerative diseases (modified from DeGeer et al., 2013 [112]). AD: Alzheimer`s disease, HD: Huntington`s disease, PD: Parkinson`s disease, CMTD4H: Charcot-Marie-Tooth Neuropathy Type 4H

	Name	Effector	Associated pathology/setting	Reference
GTPases	Cdc42	CIP4	AD, HD, PD, CMTD4H	113
	Rac1		Nerve injury, early AD, PD, HD	108,114–116
	RhoA	ROCK	Nerve injury AD, degeneration, HD, PD, CMTD, lower motor neuron disease	110,114,117–123
GEFs	Alsin	Rab5, Rac1	ALS/Upper motor neuron disease	113
	ARHGEF10	RhoA	Peripheral nerve disease	124
	Dock3	Rac1	AD	125–128
	Frabin/FGD4	Cdc42	CMTD4H	129
	GEF-H1	RhoA	HD	130
	PLEKHG5/Syx	RhoA	Lower motor neuron disease	123
	Kalirin 7	Rac1	AD, HD, PD	131–133
	Kalirin 9	RhoA, Rac1	Nerve injury/axon pruning	134
	Tiam1	Rac1	AD	115
	Trio	RhoA, Rac1, RhoG	HD	135
	Vav2/Vav3	RhoA/B/G	Glaucoma	136
GAPs	BARGIN	Rac1	AD	137
	NOMA-GAP	Cdc42	AD	138
	p250GAP	RhoA, Rac1, Cdc42	HD	139
	p190RhoGAP	RhoA	Injury/Axon pruning	140
GDIs	RhoGDI	RhoA	Injury/Axon pruning	141

1.3 Deoxysphingolipids in neurodegeneration

1.3.1 An introduction to sphingolipids

When sphingolipids (SL) were discovered in brain extracts in the 1870s they were named after the Greek mythological creature Sphinx due to their enigmatic structure [142]. They consist of a sphingoid base backbone that is linked to a polar head group like serine, choline and ethanolamine and an acyl group like fatty acid. The combination of different head groups, fatty acids and sphingoid bases results in a variety of individual lipids. SL are bioactive molecules found in plasma membranes and especially lipid rafts [143] and are involved in various signaling processes. Especially ceramide and S1P are important regulatory molecules with ceramide mediating apoptosis and senescence and S1P promoting cell survival, migration and inflammation [144–147]. In general SL are highly abundant in the nervous system controlling survival, differentiation, responsiveness to trophic factors, synaptic stability and transmission and the formation of central and peripheral myelin [148].

SL metabolism is found in eukaryotic cells and in *Sphingomonas* bacteria. *De novo* synthesis of SL (Fig. 6A) starts in the ER with the conjugation of serine and palmitoyl-CoA resulting in the formation of 3-keto-sphinganine. This first rate-limiting step is catalyzed by serine palmitoyltransferase (SPT). SPT is a heteromeric protein consisting of three subunits SPTLC1, SPTLC2 and SPTLC3 [149–152]. The first product of the SL synthesis 3-keto-sphinganine is immediately reduced to sphinganine by the enzyme 3-keto-sphinganine reductase (KSR), [153] and sphinganine is then further metabolized to dihydro-ceramide by ceramide synthase (CerS), [155]. Six different family members of CerS have been identified

with distinct tissue and substrate specificity creating a variety of different fatty acid species with individual carbon chain length (C_{12} to C_{26}), double bonds and hydroxylations [155]. Ceramide is then synthesized by the enzyme Δ4dihydro-ceramide desaturase (DES) by inducing a *trans*-double bond into the sphinganine backbone [156,157]. The further metabolism of ceramides is located at the Golgi [158]. Here sphingomyelin synthase forms sphingomyelin and diacylglycerine in one reaction [159]. Notably, sphingomyelin is an important component of the myelin sheath that surrounds neuronal axons [160]. Also ceramides can be glycosylated to glucoceramides and conjugated to galactose to form galactosyl-ceramide [161]. Degradation of sphingomyelin and glycosphingolipids can in turn be degraded via ceramide that is then hydrolyzed to sphingosine by the enzyme ceramidase [162,163]. Sphingosine can be used to reform ceramide or can be phosphorylated by sphingosine kinases (SphK) to form sphingosine 1-phosphate (S1P) [164]. S1P lyase catalyzes the breakdown of S1P into the non-sphingolipid molecules ethanolamine phosphate and hexadecenal [165].

Importantly, deregulation of SL metabolism, transport and storage is tightly associated with numerous neurodegenerative disorders including Alzheimer`s disease, Parkinson`s disease and Huntington`s disease (for review see [148]). Moreover disturbed SL regulation contributes to the pathogenesis of cardiovascular and metabolic diseases (for review see [166,167]). Particularly the formation of atypical SLs has been associated with metabolic syndrome, diabetes and neuropathies [168–170].

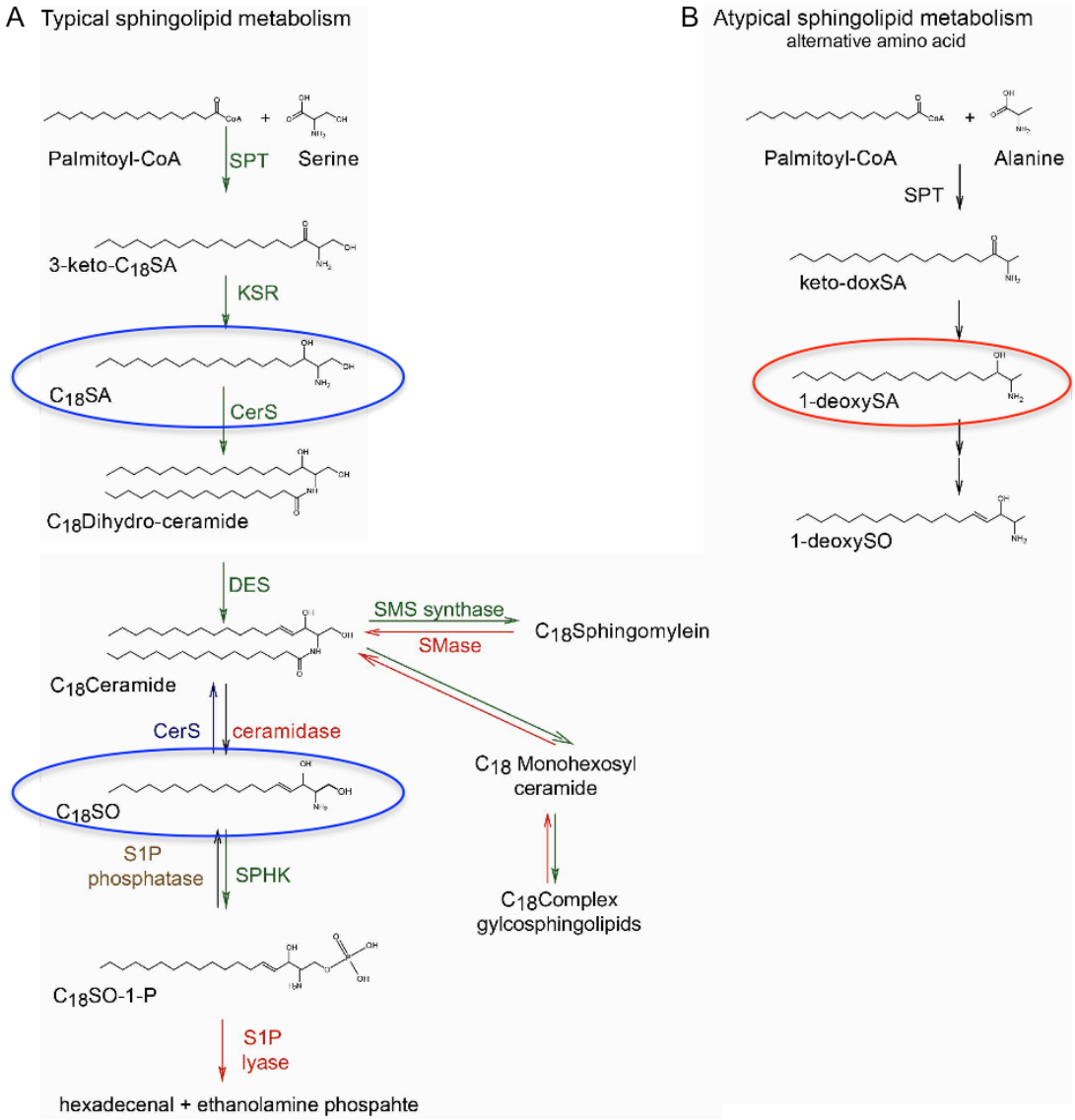

Figure 6: Metabolism of sphingolipids. A, shows the typical pathway starting with conjugation of palmitoyl-CoA and serine and the involved enzymes. B, atypical formation of deoxysphingoid bases resulting from using alanine as a substrate in the first step of sphingolipid synthesis instead of serine. SPT, serine palmitoyltransferase; KSR, keto-sphinganine reductase; CerS, ceramide synthase; DES dihydro-ceramide reductase; S1P phosphatase/lyase, sphingosine 1-phosphatase/ lyase; SPHK, Sphingosine kinases, SMS synthase, sphingomyelin synthase; SMases, sphingomyelinase; 1-deoxySA, 1-deoxysphinganine; 1-deoxySO; 1-deoxyssphingosine. Green color represents the biosynthetic and red color the degradation pathway. Adapted from Othman, 2003 [154]. The sphingolipids highlighted in blue were used as control lipids in our study. The red-highlighted atypical lipid 1-deoxySA was investigated in our study with regard to its neurotoxicity.

1.3.2 Deoxysphingolipids

As introduced above the enzyme serine palmitoyltransferase (SPT) catalyzes the first step of the *de novo* sphingolipid synthesis, the conjugation of palmitoyl-CoA and serine. Mutations and other so far unidentified conditions induce a switch of substrate specificity and SPT uses acyl-CoA others than palmitoyl-CoA or alanine instead of serine thereby forming atypical SLs. When palmitoyl-CoA is conjugated with alanine 1-deoxyspingolipids (deoxySL) are produced, named 1-deoxysphinganine (1-deoxySA) and 1-deoxysphingosine (1-deoxySO), (Fig. 6B), [170,171]. This class of lipids misses the C_1 hydroxyl group thus their metabolism to complex SL as well as their degradation is prevented and consequently accumulation of deoxySL occurs that induce toxicity in different cell types [172–175]. 1-deoxySA was first discovered in the marine organism *Spisula polynyma* as a potential anti-cancer drug, first termed spisulosine [172]. It has been demonstrated that this compound shows anti-proliferative effects on mammalian cells and induces disassembly of actin stress fibers. It was hypothesized that the observed cytoskeletal alterations might be due to decreases activity of Rho GTPases [172].

1.3.3 Deoxysphingolipids and disease

Our collaboration partners identified 1-deoxySA as product of palmitoyl-CoA and alanine catalyzed directly by SPT [170] and further investigated it mainly in the context of metabolic disease. Elevated plasma levels of deoxySL, including 1-deoxySA, have been identified as new biomarkers for diabetes mellitus and metabolic syndromes [168,169]. Very recently we have shown that 1-deoxySA

directly induces apoptosis and senescence in insulin-producing cells accompanied by cytoskeleton rearrangements and Rho GTPase deregulation [175].

Hereditary sensory and autonomic neuropathy type 1 (HSAN1) is a rare autosomal dominantly inherited axonal neuropathy. Interestingly it has been discovered that certain missense mutation in the genes encoding SPTLC1 and SPTLC2 cause this disease [176]. Symptoms of HSAN1 are progressive loss of pain and temperature sensation starting in the lower limbs and expanding to upper extremities [177]. Post-mortal examination of HSAN1 patients demonstrated extreme degeneration of dorsal root ganglion cells and destroyed myelin sheath form peripheral nerves [177]. The mentioned HSAN1 mutant SPT variants show increased substrate specificity for alanine thus inducing accumulation of deoxySL. In accordance highly elevated deoxySL levels were found in plasma and tissue of an HSAN1 mouse model [178]. The neurotoxic effect of 1-deoxySA was confirmed on cultured chicken dorsal root ganglion cells where a reduction of neurite number and length was detected [170]. However the mechanisms by which deoxySL induce neuronal death remains to be unraveled. Notably diabetic sensory neuropathy (DSN), the most common chronic complication of diabetes mellitus, is clinically very similar to HSAN1. As mentioned above diabetics have been shown to frequently have elevated deoxySL plasma levels and hence the formation of deoxysphingolipids might be even associated with DSN. However, not much is known about these deoxySL and thus much more research is required to understand their mode of action. Part of this thesis work was focused to unravel the molecular mechanisms of 1-deoxySA-induced neurotoxicity to make the first step towards the development of therapeutic approaches to prevent deoxysphingolipid-triggered neuropathies.

2. PhD thesis projects

Two main projects were performed during my PhD studies. Both dealt with the neuronal response to a pathological stimulus and focused particularly on Rho GTPase signaling and downstream cascades.

In both studies we used isolated cortical neurons from E14 mouse embryos. Notably around day 12 *in vitro* cultured neurons have set up a complex neuronal network and synaptogenesis is completed. By that time they express all receptors that are characteristic for mature neurons [179]. Thus we use 6 DIV cells as a model for immature and 17 DIV cell as a model for mature neuronal cells. Figure 7 shows brightfield images of 6 DIV and 17 DIV cultured neurons. For hypoxia experiments cells were exposed to 1 %.

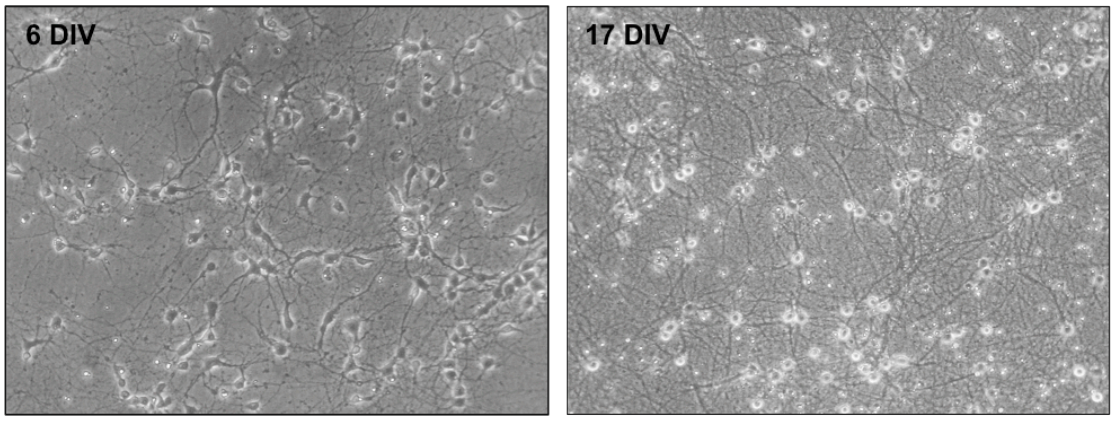

Figure 7: Brightfield image of cultured cortical mouse neurons. 17 DIV neurons have developed more neurite connetions and build a more complex network than 6 DIV neurons.

2.1 Role of Rac1 in the neuronal response to hypoxia

The goal of this study was to assess the contribution of the Rho GTPase Rac1 to the neuronal hypoxic response. The understanding of the neuronal answer to hypoxia is beneficial for elaborating strategies to prevent neuronal loss due to hypoxic insults.

Rac1 in mature (17 DIV) hypoxic neurons

- Analysis of hypoxia-dependent Rac1 regulation in mature neurons
- Effects of Rac1 inhibition on HIF-1α induction and subsequent adaptive gene expression
- Consequences of acute hypoxia and Rac1 inhibition on survival of mature neurons
- Identification of pathways mediating Rac1-dependent neuronal HIF-1α induction

The data of these investigations resulted in a submitted manuscript in which I am first author ("Rac1 plays a crucial role for neuronal adaptation to hypoxia", chapter 7.1).

Rac1 in young (6 DIV) hypoxic neurons

- Analysis of acute hypoxic Rac1 regulation in young neurons
- Determination of the effect of Rac1 inhibition of HIF-1α induction
- Survival of young neurons during acute hypoxia and Rac1 inhibition
- Effects of GSK3 inhibition on hypoxic HIF-1α accumulation

Rac1 in the response of mature neurons to prolonged hypoxia

- Analysis of the effect of Rac1 and GSK3 inhibition on HIF-1α induction and on survival of mature neurons after 24h of hypoxia

These results are presented in chapter 4.1.

2.2 Deoxysphingolipid-induced neurotoxicity

This second study determined the effect of the atypical sphingoid base, 1-deoxySA, on survival of cultured cortical neurons with a special emphasis on modulation of cytoskeleton integrity and Rho GTPase regulation. Most importantly we intended to resolve the molecular mechanisms involved in 1-deoxySA-induced neurotoxicity since this is a prerequisite to identify clinically relevant strategies to prevent deoxy-sphingolipid-mediated neurodegeneration.

Effects of deoxysphingolipid treatment on mature (17 DIV) neurons

- Effect of 1-deoxysphinganine (1-deoxySA) and its metabolites on survival of mature neurons
- Characterization of 1-deoxySA effects on the neuronal cytoskeleton
- Identification of cytoskeleton-associated proteins regulated by 1-deoxySA
- Contribution of Rac1 and JNK to 1-deoxySA-triggered neuronal death
- Analysis of involvement of NMDAR signaling in 1-deoxySA-induced neurotoxicity

The results of these investigations are presented in a submitted manuscript in which I am first author ("1-Deoxysphingolipid-induced neurotoxicity involves N-methyl-D-aspartate receptor signaling", chapter 7.2).

Effects of deoxysphingolipid treatment on young (6 DIV) neurons

- Effect of 1-deoxy-sphinganine on survival of young neurons
- 1-deoxySA effects on the young neuronal cytoskeleton and Rac1 activity
- Consequences of 1-deoxySA exposure on JNK phosphorylation and on p35 levels

The results of this study are presented in chapter 4.2.

3. Results

3.1 Rac1 in the neuronal response to hypoxia

3.1.1 Rac1 in the hypoxic response of young neurons

The submitted manuscript describes the contribution of Rac1 to the acute hypoxic response of mature (17) DIV neurons. To explore whether young neurons display a similar tolerance survival of 6 DIV neurons exposed to short periods of hypoxia was assessed. Whether HIF-1α stabilization in young neurons was regulated by Rac1- and GSK3-dependent mechanisms as observed in the older cells was also studied.

Rac1 is upregulated and activated in young neurons during hypoxia

We first studied hypoxic Rac1 regulation in 6 DIV primary cortical mouse neurons. Western blot analysis showed after 4h and 6h of hypoxia increased Rac1 protein levels compared to normoxic control samples (Fig. 8A). Immunocytochemistry confirmed this observation as normoxic cells showed very weak staining for Rac1 whereas hypoxic cells showed a bright and clear signal after 6h (Fig. 8B). To examine neuronal Rac1 activity state we used Rac G-LISA. Hypoxic exposure strongly increased Rac activity after 2h (204.0 ± 10.8, $p<0.01$) and remained elevated up to 6h (192.7 ± 1.7, $p<0.01$) compared to the normoxic control (Fig. 8C). These results show that the response to acute hypoxia of 6 DIV neurons activates Rac1 as observed in mature cells.

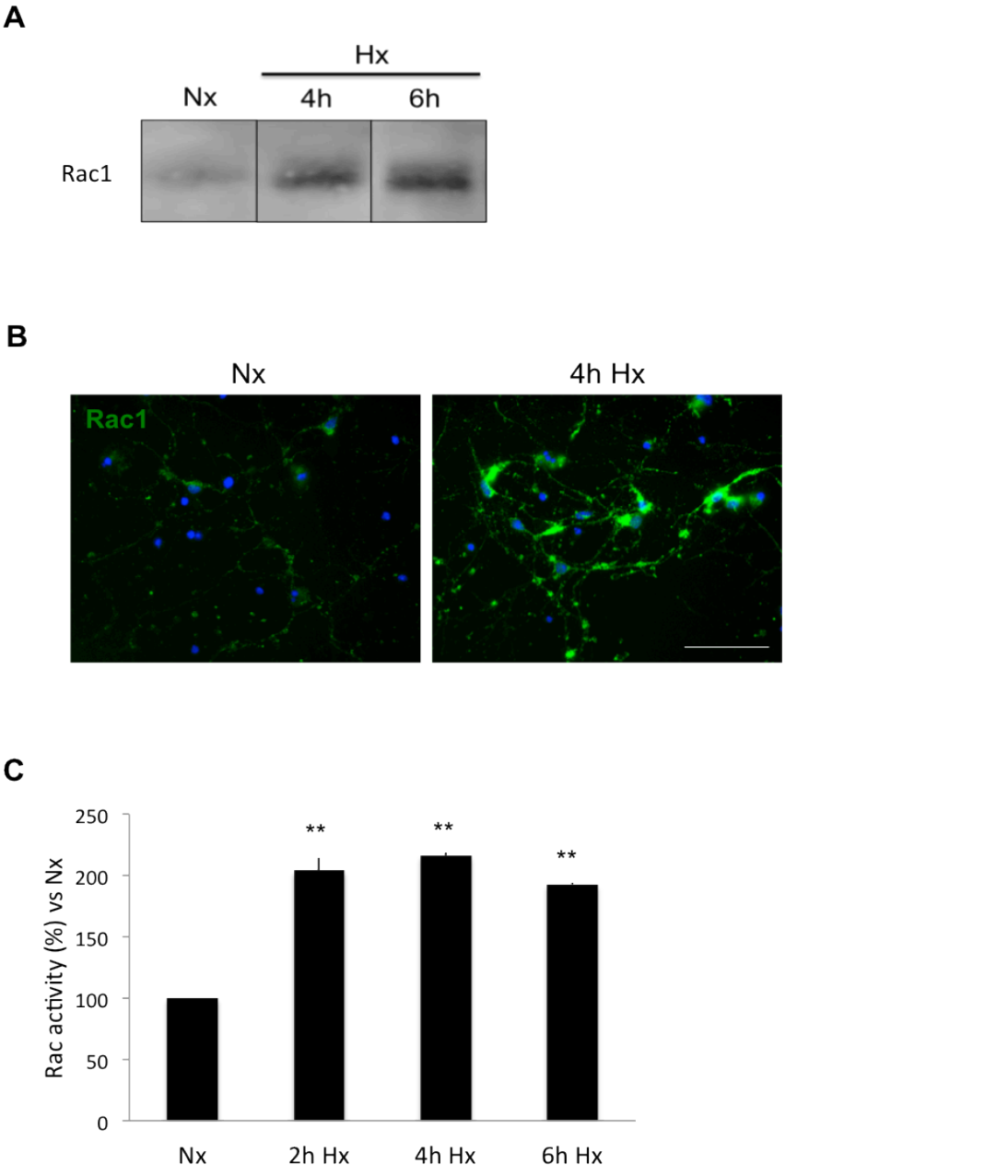

Figure 8. Rac1 is upregulated and activated during hypoxia. Cells were incubated for 4h and 6h under normoxic (Nx) or hypoxic (Hx) conditions. A, Cell lysates were used to detect total Rac1 protein levels by Western blot (N=3). B, Cellular Rac1 levels were additionally analyzed by Immunocytochemistry (N=2). Green: Rac1, blue: DAPI, scale bar: 50 µm. C, Cells lysates were used to determine active Rac by G-LISA (N=3). ** $p<0.01$ versus normoxia. Data were analyzed using one-way ANOVA followed by Bonferroni post-hoc test.

Rac1 is crucial for HIF-1α stabilization in young neurons

To prove that hypoxia-activated Rac1 is critical for HIF-1 signaling in 6 DIV cells we treated young neurons with 50 μM and 100 μM of a specific Rac1 inhibitor prior to hypoxic exposure. Western blot data show HIF-1α accumulation after 4h and 6h, however inhibitor treatment completely abrogated of hypoxic HIF-1α accumulation (Fig. 9A). Immunocytochemistry again confirmed these results showing basal HIF-1α signal with hypoxic exposure inducing nuclear HIF-1α staining. Similar to Western blot results Rac1 inhibition strongly suppressed HIF-1α accumulation in both normoxic and hypoxic cells (Fig. 9B). Thus Rac1 is a critical induced of HIF-1α stabilization in young neurons.

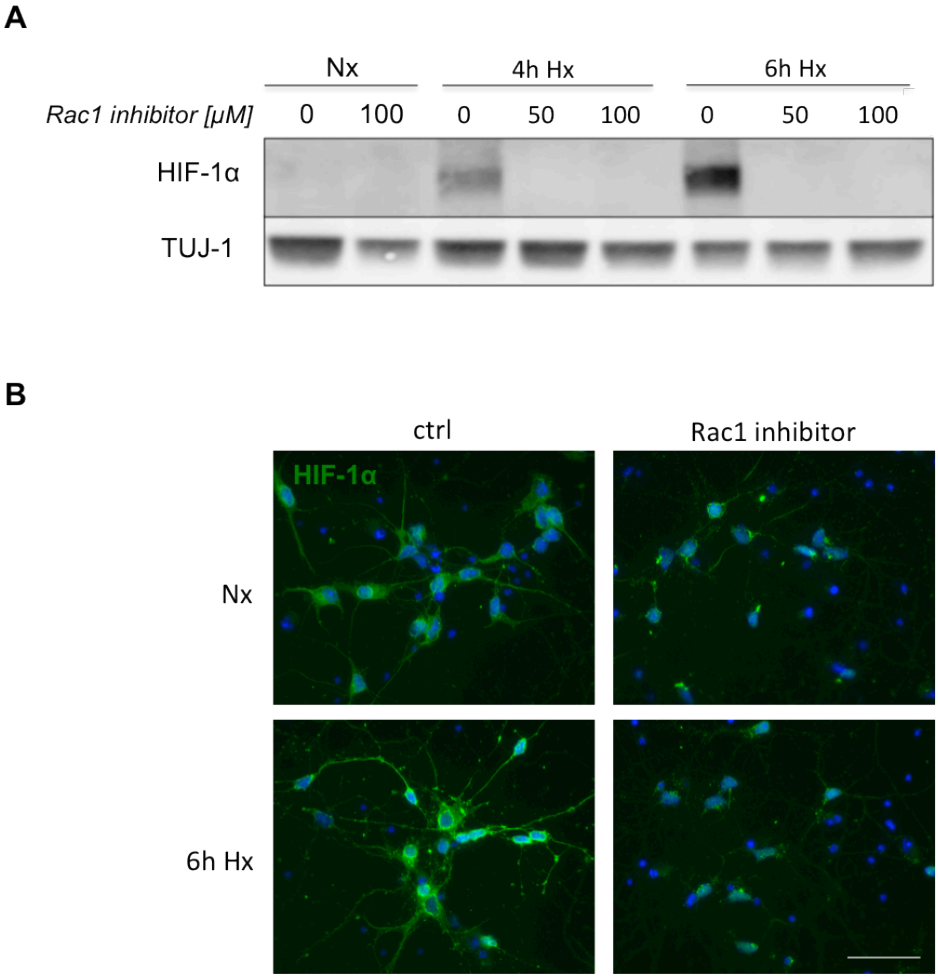

Figure 9: Rac1 is crucial for HIF-1α stabilization in young neurons. A, Representative Western blot analysis shows HIF-1α protein levels of normoxic (Nx) and hypoxic (Hx) cells treated with 50 or 100 µM Rac1 inhibitor (N=4). TUJ-1 was used as loading control. B, Immunocytochemistry demonstrate localization of HIF-1α (green) in the presence or absence or 100 µM Rac1 inhibitor (N=2). DAPI (blue), scale bar: 50 µm.

Young neurons survive acute hypoxia in absence of Rac1 and HIF-1α

To demonstrate the effect of acute hypoxia and Rac1 inhibition on survival of young neurons, cells were treated with Rac1 inhibitor prior to hypoxic exposure and cell survival was assessed using MTT (Fig. 10A) and LDH (Fig. 10B) assays. Both assays data show that neither acute hypoxia nor Rac1 inhibition alters survival of immature neurons. Thus tolerance to short periods of reduced oxygen levels do not depend on Rac1 and HIF-1α.

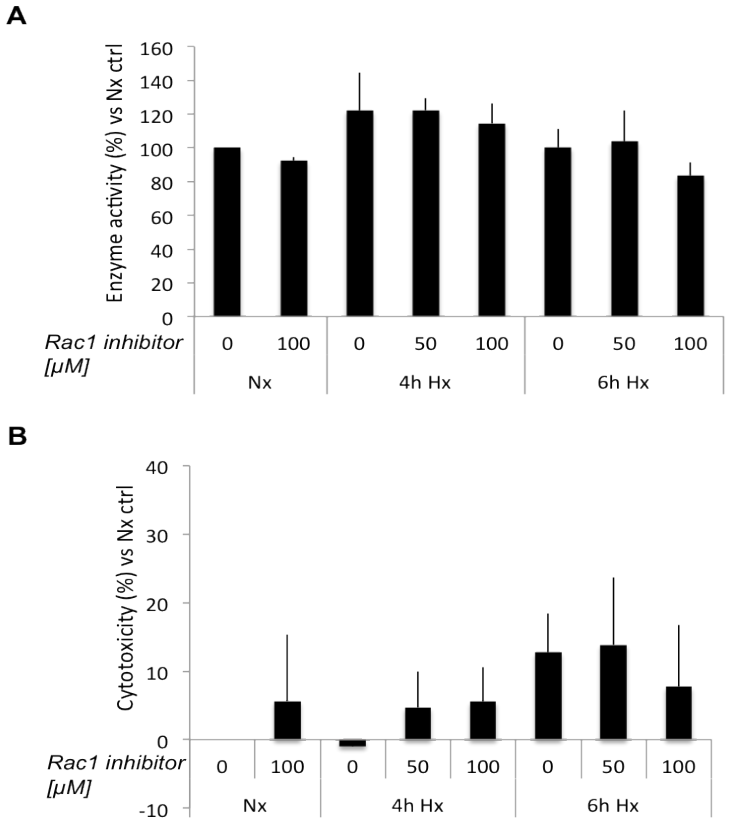

Figure 10: Neurons survive acute hypoxia in absence of Rac1 and HIF-1α. Cells were treated with Rac1 inhibitor and kept under normoxic (Nx) or hypoxic conditions (Hx). And cell survival determined by two methods. A, MTT assay was used as an indicator for cell survival (N=4). B, LDH release into the culture medium was measured to detect cytotoxicity (N=3). No significant changes were observed.

Active GSK3 is critical for hypoxic HIF-1α accumulation in neurons

We prevented GSK3 activation by LiCl treatment of young neurons to verify our hypothesis that Rac1-dependent HIF-1α induction involves activation of GSK3. Western blot analysis demonstrated that HIF-1α accumulation in hypoxic cells was reduced in cells treated with 25 mM LiCl and completely blocked by higher concentrations of LiCl (Fig. 11A). Immunohistochemical analysis comfirmed LiCl-dependent interference with hypoxic HIF-1α stabilization (Fig. 11B). Our results identify GSK3 as an inducer of hypoxic HIF-1α accumulation in young neurons.

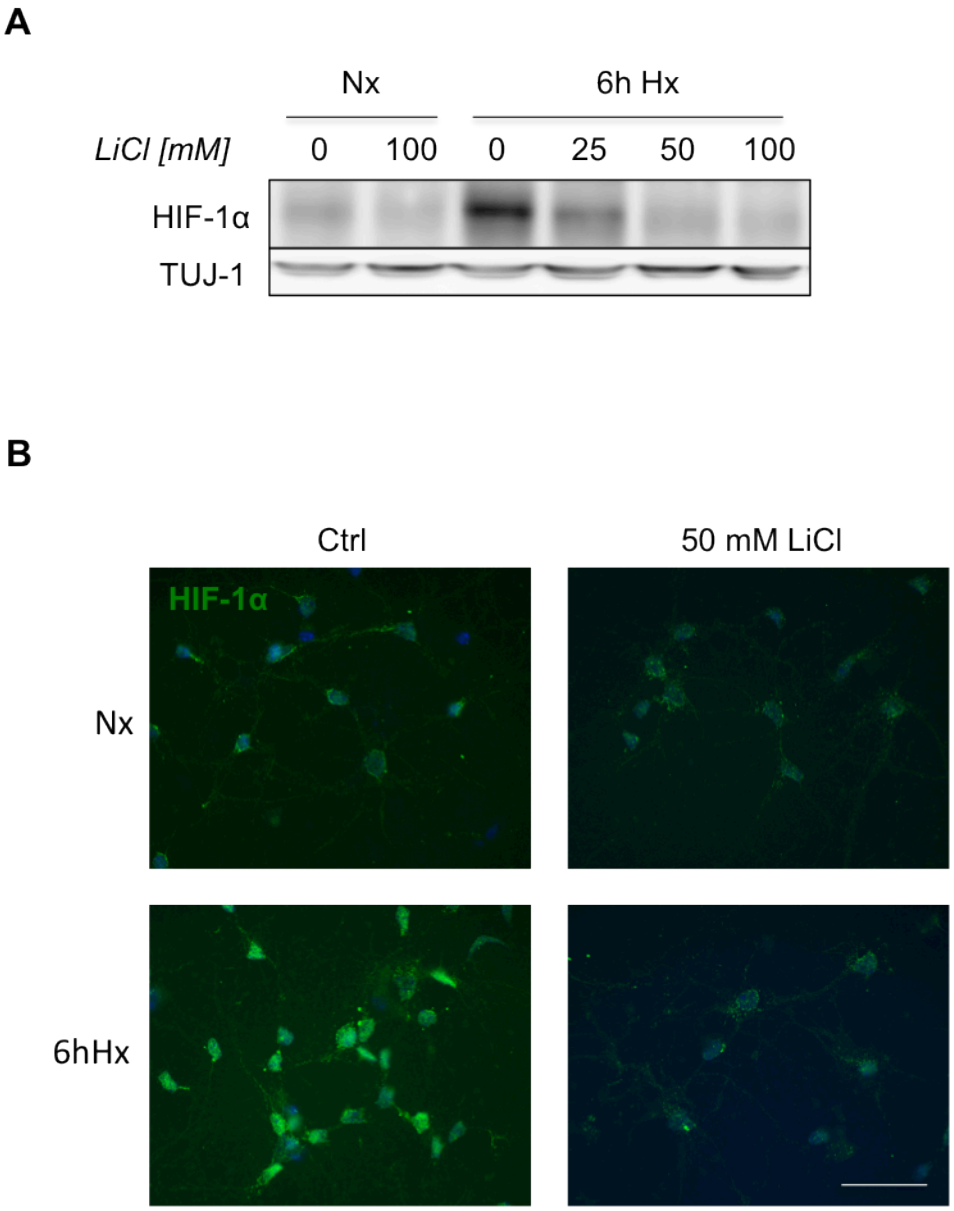

Figure 11: Active GSK3 is critical for hypoxic HIF-1a accumulation in neurons. A, Activation of GSK3 was prevented by exposure of neurons to 25 mM, 50 mM and 100 mM LiCl prior to hypoxia (Hx) and normoxia (Nx). HIF-1α induction was compared to untreated samples by Western blot and TUJ-1 was used as loading control (N=3). B, Immunocytochemistry identified localization of HIF-1α in normoxia and hypoxia in the presence or absence of 50 mM LiCl (N=1). Green: HIF-1α, blue: DAPI, Scale bar: 50 µM.

3.1.2 Rac1 and the response of mature neurons to prolonged hypoxia

Our manuscript describes that neither acute hypoxia alone nor Rac1 or GSK3 inhibition induced cell death in mature neurons. However since a number of studies have shown conclusively that prolonged hypoxia induces cell death [63,180], we assessed the sensitivity of mature neurons to prolonged hypoxia. Furthermore we determined the effect of continuous inhibition of Rac1 and GSK3 on survival.

Rac1 and active GSK3 induce HIF-1α accumulation in mature neurons during prolonged hypoxia

First we disclosed whether Rac1 is needed for HIF-1 induction during prolonged hypoxia. Western blot studies demonstrated that pharmacological blockade of Rac1 in 17 DIV neurons prior to 24h hypoxic exposure totally abrogated in inhibitor-treated neurons (Fig. 12A). Similar results were obtained when neurons were pretreated with 5 mM and 10 mM of LiCl or 5 μM and 10 μM SB216763 (SB), a specific inhibitor of GSK3, and HIF-1α levels after 24h were monitored by Western blot (Fig. 12B). Similar to the acute response (see manuscript, Fig. 5B) 5 mM LiCl was not enough but 10 mM of LiCl, and 10 μM SB treatment, interfered with hypoxic HIF-1α stabilization. These preliminary data suggest that Rac1 and GSK3 seem to be potent mediators of neuronal HIF-1α stabilization even during prolonged hypoxia.

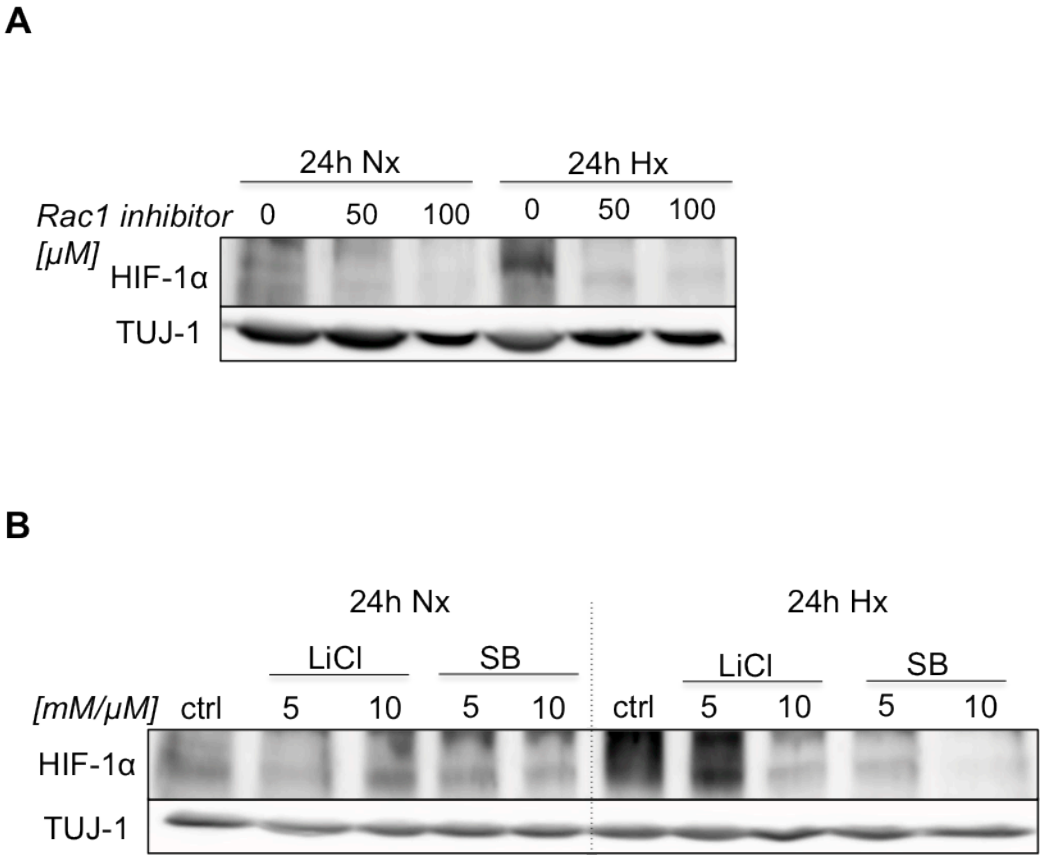

Figure 12: Rac1 and active GSK3 induce HIF-1α accumulation in mature neurons during prolonged hypoxia. A, Western blot analysis of HIF-1α protein levels after 24h oxygen deprivation (Hx) or normoxia (Nx) in 17 DIV in the presence or absence of Rac1 (N=2). B, Western blot showing HIF-1α induction of cells treated with LiCl [mM] and SB216763 (SB, μM) to inhibit GSK3 during 24h of Nx and Hx. TUJ-1 was used as loading control (N=1).

Contribution of Rac1 and active GSK3 to neuronal survival during prolonged hypoxia

To evaluate the tolerance of mature neurons to prolonged hypoxic exposure and to Rac1-inhibiton-mediated HIF-1α blockade we performed MTT assay (Fig. 13A). Contrary to acute hypoxia prolonged oxygen deprivation reduced cell survival approximately 50% compared to normoxia (53.2 ± 14.9, $p<0.0001$). Additional inhibition of Rac1 for 24h had a further negative effect on cell survival. Normoxic Rac1 inhibition reduced cell survival compared to the untreated control by 40 % (59.3 ± 19.1, $p<0.001$) and hypoxic Rac1 blockade further amplified hypoxia-induced cell death (19.6 ± 6.3, $p<0.01$ versus 24h Hx). Notably consequences of Rac1 inhibition were dose-dependent

To assess the effect of GSK3 inhibition on cell survival neurons were treated with 10 mM LiCl or 10 μM SB and MTT assay was performed (Fig. 13B). Again, 24h of hypoxia reduces neuronal survival. However both GSK3 inhibitors had the tendency to reduce hypoxia-induced cell death as well as improve survival in normoxic conditions although these changes did not reach significance. Thus prolonged inhibition of Rac1 and GSK3 both abrogated hypoxic HIF-1α induction but had a different outcome with regard to cell survival.

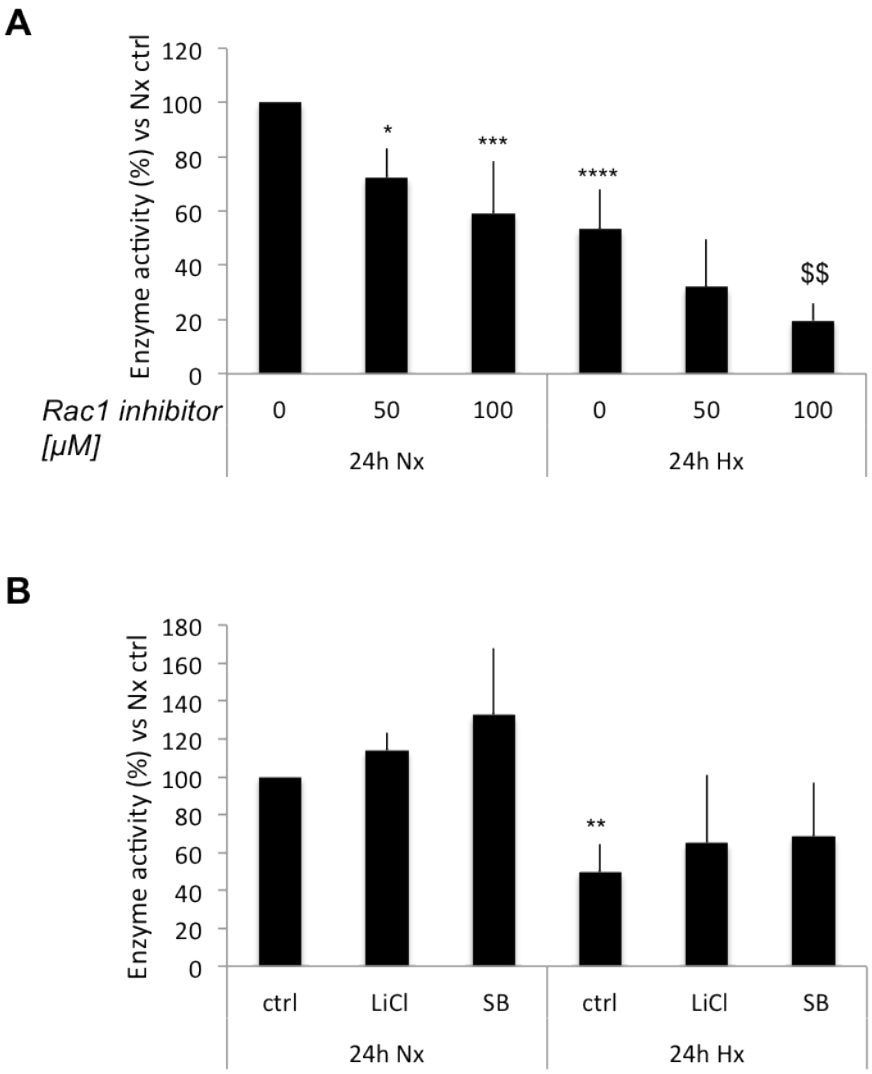

Figure 13: Impact of prolonged hypoxia and inhibition of Rac1 and GSK3 on neuronal survival. A, MTT assay of 17 DIV neurons treated with 50 or 100 μM Rac1 inhibitor just prior to 24h of normoxic (Nx) or hypoxic (Hx) exposure (N=5). * $p<0.05$, *** $p< 0.001$, **** $p<0.0001$ versus Nx ctrl, $$ $p<0.01$ versus 24h Hx. B, MTT assay was used to assess neuronal survival after 24h of hypoxia in the presence or absence of GSK3 inhibitors (each 10 μM), (N=4). Normoxic untreated cells were set to 100%. ** $p<0.01$ versus Nx ctrl. Data analysis was performed using two-way ANOVA followed by Bonferroni post-hoc test.

3.2 Deoxysphingolipid-induced neurotoxicity

We have described the effect of 1-deoxysphinganine (1-deoxySA) treatment on the cytoskeleton, cytoskeleton regulators and on survival of mature (17 DIV) neurons in our manuscript (chapter 7.2). Since neurodegeneration correlates with aging [181,182], we further hypothesized that young (6 DIV) neurons would be less susceptible to 1-deoxySA. Thus we assessed how 1-deoxySA treatment affects cell survival and cytoskeletal organization in immature neurons. Furthermore we addressed the modulation of Rac1, JNK and p35 levels in young neurons since their deregulation seem to participate in mediation of 1-deoxySA-induced neurotoxic effects in mature cells.

1-deoxySA induces cell death in young neurons

6 DIV neurons were treated with 0.5 µM and 2 µM of 1-deoxySA, C18SA or C18SO or with BSA for 24 hours to assess the effect of lipid treatment on neuronal survival using MTT (Fig. 14A) and LDH (Fig. 14B). MTT data of 6 DIV neurons show that both 0.5 µM and 2 µM of 1-deoxySA induced significant cell death compared to controls (48.8 ± 11.6, $p<0.01$ and 38.2 ± 5.5, $p<0.001$, respectively). A similar trend, although not as dramatic, was observed by LDH assay. 1-deoxySA induced cell death in young neurons in a concentration dependent manner (8.1 ± 2.8, $p<0.05$ and 14.5 ± 4.5, $p<0.0001$). In both MTT and LDH assay neither C18SO and C18SA had a negative effect on cell survival.

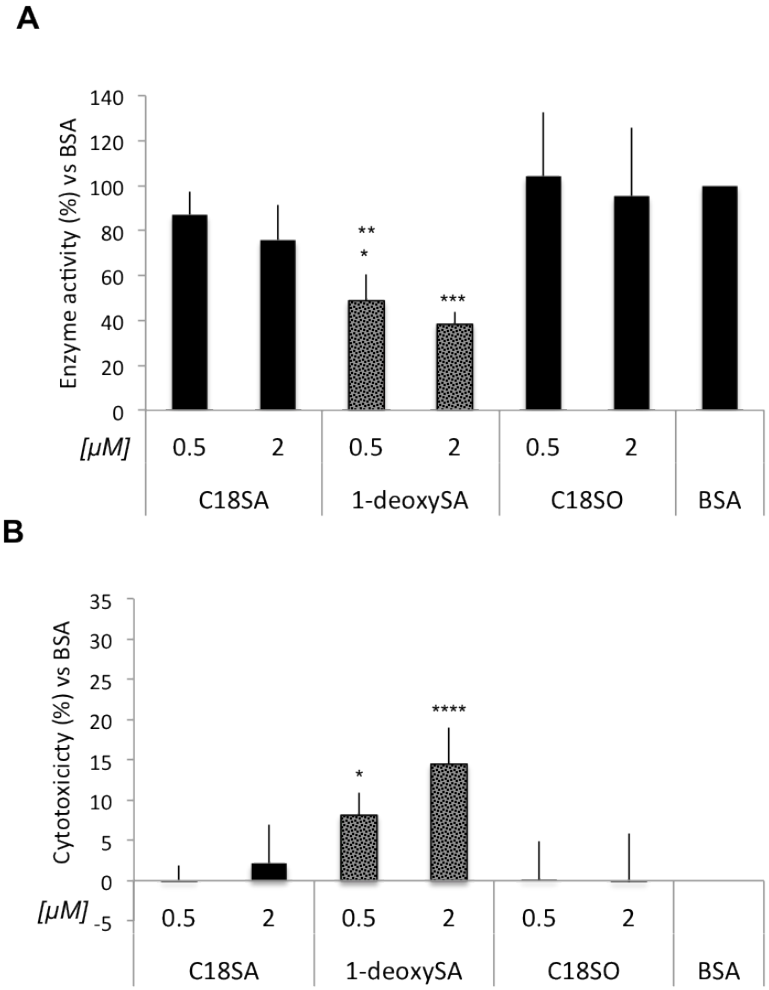

Figure 14: 1-deoxySA induces cell death in young neurons. 1-deoxySA, C18SA or C18SO or BSA control and cell death was assessed by MTT (BSA=100%) and LDH (BSA=0%) assays. A, MTT assay was used to detect enzymatic activity in 6 DIV neurons (N=4). * $p<0.05$ versus 0.5 SA, ** $p<0.01$ versus C18SO and BSA, *** $p<0.001$ versus 0.5 µM C18SA, C18SO and BSA. B, LDH showing lipid-induced cell death in 6 young neurons (N=5). * $p<0.05$, **** $p<0.0001$ both versus C18SA, C18SO and BSA. Data were analyzed using two-way ANOVA followed by Bonferroni post-hoc test.

Exposure to 1-deoxySA leads to cytoskeletal disruption in young neurons

1-deoxySA induced alterations in neurofilament structure and loss of neurites in 17 DIV neurons we assessed its effect on the cytoskeleton of young neurons cells by immunocytochemistry (Fig. 15). Although 1-deoxySA did not alter neurofilament heavy (NF-H) staining both 0.5 µM and 2 µM 1-deoxySA strongly reduced staining for neurofilament light (NF-L) compared to controls. Visualization of filamentous actin (F-actin) using phalloidin underlining the 1-deoxySA-induced alterations compared to other lipid treatments wherein neurites looked less distinct and the staining became punctuated. Thus 1-deoxySA also causes cytoskeleton rearrangement in young neurons. However effects were less pronounced than in mature neurons.

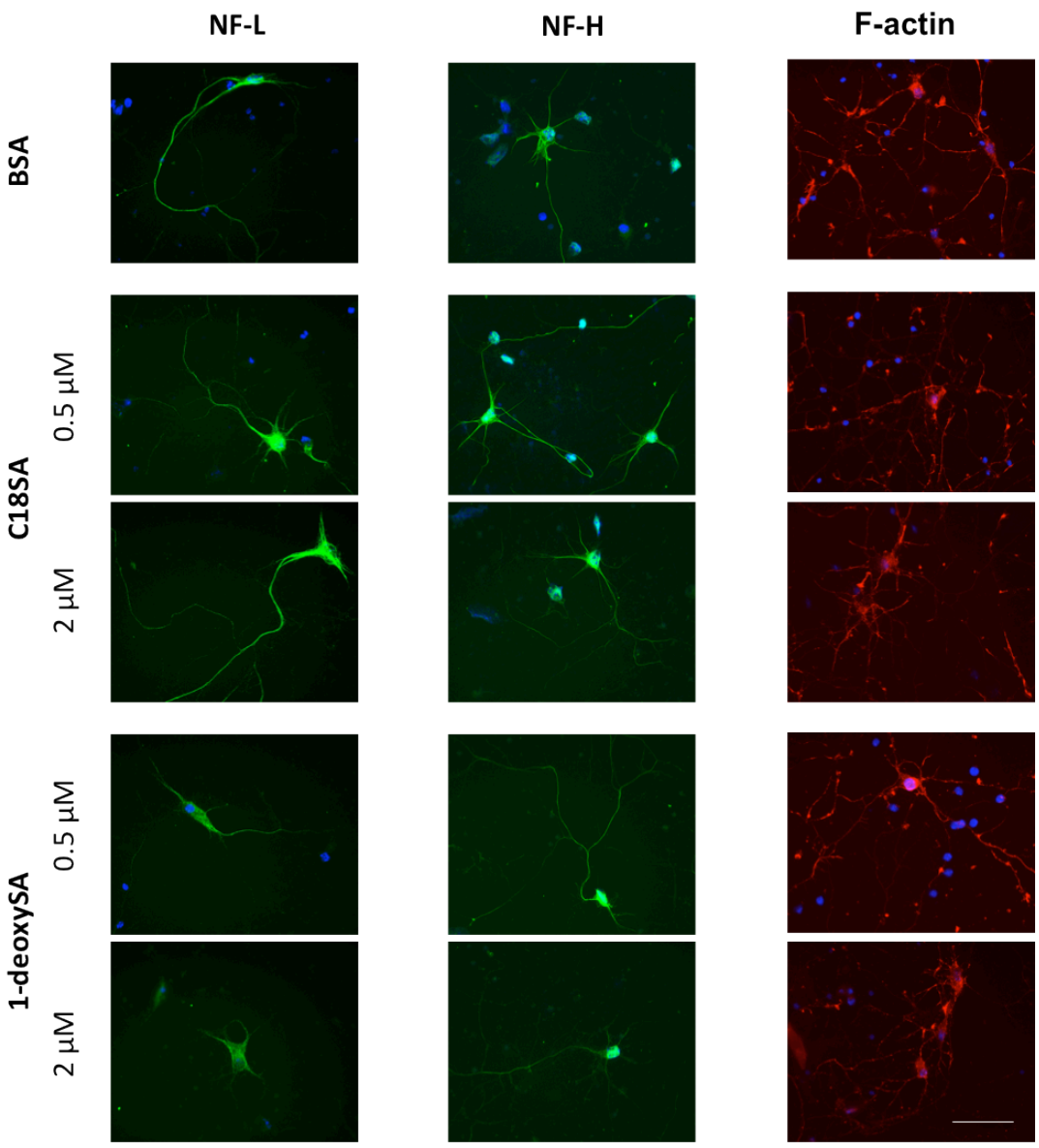

Figure 15: 1-deoxySA causes cytoskeleton disruption in young neurons. 6 DIV neurons were treated with 0.5 and 2 µM C18SA or 1-deoxySA or with the BSA control for 24h prior to immunocytochemistry. Anti neurofilament light (NF-L) and anti heavy (NF-H) chain antibodies were used to observe neurites and phalloidin staining was used to visualize filamentous actin (F-actin) Nuclei were counterstained with DAPI (blue). Scale bar: 50 µM. N=3.

Involvement of Rac1 in 1-deoxySA-mediated death of young neurons

We suggested that Rac1 deregulation was associated with the observed cytoskeleton alterations similar to our data on 17 DIV cells. Thus after 24h-treatment with lipids or BSA as control 6 DIV lysates were profiled using G-LISA assay. 2 μM 1-deoxySA reduced Rac1 activity within the cells (69.5 ± 11.8, $p<0.01$ versus all other treatments) (Fig. 16A), although total Rac1 proteins remained stable in all treatments as shown by Western blot (Fig. 16B). To answer whether deregulated Rac1 and RhoA contributed to 1-deoxySA-induced neurotoxicity cells were pre-incubated with specific inhibitors prior to lipid exposure and cell survival was determined using MTT (Fig. 16C). Similar to our 17 DIV data 24h-treatment with Rho inhibitor did not affect survival but inhibition of Rac1 reduced cell survival approximately 50 % in both BSA control and in C18SA samples (52.2 ± 16.9 and 48.8 ± 17.0, respectively, both $p<0.001$) and further enhanced cell death in 1-deoxySA-treated neurons (27.0 ± 13.7). Thus 2 μM 1-deoxySA-induced Rac1 inhibition might be mechanism contributing to impaired neuronal survival.

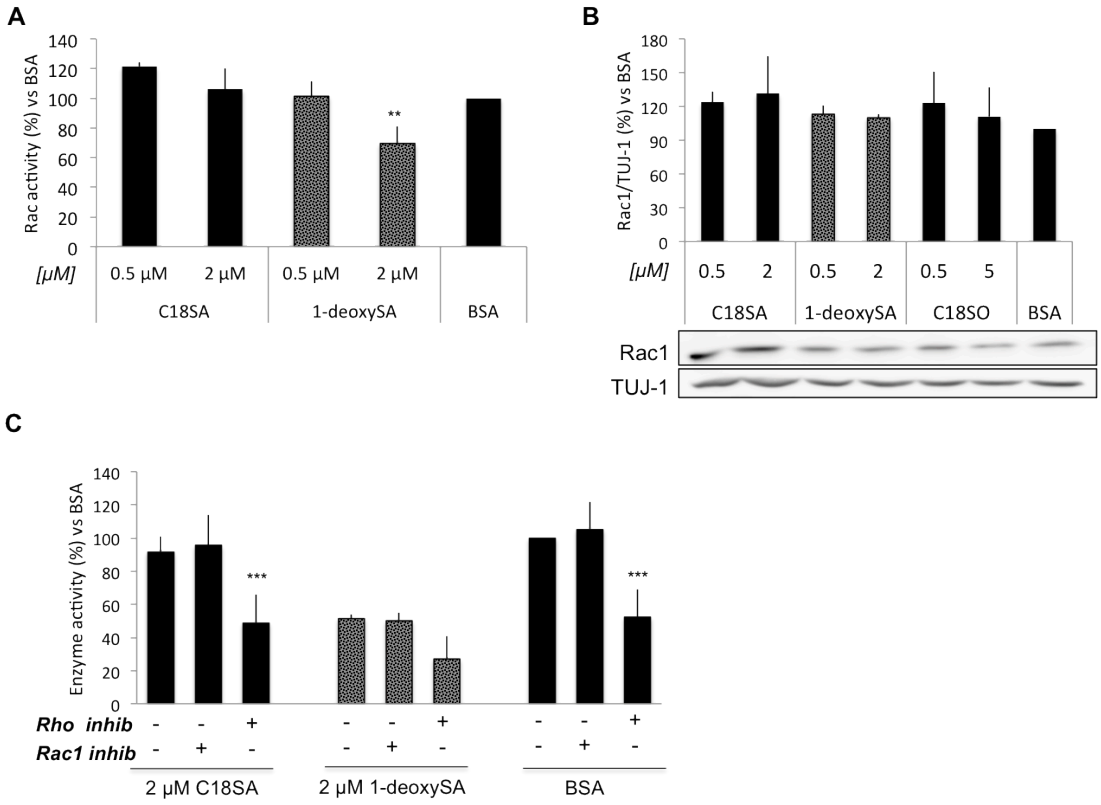

Figure 16: Involvement of Rac1 in 1-deoxySA-mediated death of young neurons.
6 DIV neurons were incubated for 24h with 0.5 µM and 2 µM 1-deoxSA or C18SA or with BSA as a control. A, Rac1 activity was determined using G-LISA (N=3). ** $p<0.01$ versus all other treatments. B, Western blot show total Rac1 levels (N=4). C, MTT was used to determine the effect of Rho GTPase inhibition on cell survival (N=3). Cells were pre-incubated with 100 µM Rac1 inhibitor (Rac1 inhib) or Rho inhibitor (Rho inhib) for 30 min before treatment with 2 µM 1-deoxySA or C18SA or with BSA as control for 24h. Ctrl samples were treated with the lipids only. *** $p<0.001$ versus control and Rho inhib within the group. Data were analyzed using two-way ANOVA followed by Bonferroni post-hoc test.

1-deoxySA deregulates JNK activity and p35 levels in young neurons

We performed Western blot to establish whether reduced JNK activity and p35 levels effects can be observed in 1-deoxySA treated young neurons (Fig. 17). Indeed 2 μM 1-deoxySA tended to reduce phospho-JNK levels in comparison to other lipid treatments (76.4 ± 15.9) while total levels remained stable. However changes did not reach significance (Fig. 17A). Western blot for p35 shows that 2 μM of 1-deoxySA suppressed p35 levels (68.5 ± 19.4) but again the reduction was not significant (Fig. 17B).

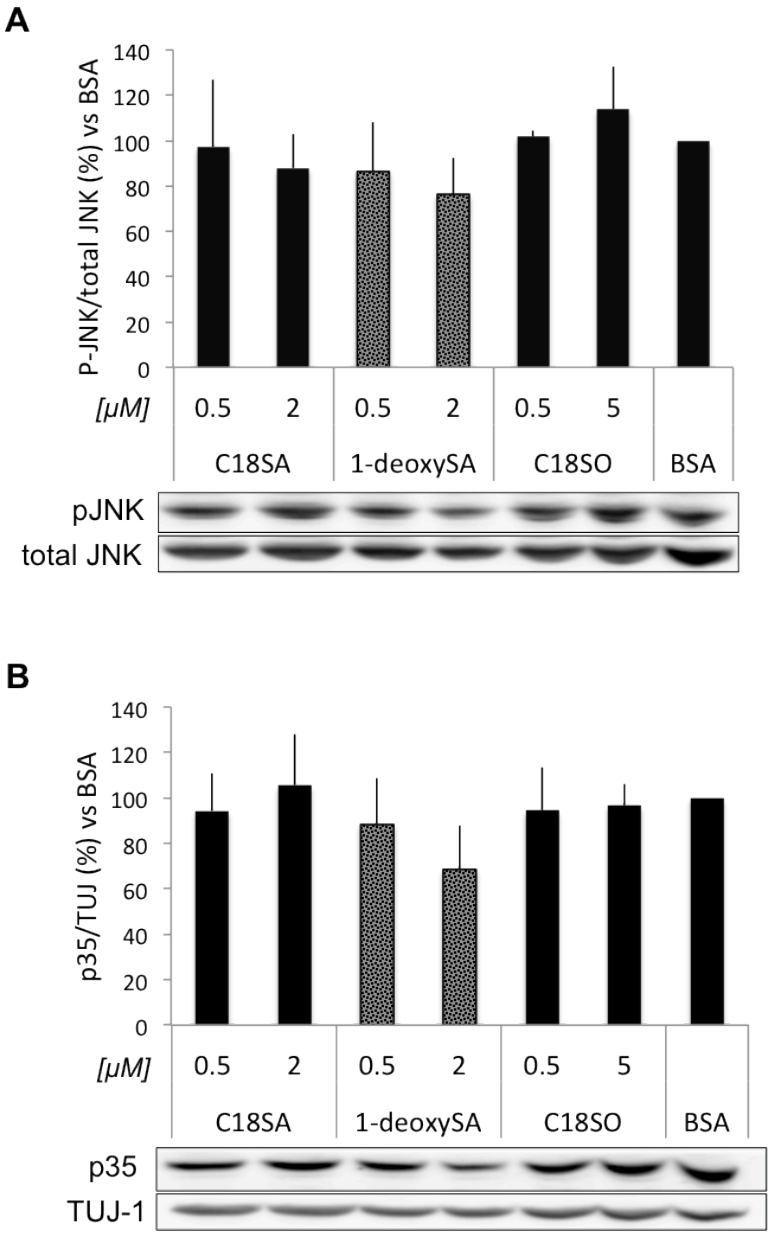

Figure 17: 1-deoxySA deregulates JNK activity and p35 levels. After treatment of 6 DIV neurons with 0.5 µM and 2 µM 1-deoxySA, C18SA or C18SO or with BSA as a control for 24h Western blot was performed to detect JNK phosphorylation status (A) and protein levels of p35 (B), (both N=3). A, Results are expressed as the ratio of phosphorylated (pJNK) and total protein and were compared to BSA. B, Graph shows Western blot analysis of p35 levels normalized to TUJ-1. Data were analyzed using two-way ANOVA followed by Bonferroni post-hoc test.

4. Discussion

4.1 Role of Rac1 in the neuronal response to hypoxia

Rho GTPases are molecular switches that are known to be involved in a wide range of processes from mediating cell survival to transferring stress response. In particular Rac1 has been demonstrated in some cells to contribute to hypoxic signaling [98,99]. However it remains unclear whether such pathways also underlie neuronal hypoxic adaptation. Notably, diseases like respiratory and cardiovascular disorders can cause periods of continuous or intermittent cerebral hypoxia and disturb neuronal function thus increasing predisposition for neuropathologies and neurodegenerative diseases. Hence it is of special interest to better understand neuronal molecular responses during reduced oxygen concentrations since such knowledge will be beneficial for the development of therapeutic strategies to prevent neuronal loss due to limited oxygen supply.

This project investigated the role of Rac1 in the neuronal hypoxic response and aimed to identify the putative molecular mechanisms through which Rac1 acts. We used both young (6 DIV) and mature (17 DIV) primary cortical mouse neurons exposed to 1% oxygen, since an age-dependent susceptibility was suggested [183–185].

Rac1 and neuronal survival during hypoxia

Surprisingly, both young and mature neurons tolerated acute periods of hypoxia. It has been suggested by various studies that during maturation neurons develop strategies to restrict apoptosis and thereby increase their tolerance to stress.

Cortical and cerebellar neurons decrease Apaf-1 levels [186,187], Bax levels were diminished during maturation in DRG and forebrain neurons [188,189] and cortical neurons and photoreceptors even shut down caspase-3 expression [190,191]. Other studies propose that susceptibility to stress increases with maturation. It is has been reported that younger animals tolerate hypoxic/ischemic conditions better than adults [184,185] and additionally neuronal maturation over days *in vitro* correlates with increased susceptibility to excitotoxic stimuli [192]. Although we could not detect any difference in vulnerability during acute hypoxia survival of mature neurons during prolonged hypoxia was reduced by around 50%. In agreement with this Zhang and colleagues suggested that only severe or prolonged hypoxia induces neuronal death [180]. Further experiments investigating the effect of prolonged hypoxia on young neurons remain to be preformed, however a similar study with cortical neurons demonstrated that 6 DIV neurons tolerate 1% of oxygen up to 24h whereas by that time cell death was already significantly induced in 12 DIV neurons, underlying higher vulnerability of older neurons [193].

Surprisingly, since it is required for HIF-1 stabilization, Rac1 blockade did not impair neuronal survival during acute hypoxia whereas prolonged inhibition had a strong negative effect on neuronal survival in both normoxia and hypoxia. This data agrees with the study of Le and colleagues on cerebellar granule neurons showing that Rac1 inhibition induces the mitochondrial apoptotic cascade [194]. Similarly, decreased Rac1 activity correlated with down-regulation of survival signaling after 24h of global cerebral ischemia *in vivo* [95]. Interestingly, an independent study on endothelial cells by our group showed that both Rac1 activity and HIF-1α levels decrease after 24h (unpublished data). For mature

neurons I demonstrated that prolonged hypoxic HIF-1α accumulation is still dependent on Rac1. Hence sustained hypoxia might similarly suppress Rac1 activity in mature neurons in turn preventing HIF-1α accumulation and impairing neuronal survival due to diminished adaptive HIF-1 signaling. Conclusively, the duration of hypoxic insult is decisive for survival or death of mature neurons. Despite being able to tolerate acute hypoxic stress in the absence of Rac1, during prolonged stress Rac1 seems to be beneficial for neuronal survival.

JNK as a mediator of Rac1-dependent HIF-1α stabilization

As a possible candidate that mediates Rac-1-driven HIF-1α accumulation we nominated JNK since its activity is regulated by Rac1 [195,196] and is involved in hypoxic HIF-1α modulation [197–199]. Furthermore JNK activity was shown to be hypoxia-responsive [200,201]. Accordingly we demonstrate that in mature neurons JNK was activated by hypoxia and its activity was strongly dependent on Rac1. Indeed JNK seems to be an inducer of HIF-1α since direct inhibition led to reduced hypoxic HIF-1α accumulation. Although the involvement of JNK in HIF-1 regulation in immature neurons remains to be determined I hypothesize that a comparable mechanism occurs in young cells. Generally, JNK activity is highly dependent on Rac1 and hypoxic activation of Rac1 in young neurons was even increased compared to mature neurons suggesting a strong activation of JNK and thus contribution to HIF-1α induction. Thus Rac1-dependent promotion of HIF-1 signaling during acute hypoxia may be regulated via JNK activation.

GSK3 as a mediator of Rac1-dependent HIF-1α stabilization and its role for neuronal survival during prolonged hypoxia

As discussed earlier we suggest active GSK3 is another mediator of Rac1-driven HIF-1α induction during acute hypoxia. As for Rac1, we asked whether GSK3 also contributes to HIF-1α accumulation also during prolonged periods of oxygen deprivation. We observed that HIF-1α accumulation was strongly dependent on active GSK3 since its blockade suppressed HIF-1α levels during acute and prolonged hypoxic conditions. Hence GSK3 is likely an important inducer of neuronal HIF-1α stabilization. In contrast, other studies reported that inhibition of GSK3 enhanced hypoxic HIF-1α accumulation [11,57,202]. Those studies suggest that GSK3 phosphorylates HIF-1α thereby targeting it for proteasomal degradation. The mechanism how GSK3 might induce neuronal HIF-1 is unclear at the moment but GSK3 may phosphorylate other residues of HIF-1α that could support protein stability. Regardless whether it would be a direct or indirect interaction we hereby provide strong evidence for a cell-type specific mechanism in neurons wherein active GSK3 is critical for full HIF-1α induction.

Interestingly the suppressive effect of GSK3-blockade on HIF-1α levels was even stronger after 24h of hypoxia than after acute hypoxic exposure. This might be due to an increased activation of GSK3 during prolonged hypoxia hence blockade of GSK3 would consequently have a greater effect on downstream targets such as HIF-1α. Indeed a study by Mottet and collegaues demonstrated that prolonged hypoxia strongly increased GSK3 activity compared to short hypoxic exposure in HepG2 cells [203]. Enhanced GSK3 activity may also contribute to neuronal death after 24h of hypoxia. It has been shown that elevated activation of GSK3 mediates hypoxia-induced apoptosis of vascular smooth muscle cells [204].

Furthermore, lithium chloride treatment reduces autophagy and apoptosis after neonatal hypoxia-ischemia and GSK3 inhibition reduced ischemic cerebral damage [205–207]. In agreement with that data we observed that prolonged exposure to both GSK3 inhibitors were beneficial for survival of mature cell during both hypoxia and normoxia.

Notably, both Rac1 and GSK3 inhibition abrogated HIF-1α accumulation but had different effects on neuronal survival supporting the hypothesis that beside HIF-1α other factors are involved in regulating survival during hypoxia. We propose that during acute hypoxia overactivation of PI3K/AKT resulting from Rac1 inhibition might counterbalance the absence of Rac1 and HIF-1α. During prolonged hypoxic stress the inhibition of GSK3 was beneficial for cell survival although HIF-1α was suppressed. Thus modulation of certain pathways seems to enable compensation of interrupted HIF-1 signaling under particular conditions highlighting that hypoxic neuronal survival does not seem to solely depend on HIF-1α.

Overall Rac1 and active GSK3 are crucial for HIF-1α accumulation independent of the duration of hypoxic exposure. However we suggest that Rac1 and GSK3 might be differently modulated during short and long periods of oxygen deprivation and thus influence neuronal survival in different manners. It would be a very interesting future study to directly compare Rac1 activity, HIF-1α levels and GSK3 activation of young and mature neurons after prolonged hypoxia to determine whether differential modulation is a reason for increased susceptibility of mature neurons to hypoxic insults. Furthermore directly blocking HIF-1α would demonstrate how important HIF-1-signaling really is for

neuronal survival during the different phases of hypoxic adaptation. Although the Rac1-triggered pathways and mechanisms may partly be cell type-specific we suggest a neuronal-specific role for GSK3 in hypoxic HIF-1α accumulation. Moreover acute hypoxia can be tolerated by young and mature neurons independent of HIF-1α, however prolonged hypoxia strongly impairs survival of mature cells. I hypothesize that GSK3 inhibition in combination with enhancement of HIF-1α levels might be beneficial for neuronal survival during sustained hypoxia.

This study presents new insights into neuronal hypoxic responses and identifies candidates involved in neuronal of HIF-1α regulation. We propose simultaneous modulation of HIF-1α levels and Rac-1-dependet downstream pathways that influence survival independent of HIF-1 as possible approach to prevent neuronal loss due to prolonged hypoxic insults.

4.2 Deoxysphingolipid-induced neurotoxicity

Recently it was discovered that the formation of deoxy-long chain bases (deoxyLCBs) including 1-deoxysphinganine (1-deoxySA) is associated with metabolic diseases and neurodegenerative disorders like HSAN1 [168–170]. However the molecular mechanism by which deoxyLCBs mediate neurotoxicity is unknown und thus therapeutic strategies to prevent neuronal loss in deoxyLCB-associated diseases remain to be developed. This study explored the effect of 1-deoxySA-treatment on cultured primary neurons with emphasis on cytoskeleton integrity and neuronal survival and identified pathways that

mediate deoxyLCB-induced neurotoxicity. Our data suggests NMDAR as new therapeutic target to prevent 1-deoxySA induced neurotoxicity.

Effect of 1-deoxySA-treatment on neuronal survival and cytoskeletal integrity

It has been shown that deoxyLCBs cause cell death in various cell types [172–175]. In agreement both young and mature neurons were similarly impaired by low concentrations of 1-deoxySA however increased concentrations of 1-deoxySA reduced survival of mature neurons more than young cells. As suggested for hypoxic responses an increased susceptibility of aged neurons to injury stimuli is apparent. This underlines the usefulness of such models since prevalence of neurodegeneration increases with aging. Further investigations on mature neurons showed that indeed 1-deoxySA gets internalized and metabolized to deoxydihydroceramide. Similar to the study of Zuellig and colleagues on pancreatic cells [175] blockade of ceramide synthase however could rescue neurons from 1-deoxySA-induced death suggesting that deoxydihydroceramide is the causal factor that triggers DSB neurotoxicity. However, ceramide synthesis is essential and Fumonisin B1 is toxic *in vivo* (for review see [208]) and genetic deletion of ceramide synthase has been shown to results in detrimental phenotypes [209–211]. Thus inhibition of ceramide synthase cannot be considered as therapeutic approach to prevent 1-deoxySA induced toxicity.

It has been highlighted that deoxyLCBs induce cytoskeleton rearrangements in sensory neurons and insulin-producing cells [170,175]. Indeed 1-deoxySA induced loss of neurites in mature neurons. Similarly young neurons treated with 1-

deoxySA showed disassembled actin filaments and loss of neurofilament light structures although neurofilament heavy chain components were little affected. Cytoskeleton alterations, especially impaired axonal transport, have been described for diabetic sensory neuropathy (DSN) that is clinically highly similar to hereditary sensory and autonomic neuropathy type I (HSAN1) [212]. Medori and collegaues (1985, 1988) demonstrated impaired of axonal transport of neurofilament, actin and tubulin and described distal axonal atrophy accompanied by substantial loss of neurofilaments in a rat diabetes model [213,214]. In a similar animal model reduced cytoskeleton proteins like synaptophysin and sytaxin were also detected [215]. Hence 1-deoxySA-treatment induces cytoskeleton alterations similar to those described for peripheral neuropathies and confirms the usefulness of our model system.

Role of Rac1 in 1-deoxySA-induced cytoskeletal rearrangements and neuronal death

Rho GTPases are suggested to drive deoxyLCBs-induced cytoskeleton alterations [172,175], and downregulation of Rac1 in neurons correlated with loss of filamentous actin [216]. Furthermore Rac1 inhibition has been demonstrated to induce mitochondrial apoptotic cascade in cerebellar granule neurons [194]. In agreement 1-deoxySA-treated neurons also had significantly attenuated Rac1 activity independent of their age. However as shown by direct Rac1 blockade survival of mature neurons was more impaired than young cells indicating that mature neurons become more sensitive to 1-deoxySA-triggered Rac1 deregulation that occurs prior to death.

Since JNK, a signaling kinase involved in regulating cell death and survival [217–220], is dependent on Rac1 [196,221], we investigated if its modulation by 1-deoxySA was similar to Rac1. JNK activity was indeed abrogated by 1-deoxySA and again the effect was stronger in mature neurons. Furthermore direct inhibition of JNK induced massive cell death suggesting that 1-deoxySA-induced deregulation of JNK may contribute to increased neuronal death in mature neurons. Similarly it has been proposed that activation of JNK improves neuritogenesis and counteracts neurodegeneration in an *in vitro* model of Charcot-Marie-tooth disease [222].

With regard to 1-deoxySA-induced cytoskeletal alterations via Rac1 we discussed in our manuscript that CDK5-dependent phosphorylation of Ezrin may be responsible for 1-deoxySA-induced reduction of Rac1 activity as it is suggested in senescent cells [223]. We further propose that diminished Rac1 activity subsequently disturbs IRSp53/WAVE2 signaling cascade thereby altering actin structures. The effect of 1-deoxySA on Ezrin phosphorylation and IRSp53 levels in young neurons remains to be established however I hypothesize that the impact might be stronger in mature neurons thus contributing to more severe cytoskeletal alterations.

Taken together, 1-deoxySA-triggered deregulation of Rac1 activity may not only induce loss of neurites but also contribute to the increased susceptibility of mature neurons via its downstream target JNK.

Involvement of NMDAR signaling in 1-deoxySA-triggered neuronal death

As discussed in our manuscript we propose that 1-deoxySA mediates death of mature neurons by activation of NMDAR and the subsequent cleavage of p35

since inhibition of NMDAR activation prevented p35 cleavage and partly rescued neurons from 1-deoxySA-induced death. A positive correlation between p35 cleavage and neuronal death has been demonstrated in many neurodegenerative diseases [224,225] and we show that p35 is much more cleaved in mature neurons than in young neurons. Thus we hypothesize that 1-deoxySA-induced NMDAR activation is higher in mature neurons. Notably the NMDAR is heterotetramer [226,227] and the composition and the distribution changes during neuronal development [228–230]. Indeed, surface-expression of both AMPA and NMDA receptors was increased in 10 DIV hippocampal neurons compared to 3 DIV [230]. Thus different receptor composition and surface expression levels might explain the variation of 1-deoxySA-induced neurotoxicity between young and mature neurons. Notably, both NMDA and AMPA receptors are also expressed in the peripheral nervous system [231,232] further supporting the validity of our model system for peripheral neuropathy.

In summary, this second study demonstrated that 1-deoxySA, more precisely its metabolite deoxydihydroceramide triggers neuronal death in a time and concentration dependent manner with mature neurons more vulnerable than young cells. Significant alterations in cytoskeleton structures and cytoskeleton-associated proteins suggest that 1-deoxySA induced neurotoxicity, either directly or indirectly, via promoting NMDAR activation. The increased sensitivity of mature neurons to Rac1 and JNK deregulation together with possibly distinct NMDAR subunit composition and elevated expression levels likely underlies their greater susceptibility to deoxyLCB-induced neurotoxicity. As a next step we

plan to detect functional NMDAR activation upon 1-deoxySA-treatment via patch-clamp technique.

With this study we set the cornerstone for new therapeutic approaches to prevent or treat deoxyLCB-associated neurodegenerative disease since we demonstrate for the first time some of the molecular mechanisms involved in 1-deoxySA-induced neurotoxicity. Inhibition of glutamate receptors might represent a strategy to counteract neuronal loss due to deoxyLCB formation.

4.3 Limitations of the studies

Role of Rac1 in the neuronal response to hypoxia

The current project is an *in vitro* study that uses pharmacological inhibition to define the importance of Rac1 in neuronal hypoxic signaling. Using this approach we demonstrate that in neurons Rac1 is crucial for HIF-1α stabilization and subsequent HIF-1 target gene induction. In contrast to prolonged hypoxia during acute hypoxia Rac1 does not seem to have a critical role for neuronal survival. However this project is not fully conclusive since it leans on a pharmacological inhibitor thus a genetic knockdown of Rac1 would be a final proof of the current results. In addition the *in vivo* effects of a neuron-specific knockout of Rac1 on stabilization of HIF-1α and on neuronal survival during hypoxia remain to be investigated. Furthermore we assume a cell-type specific regulation of HIF-1α by GSK3 during hypoxia. However studies that demonstrate GSK3-dependent phosphorylation and subsequent degradation of HIF-1α have been performed

with human cell lines while our study uses murine cells. Thus a species-specific regulation could be the explanation for the differential effects. Sequence comparison of HIF-1α would demonstrate if GSK3-phosphorylated residues within the human protein might be absent in the murine variant.

Conclusively, understanding the role of Rac1 for HIF-1α stabilization and for neuronal survival during hypoxia might be clinically very important to develop strategies to rescue damaged neurons after injury. Thus regardless of the current limitations of this study the data herein still provides a significant advantage to current knowledge.

Deoxysphingolipid-induced neurotoxicity

This study shows that the atypical sphingoid base 1-deoxysphinganine is neurotoxic and induces cytoskeletal alterations that are associated with Rac1 deregulation and suggests that inhibition of the NMDA receptor could significantly prevent neuronal death due to 1-deoxySA exposure. . Clearly some questions remain to be answered, for example whether NMDAR blockade will protect the cytoskeleton from 1-deoxySA-triggered disruptions. The current study also does not answer the question if 1-deoxySA interacts with the NMDA receptor directly or indirectly. Software-based structural analysis could give an indication whether a direct binding is possible. Preliminary patch-clamp data demonstrate that indeed 1-deoxySA induces activation of the NMDAR. Overexpression of different NMDAR subunits in HeLa or HEK-293 cells (neither express the receptor endogenously) and subsequent patch-clamp analysis could demonstrate whether 1-deoxySA-induced activation of the receptor depends on a special subunit or subunit composition. Particularly it would be very

interesting to assess whether NMDAR antagonist treatment could prevent onset or progression of neuropathy in a HSAN1 mouse model.

However the current study represents the first step towards the development of therapeutic strategies to prevent neuropathology due to deoxyLCB accumulation.

5. References

1. Sharp, F. R. & Bernaudin, M. HIF1 and oxygen sensing in the brain. *Nat. Rev. Neurosci.* **5,** 437–48 (2004).

2. Wang, G. L., Jiang, B. H., Rue, E. a & Semenza, G. L. Hypoxia-inducible factor 1 is a basic-helix-loop-helix-PAS heterodimer regulated by cellular O2 tension. *Proc. Natl. Acad. Sci. U. S. A.* **92,** 5510–4 (1995).

3. Wang, G. & Semenza, G. Purification and characterization of hypoxia-inducible factor 1. *J. Biol. Chem.* **270,** 1230–1237 (1995).

4. Jiang, B. *et al.* Dimerization , DNA Binding , and Transactivation Properties of Dimerization , DNA Binding , and Transactivation Properties of Hypoxia-inducible Factor 1. *J. Biol. Chem.* **271,** 17771–17778 (1996).

5. Epstein, a C. *et al.* C. elegans EGL-9 and mammalian homologs define a family of dioxygenases that regulate HIF by prolyl hydroxylation. *Cell* **107,** 43–54 (2001).

6. Appelhoff, R. J. *et al.* Differential function of the prolyl hydroxylases PHD1, PHD2, and PHD3 in the regulation of hypoxia-inducible factor. *J. Biol. Chem.* **279,** 38458–65 (2004).

7. Siddiq, A., Aminova, L. & Ratan, R. R. Prolyl 4-hydroxylase activity-responsive transcription factors: from hydroxylation to gene expression and neuroprotection. *Front. Biosci.* **13,** 2875–2887 (2008).

8. Cockman, M. E. *et al.* Hypoxia inducible factor-alpha binding and ubiquitylation by the von Hippel-Lindau tumor suppressor protein. *J. Biol. Chem.* **175,** 25733–25741 (2000).

9. Hon, W.-C. *et al.* Structural basis for the recognition of hydroxyproline in HIF-1 alpha by pVHL. *Nature* **417,** 975–8 (2002).

10. Jaakkola, P. *et al.* Targeting of HIF-alpha to the von Hippel-Lindau ubiquitylation complex by O2-regulated prolyl hydroxylation. *Science* **292,** 468–72 (2001).

11. Flügel, D., Görlach, A., Michiels, C. & Kietzmann, T. Glycogen synthase kinase 3 phosphorylates hypoxia-inducible factor 1alpha and mediates its destabilization in a VHL-independent manner. *Mol. Cell. Biol.* **27,** 3253–65 (2007).

12. Kallio, P. J. *et al.* Signal transduction in hypoxic cells : inducible nuclear translocation and recruitment of the CBP / p300 coactivator by the hypoxia-inducible factor-1 α. *EMBO* **17,** 6573–6586 (1998).

13. Wang, F., Zhang, R., Wu, X. & Hankinson, O. Roles of coactivators in hypoxic induction of the erythropoietin gene. *PLoS One* **5,** e10002 (2010).

14. Lando, D. *et al.* FIH-1 is an asparaginyl hydroxylase enzyme that regulates the transcriptional activity of hypoxia-inducible factor. *Genes Dev.* **16,** 1466–1471 (2002).

15. Mahon, P. C., Hirota, K. & Semenza, G. L. FIH-1 : a novel protein that interacts with HIF-1 alpha and VHL to mediate repression of HIF-1 transcriptional activity. *Genes Dev.* **15,** 2675–2686 (2001).

16. Kim, S. Y., Lee, M. J., Na, Y.-R., Kim, S. Y. & Yang, E. G. Visualization of hypoxia-inducible factor 1α-p300 interactions in live cells by fluorescence resonance energy transfer. *J. Cell. Biochem.* **115,** 271–80 (2014).

17. Lando, D., Gorman, J. J., Whitelaw, M. L. & Peet, D. J. Oxygen-dependent regulation of hypoxia-inducible factors by prolyl and asparaginyl hydroxylation. *Eur. J. Biochem.* **270,** 781–790 (2003).

18. Østergaard, L. & Gassmann, M. Hypoxia Inducible Factor and Hypoxia-mediated Pulmonary Hypertension. *PVRI Rev.* **3,** 5 (2011).

19. Luo, W. *et al.* Hsp70 and CHIP selectively mediate ubiquitination and degradation of hypoxia-inducible factor (HIF)-1alpha but Not HIF-2alpha. *J. Biol. Chem.* **285,** 3651–63 (2010).

20. Minet, E. *et al.* Hypoxia-induced activation of HIF-1: role of HIF-1alpha-Hsp90 interaction. *FEBS Lett.* **460,** 251–6 (1999).

21. Isaacs, J. S. *et al.* Hsp90 regulates a von Hippel Lindau-independent hypoxia-inducible factor-1 alpha-degradative pathway. *J. Biol. Chem.* **277,** 29936–44 (2002).

22. Gogate, S., Fujita, N., Skubutyte, R., Shapiro, I. & Risbud, M. Tonicity enhancer binding protein (TonEBP) and hypoxia-inducible factor (HIF) coordinate heat shock protein 70 (Hsp70) expression in hypoxic nucleus pulposus cells: role of Hsp70 in HIF-1α degradation. *J. Bone Miner. Res.* **27,** 1106–1117 (2012).

23. Blagosklonny, M. V. Do VHL and HIF-1 mirror p53 and Mdm-2? Degradation-transactivation loops of oncoproteins and tumor suppressors. *Oncogene* **20,** 395–8 (2001).

24. Semenza, G. *et al.* Structural and functional analysis of hypoxia-inducible factor-1. *Kidney Int.* **51,** 553–5 (1997).

25. Brahimi-Horn, C., Mazure, N. & Pouysségur, J. Signalling via the hypoxia-inducible factor-1alpha requires multiple posttranslational modifications. *Cell. Signal.* **17,** 1–9 (2005).

26. Jeong, J.-W. *et al.* Regulation and Destabilization of HIF-1α by ARD1-Mediated Acetylation. *Cell* **111,** 709–720 (2002).

27. Sodhi, A., Montaner, S., Patel, V. & Factor, H. The Kaposi ' s Sarcoma-associated Herpes Virus G Protein-coupled Receptor Up-Regulates Vascular Endothelial Growth Factor Expression and Secretion through Mitogen-activated Protein Kinase and p38 Pathways Acting on Hypoxia-inducible Factor 1 α The Kaposi. *Cancer Res.* **60,** 4873–4880 (2000).

28. Richard, D. E. p42/p44 Mitogen-activated Protein Kinases Phosphorylate Hypoxia-inducible Factor 1alpha (HIF-1alpha) and Enhance the Transcriptional Activity of HIF-1. *J. Biol. Chem.* **274,** 32631–32637 (1999).

29. Toffoli, S., Feron, O., Raes, M. & Michiels, C. Intermittent hypoxia changes HIF-1alpha phosphorylation pattern in endothelial cells: unravelling of a new PKA-dependent regulation of HIF-1alpha. *Biochim. Biophys. Acta* **1773,** 1558–71 (2007).

30. Yasinska, I. M. & Sumbayev, V. V. S-nitrosation of Cys-800 of HIF-1α protein activates its interaction with p300 and stimulates its transcriptional activity. *FEBS Lett.* **549,** 105–109 (2003).

31. Ema, M. *et al.* A novel bHLH-PAS factor with close sequence similarity to hypoxia-inducible factor 1alpha regulates the VEGF expression and is potentially involved in lung and vascular development. *Proc. Natl. Acad. Sci. U. S. A.* **94,** 4273–8 (1997).

32. Tian, H., McKnight, S. L. & Russell, D. W. Endothelial PAS domain protein 1 (EPAS1), a transcription factor selectively expressed in endothelial cells. *Genes Dev.* **11,** 72–82 (1997).

33. Wiesener, M. *et al.* Widespread hypoxia-inducible expression of HIF-2alpha in distinct cell populations of different organs. *FASEB J.* **17,** 271–273 (2002).

34. Prabhakar, N. R., Kumar, G. K. & Nanduri, J. Intermittent hypoxia-mediated plasticity of acute O2 sensing requires altered red-ox regulation by HIF-1 and HIF-2. *Ann. N. Y. Acad. Sci.* **1177,** 162–8 (2009).

35. Bacon, A. L. & Harris, A. L. Hypoxia-inducible factors and hypoxic cell death in tumour physiology. *Ann. Med.* **36,** 530–9 (2004).

36. Hu, C., Wang, L., Chodosh, L. A., Keith, B. & Simon, M. C. Differential Roles of Hypoxia-Inducible Factor 1 alpha (HIF-1 alpha) and HIF-2 alpha in Hypoxic Gene Regulation. *Mol Cell Biol* **23,** 9361–9374 (2003).

37. Makino, Y. *et al.* Transcriptional up-regulation of inhibitory PAS domain protein gene expression by hypoxia-inducible factor 1 (HIF-1): a negative feedback regulatory circuit in HIF-1-mediated signaling in hypoxic cells. *J. Biol. Chem.* **282,** 14073–82 (2007).

38. Tanaka, T., Wiesener, M., Bernhardt, W., Eckardt, K.-U. & Warnecke, C. The human HIF (hypoxia-inducible factor)-3alpha gene is a HIF-1 target gene and may modulate hypoxic gene induction. *Biochem. J.* **424,** 143–51 (2009).

39. Makino, Y. *et al.* Inhibitory PAS domain protein is a negative regulator of hypoxia-inducible gene expression. *Nature* **414,** 550–4 (2001).

40. Makino, Y., Kanopka, A., Wilson, W. J., Tanaka, H. & Poellinger, L. Inhibitory PAS domain protein (IPAS) is a hypoxia-inducible splicing variant of the hypoxia-inducible factor-3alpha locus. *J. Biol. Chem.* **277,** 32405–8 (2002).

41. Kotch, L. E., Iyer, N. V, Laughner, E. & Sem, G. L. Defective Vascularization of HIF-1 alpha-Null Embryos Is Not Associated with VEGF Deficiency but with Mesenchymal Cell Death. *Dev. Biol.* **267,** 254–267 (1999).

42. Iyer, N. V *et al.* Cellular and developmental control of O2 homeostasis by hypoxia-inducible factor 1 alpha. *Genes Dev.* **12,** 149–62 (1998).

43. Tomita, S. *et al.* Defective Brain Development in Mice Lacking the Hif-1 alpha Gene in Neural Cells. **23,** 6739–6749 (2003).

44. Taylor, C. T. Mitochondria and cellular oxygen sensing in the HIF pathway. *Biochem. J.* **409,** 19–26 (2008).

45. Semenza, G. L. Regulation of metabolism by hypoxia-inducible factor 1. *Cold Spring Harb. Symp. Quant. Biol.* **76,** 347–53 (2011).

46. Semenza, G. L. Targeting HIF-1 for cancer therapy. *Nat. Rev. Cancer* **3,** 721–32 (2003).

47. Lambert, C. M., Roy, M., Robitaille, G. a, Richard, D. E. & Bonnet, S. HIF-1 inhibition decreases systemic vascular remodelling diseases by promoting apoptosis through a hexokinase 2-dependent mechanism. *Cardiovasc. Res.* **88,** 196–204 (2010).

48. Qing, G. *et al.* Combinatorial regulation of neuroblastoma tumor progression by N-Myc and hypoxia inducible factor HIF-1alpha. *Cancer Res.* **70,** 10351–10361 (2010).

49. Maxwell, P. H. & Ratcliffe, P. J. Oxygen sensors and angiogenesis. *Semin. Cell Dev. Biol.* **13,** 29–37 (2002).

50. Garayoa, M. *et al.* Hypoxia-inducible factor-1 (HIF-1) up-regulates adrenomedullin expression in human tumor cell lines during oxygen deprivation: a possible promotion mechanism of carcinogenesis. *Mol. Endocrinol.* **14,** 848–62 (2000).

51. Feldser, D., Agani, F. & Iyer, N. V. Reciprocal Positive Regulation of Hypoxia-inducible Factor 1 α and Insulin-like Growth Factor 2 Growth Factor 2. *Cancer Res.* **59,** 3915–3918 (1999).

52. Ergorul, C. *et al.* NIH Public AccessHypoxia inducible factor-1α (HIF-1α) and some HIF-1 target genes are elevated in experimental glaucoma. *Journel Mol. Neurosci.* **42,** 183–191 (2010).

53. Kim, J.-Y., Ahn, H.-J., Ryu, J.-H., Suk, K. & Park, J.-H. BH3-only protein Noxa is a mediator of hypoxic cell death induced by hypoxia-inducible factor 1alpha. *J. Exp. Med.* **199,** 113–24 (2004).

54. Farrall, a L. & Whitelaw, M. L. The HIF1alpha-inducible pro-cell death gene BNIP3 is a novel target of SIM2s repression through cross-talk on the hypoxia response element. *Oncogene* **28,** 3671–80 (2009).

55. Ding, M., Xu, J. Y. & Fan, Y. Altered expression of mRNA for HIF-1alpha and its target genes RTP801 and VEGF in patients with oral lichen planus. *Oral Dis.* **16,** 299–304 (2010).

56. Halterman, M. & Federoff, H. HIF-1 alpha and p53 Promote Hypoxia-Induced Delayed Neuronal Death in Models of CNS Ischemia. *Exp. Neurol.* **159,** 65–72 (1999).

57. Cassavaugh, J. M. *et al.* Negative regulation of HIF-1α by an FBW7-mediated degradation pathway during hypoxia. *J. Cell. Biochem.* **112,** 3882–90 (2011).

58. Van Hoecke, M. *et al.* Evidence of HIF-1 functional binding activity to caspase-3 promoter after photothrombotic cerebral ischemia. *Mol. Cell. Neurosci.* **34,** 40–7 (2007).

59. Helton, R. *et al.* Brain-specific knock-out of hypoxia-inducible factor-1alpha reduces rather than increases hypoxic-ischemic damage. *J. Neurosci.* **25,** 4099–107 (2005).

60. Kunze, R. *et al.* Neuron-specific prolyl-4-hydroxylase domain 2 knockout reduces brain injury after transient cerebral ischemia. *Stroke.* **43,** 2748–56 (2012).

61. Baranova, O. *et al.* Neuron-specific inactivation of the hypoxia inducible factor 1 alpha increases brain injury in a mouse model of transient focal cerebral ischemia. *J. Neurosci.* **27,** 6320–32 (2007).

62. Aminova, L. R. *et al.* Prosurvival and prodeath effects of hypoxia-inducible factor-1alpha stabilization in a murine hippocampal cell line. *J. Biol. Chem.* **280,** 3996–4003 (2005).

63. Vangeison, G., Carr, D., Federoff, H. J. & Rempe, D. a. The good, the bad, and the cell type-specific roles of hypoxia inducible factor-1 alpha in neurons and astrocytes. *J. Neurosci.* **28,** 1988–93 (2008).

64. Halterman, M. W., Miller, C. C. & Federoff, H. J. Hypoxia-Inducible Factor-1 alphy Mediates Hypoxia-Induced Delayed Neuronal Death That Involves p53. *J. Neurosci.* **19,** 6818–6824 (1999).

65. Brahimi-Horn, C. & Pouysségur, J. The role of the hypoxia-inducible factor in tumor metabolism growth and invasion. *Bull. Cancer* **93,** E73–80 (2006).

66. Ogawa, S., Kitao, Y. & Hori, O. Ischemia-induced neuronal cell death and stress response. *Antioxid. Redox Signal.* **9,** 573–87 (2007).

67. Xu, L., Sa, M. & Giffa, G. Differential Sensitivity of Murine Astrocytes and Neurons from Different Brain Regions to Injury. *Exp. Neurol.* **169,** 416–424 (2001).

68. Almeida, A., Delgado-Esteban, M., Bolaños, J. P. & Medina, J. M. Oxygen and glucose deprivation induces mitochondrial dysfunction and oxidative stress in neurones but not in astrocytes in primary culture. *J. Neurochem.* **81,** 207–17 (2002).

69. Sochocka, E. *et al.* Cell death in primary cultures of mouse neurons and astrocytes during exposure to and "recovery" from hypoxia, substrate deprivation and simulated ischemia. *Brain Res.* **638,** 21–8 (1994).

70. Schmidt-Kastner, R. & Freund, T. Selective vulnerability of the hippocampus in brain ischemia. *Neuroscience* **40,** 599–636 (1991).

71. Pulsinelli, W. a, Brierley, J. B. & Plum, F. Temporal profile of neuronal damage in a model of transient forebrain ischemia. *Ann. Neurol.* **11,** 491–8 (1982).

72. Kietzmann, T., Knabe, W. & Schmidt-Kastner, R. Hypoxia and hypoxia-inducible factor modulated gene expression in brain: involvement in neuroprotection and cell death. *Eur. Arch. Psychiatry Clin. Neurosci.* **251,** 170–8 (2001).

73. Desmond, D. W., Moroney, J. T., Sano, M., Stern, Y. & Merino, J. G. Incidence of Dementia After Ischemic Stroke: Results of a Longitudinal Study. *Stroke* **33,** 2254–2262 (2002).

74. Correia, S. C. & Moreira, P. I. Hypoxia-inducible factor 1: a new hope to counteract neurodegeneration? *J. Neurochem.* **112,** 1–12 (2010).

75. Liu, Y., Liu, F., Iqbal, K., Grundke-Iqbal, I. & Gong, C. Decreased glucose transporters correlate to abnormal hyperphosphorylation of tau in Alzheimer disease. *FEBS Lett.* **582,** 359–364 (2008).

76. Ogunshola, O. O. & Antoniou, X. Contribution of hypoxia to Alzheimer's disease: is HIF-1alpha a mediator of neurodegeneration? *Cell. Mol. Life Sci.* **66,** 3555–63 (2009).

77. Bouvry, D., Planès, C., Malbert-Colas, L., Escabasse, V. & Clerici, C. Hypoxia-induced cytoskeleton disruption in alveolar epithelial cells. *Am. J. Respir. Cell Mol. Biol.* **35,** 519–27 (2006).

78. Oehmichen, M., Woetzel, F. & Meissner, C. Hypoxic-ischemic changes in SIDS brains as demonstrated by a reduction in MAP2-reactive neurons. *Acta Neuropathol.* **117,** 267–74 (2009).

79. Molitoris, B. a. Putting the actin cytoskeleton into perspective: pathophysiology of ischemic alterations. *Am. J. Physiol.* **272,** F430–3 (1997).

80. McMurray, C. T. Neurodegeneration: diseases of the cytoskeleton? *Cell Death Differ.* **7,** 861–5 (2000).

81. Cairns, N. J., Lee, V. M. & Trojanowski, J. Q. The cytoskeleton in neurodegenerative diseases. *J. Pathol.* **204,** 438–449 (2004).

82. Vetter, I. R. & Wittinghofer, a. The guanine nucleotide-binding switch in three dimensions. *Science* **294,** 1299–304 (2001).

83. Gosser, Y. Q. *et al.* C-terminal binding domain of Rho GDP-dissociation inhibitor directs N-terminal inhibitory peptide to GTPases. *Nature* **387,** 814–9 (1997).

84. Cherfils, J. & Chardin, P. GEFs: structural basis for their activation of small GTP-binding proteins. *Trends Biochem. Sci.* **24,** 306–11 (1999).

85. Soldati, T., Shapira, A., Svejstrp, A. & Pfeffer, S. Membrane targeting of the small GTPase Rab9 is accompanied by nucleotide exchange. *Nature* **125,** 76–78 (1994).

86. Bishop, a L. & Hall, a. Rho GTPases and their effector proteins. *Biochem. J.* **348 Pt 2,** 241–55 (2000).

87. Bustelo, X., Sauzeau, V. & Berenjeno, I. GTP-binding proteins of the Rho/Rac family: regulation, effectors and functions in vivo. *Bioessays* **29,** 356–370 (2007).

88. Zhang, B. & Zheng, Y. Regulation of RhoA GTP hydrolysis by the GTPase-activating proteins p190, p50RhoGAP, Bcr, and 3BP-1. *Biochemistry* **2960,** 5249–5257 (1998).

89. Guilluy, C., Garcia-mata, R. & Burridge, K. Rho protein crosstalk : another social network? *Trends Cell Biol.* **21,** 718–726 (2012).

90. Kozma, R., Sarner, S., Ahmed, S. & Lim, L. Rho family GTPases and neuronal growth cone remodelling: relationship between increased complexity induced by Cdc42Hs, Rac1, and acetylcholine and collapse induced by RhoA and lysophosphatidic acid. *Mol. Cell. Biol.* **17,** 1201–11 (1997).

91. Rossman, K. L., Der, C. J. & Sondek, J. GEF means go: turning on RHO GTPases with guanine nucleotide-exchange factors. *Nat. Rev. Mol. Cell Biol.* **6,** 167–80 (2005).

92. Semenova, M. M. *et al.* Rho mediates calcium-dependent activation of p38alpha and subsequent excitotoxic cell death. *Nat. Neurosci.* **10,** 436–43 (2007).

93. Trapp, T. *et al.* GTPase RhoB: an early predictor of neuronal death after transient focal ischemia in mice. *Mol. Cell. Neurosci.* **17,** 883–94 (2001).

94. Ozaki, M. *et al.* Inhibition of the Rac1 GTPase protects against nonlethal ischemia/reperfusion-induced necrosis and apoptosis in vivo. *FASEB J.* **14,** 418–29 (2000).

95. Johanna, G.-V. *et al.* Rac1 activity changes are associated with neuronal pathology and spatial memory long-term recovery after global cerebral ischemia. *Neurochem. Int.* **57,** 762–73 (2010).

96. Turcotte, S., Desrosiers, R. R. & Béliveau, R. HIF-1alpha mRNA and protein upregulation involves Rho GTPase expression during hypoxia in renal cell carcinoma. *J. Cell Sci.* **116,** 2247–60 (2003).

97. Hirota, K. & Semenza, G. L. Rac1 activity is required for the activation of hypoxia-inducible factor 1. *J. Biol. Chem.* **276,** 21166–72 (2001).

98. Zhang, P. *et al.* Rac1 activates HIF-1 in retinal pigment epithelium cells under hypoxia. *Graefes Arch. Clin. Exp. Ophthalmol.* **247,** 633–9 (2009).

99. Xue, Y. *et al.* Role of Rac1 and Cdc42 in hypoxia induced p53 and von Hippel-Lindau suppression and HIF1alpha activation. *Int. J. Cancer* **118,** 2965–72 (2006).

100. Du, J. *et al.* PI3K and ERK-induced Rac1 activation mediates hypoxia-induced HIF-1α expression in MCF-7 breast cancer cells. *PLoS One* **6,** e25213 (2011).

101. Görlach, A. *et al.* Reactive oxygen species modulate HIF-1 mediated PAI-1 expression: involvement of the GTPase Rac1. *Thromb. Haemost.* **89,** 926–35 (2003).

102. Diebold, I. *et al.* Reciprocal Regulation of Rac1 and PAK-1 by HIF-1 a : A Positive-Feedback Loop Promoting. *Antioxid. Redox Signal.* **13,** 399–412 (2010).

103. Lee, H.-Y. *et al.* Src activates HIF-1α not through direct phosphorylation of HIF-1α specific prolyl-4 hydroxylase 2 but through activation of the NADPH oxidase/Rac pathway. *Carcinogenesis* **32,** 703–12 (2011).

104. Kim, J. *et al.* Factor-1α Expression through a Rac1-dependent NF- B Pathway. **19,** 433–444 (2008).

105. Diebold, I., Djordjevic, T., Hess, J. & Görlach, A. Rac-1 promotes pulmonary artery smooth muscle cell proliferation by upregulation of plasminogen activator inhibitor-1: role of NFkappaB-dependent hypoxia-inducible factor-1alpha transcription. *Thromb. Haemost.* **100,** 1021–1028 (2008).

106. Xue, Y. *et al.* Phosphatidylinositol 3-kinase signaling pathway is essential for Rac1-induced hypoxia-inducible factor-1alpha and vascular endothelial growth factor expression. *Am J Physiol Hear. Circ Physiol.* **300,** 2169–2176 (2011).

107. Lansbury, P. T. & Lashuel, H. a. A century-old debate on protein aggregation and neurodegeneration enters the clinic. *Nature* **443,** 774–9 (2006).

108. Petratos, S. *et al.* The beta-amyloid protein of Alzheimer's disease increases neuronal CRMP-2 phosphorylation by a Rho-GTP mechanism. *Brain* **131,** 90–108 (2008).

109. Zhao, L. *et al.* Role of p21-activated kinase pathway defects in the cognitive deficits of Alzheimer disease. *Nat. Neurosci.* **9,** 234–42 (2006).

110. Pollitt, S. K. *et al.* A rapid cellular FRET assay of Polyglutamine Aggregation Identifies a Novel Inhibitor Neurotechnique. *Neuron* **40,** 685–694 (2003).

111. Holbert, S. *et al.* Cdc42-interacting protein 4 binds to huntingtin: neuropathologic and biological evidence for a role in Huntington's disease. *Proc. Natl. Acad. Sci. U. S. A.* **100,** 2712–7 (2003).

112. DeGeer, J. & Lamarche-Vane, N. Rho GTPases in neurodegeneration diseases. *Exp. Cell Res.* **319,** 2384–94 (2013).

113. Yamanaka, K., Miller, T. M., McAlonis-Downes, M., Chun, S. J. & Cleveland, D. W. Progressive spinal axonal degeneration and slowness in ALS2-deficient mice. *Ann. Neurol.* **60,** 95–104 (2006).

114. Niederöst, B., Oertle, T., Fritsche, J., McKinney, R. A. & Bandtlow, C. E. Nogo-A and myelin-associated glycoprotein mediate neurite growth inhibition by antagonistic regulation of RhoA and Rac1. *J. Neurosci.* **22,** 10368–76 (2002).

115. Mendoza-Naranjo, A., Gonzalez-Billault, C. & Maccioni, R. B. Abeta1-42 stimulates actin polymerization in hippocampal neurons through Rac1 and Cdc42 Rho GTPases. *J. Cell Sci.* **120,** 279–88 (2007).

116. Mandela, P. & Ma, X.-M. Kalirin, a key player in synapse formation, is implicated in human diseases. *Neural Plast.* **2012,** 728161 (2012).

117. Fournier, A. E., Takizawa, B. T. & Strittmatter, S. M. Rho kinase inhibition enhances axonal regeneration in the injured CNS. *J. Neurosci.* **23,** 1416–23 (2003).

118. Borisoff, J. F. *et al.* Suppression of Rho-kinase activity promotes axonal growth on inhibitory CNS substrates. *Mol. Cell. Neurosci.* **22,** 405–416 (2003).

119. Huesa, G. *et al.* Altered distribution of RhoA in Alzheimer's disease and AbetaPP overexpressing mice. *J. Alzheimers. Dis.* **19,** 37–56 (2010).

120. Zhou, Y. *et al.* Nonsteroidal anti-inflammatory drugs can lower amyloidogenic Abeta42 by inhibiting Rho. *Science* **302,** 1215–7 (2003).

121. Cook, M., Mani, P., Wentzell, J. S. & Kretzschmar, D. Increased RhoA prenylation in the loechrig (loe) mutant leads to progressive neurodegeneration. *PLoS One* **7,** e44440 (2012).

122. Chaya, T. *et al.* Identification of a negative regulatory region for the exchange activity and characterization of T332I mutant of Rho guanine nucleotide exchange factor 10 (ARHGEF10). *J. Biol. Chem.* **286,** 29511–20 (2011).

123. Maystadt, I. *et al.* The nuclear factor kappaB-activator gene PLEKHG5 is mutated in a form of autosomal recessive lower motor neuron disease with childhood onset. *Am. J. Hum. Genet.* **81,** 67–76 (2007).

124. Verhoeven, K. *et al.* Report Slowed Conduction and Thin Myelination of Peripheral Nerves Associated with Mutant Rho Guanine-Nucleotide Exchange Factor 10. *Am. J. Hum. Genet.* **73,** 926–932 (2003).

125. Kashiwa, a *et al.* Isolation and characterization of novel presenilin binding protein. *J. Neurochem.* **75,** 109–16 (2000).

126. Namekata, K. *et al.* Dock3 stimulates axonal outgrowth via GSK-3β-mediated microtubule assembly. *J. Neurosci.* **32,** 264–74 (2012).

127. Chen, Q., Kimura, H. & Schubert, D. A novel mechanism for the regulation of amyloid precursor protein metabolism. *J. Cell Biol.* **158,** 79–89 (2002).

128. Bassermann, F. *et al.* Association of Bcr-Abl with the proto-oncogene Vav is implicated in activation of the Rac-1 pathway. *J. Biol. Chem.* **277,** 12437–45 (2002).

129. Stendel, C. *et al.* Peripheral nerve demyelination caused by a mutant Rho GTPase guanine nucleotide exchange factor, frabin/FGD4. *Am. J. Hum. Genet.* **81,** 158–64 (2007).

130. Varma, H., Yamamoto, A., Sarantos, M. R., Hughes, R. E. & Stockwell, B. R. Mutant huntingtin alters cell fate in response to microtubule depolymerization via the GEF-H1-RhoA-ERK pathway. *J. Biol. Chem.* **285,** 37445–57 (2010).

131. Youn, H., Ji, I., Ji, H. P., Markesbery, W. R. & Ji, T. H. Under-expression of Kalirin-7 Increases iNOS Activity in Cultured Cells and Correlates to Elevated iNOS Activity in Alzheimer ' s Disease Hippocampus. *J. Alzheimers. Dis.* **12,** 271–281 (2007).

132. Colomer, V. *et al.* Huntingtin-associated protein 1 (HAP1) binds to a Trio-like polypeptide, with a rac1 guanine nucleotide exchange factor domain. *Hum. Mol. Genet.* **6,** 1519–25 (1997).

133. Tsai, Y.-C., Riess, O., Soehn, A. S. & Nguyen, H. P. The Guanine nucleotide exchange factor kalirin-7 is a novel synphilin-1 interacting protein and modifies synphilin-1 aggregate transport and formation. *PLoS One* **7,** e51999 (2012).

134. Harrington, A. W. *et al.* The role of Kalirin9 in p75/nogo receptor-mediated RhoA activation in cerebellar granule neurons. *J. Biol. Chem.* **283,** 24690–7 (2008).

135. Peng, Y.-J. *et al.* Trio is a key guanine nucleotide exchange factor coordinating regulation of the migration and morphogenesis of granule cells in the developing cerebellum. *J. Biol. Chem.* **285,** 24834–44 (2010).

136. Fujikawa, K. *et al.* VAV2 and VAV3 as candidate disease genes for spontaneous glaucoma in mice and humans. *PLoS One* **5,** e9050 (2010).

137. Huang, T. Y. *et al.* A novel Rac1 GAP splice variant relays poly-Ub accumulation signals to mediate Rac1 inactivation. *Mol. Biol. Cell* **24,** 194–209 (2013).

138. Rosário, M., Schuster, S., Jüttner, R., Simó, S. & Cooper, J. A. Neocortical dendritic complexity is controlled during development by NOMA-GAP-dependent inhibition of Cdc42 and activation of cofilin. *Genes Dev.* **26,** 1743–1757 (2012).

139. Vo, N. *et al.* A cAMP-response element binding protein-induced microRNA regulates neuronal morphogenesis. *PNAS* **103,** 16426–31 (2006).

140. Schulz, A. *et al.* Merlin isoform 2 in neurofibromatosis type 2-associated polyneuropathy. *Nat. Neurosci.* **16,** 426–33 (2013).

141. Yamashita, T. & Tohyama, M. The p75 receptor acts as a displacement factor that releases Rho from Rho-GDI. *Nat. Neurosci.* **6,** 461–7 (2003).

142. Spiegel, S. & Milstien, S. Sphingosine-1-phosphate: an enigmatic signalling lipid. *Nat. Rev. Mol. Cell Biol.* **4,** 397–407 (2003).

143. Brown, D. Structure and function of membrane rafts. *Int. J. Med. Microbiol.* **291,** 433–7 (2002).

144. Obeid, L. M., Linardic, C. M., Karolak, L. a & Hannun, Y. a. Programmed cell death induced by ceramide. *Science* **259,** 1769–71 (1993).

145. Hla, T. Physiological and pathological actions of sphingosine 1-phosphate. *Semin. Cell Dev. Biol.* **15,** 513–20 (2004).

146. Calise, S. *et al.* Sphingosine 1-phosphate stimulates proliferation and migration of satellite cells: role of S1P receptors. *Biochim. Biophys. Acta* **1823,** 439–50 (2012).

147. Chen, H. *et al.* Inhibition of de novo ceramide biosynthesis by FTY720 protects rat retina from light-induced degeneration. *J. Lipid Res.* **54,** 1616–29 (2013).

148. Piccinini, M. *et al.* Deregulated sphingolipid metabolism and membrane organization in neurodegenerative disorders. *Mol. Neurobiol.* **41,** 314–40 (2010).

149. Weiss, B. & Stoffel, W. Human and murine serine-palmitoyl-CoA transferase-cloning, expression and characterization of the key enzyme in sphingolipid synthesis. *Eur. J. Biochem.* **249,** 239–47 (1997).

150. Hanada, K. A Mammalian Homolog of the Yeast LCB1 Encodes a Component of Serine Palmitoyltransferase, the Enzyme Catalyzing the First Step in Sphingolipid Synthesis. *J. Biol. Chem.* **272,** 32108–32114 (1997).

151. Buede, R., Rinker-Schaffer, C., Pinto, W. J., Lester, R. L. & Dickson, R. C. Cloning and characterization of LCB1, a Saccharomyces gene required for biosynthesis of the long-chain base component of sphingolipids. *J. Bacteriol.* **173,** 4325–32 (1991).

152. Hornemann, T., Wei, Y. & von Eckardstein, A. Is the mammalian serine palmitoyltransferase a high-molecular-mass complex? *Biochem. J.* **405,** 157–64 (2007).

153. Beeler, T. The Saccharomyces cerevisiae TSC10/YBR265w Gene Encoding 3-Ketosphinganine Reductase Is Identified in a Screen for Temperature-sensitive Suppressors of the Ca2+-sensitive csg2Delta Mutant. *J. Biol. Chem.* **273,** 30688–30694 (1998).

154. Othman, A. M. A. Atypical Sphingolipids as Biomarkers and Therapeutic Targets in Cardio-metabolic Diseases. 130 (2013).

155. Levy, M. & Futerman, A. H. Mammalian Ceramide Synthases. *IUBMB Life* **62,** 347–356 (2011).

156. Michel, C. *et al.* Characterization of ceramide synthesis. A dihydroceramide desaturase introduces the 4,5-trans-double bond of sphingosine at the level of dihydroceramide. *J. Biol. Chem.* **272,** 22432–22437 (1997).

157. Ternes, P., Franke, S., Zähringer, U., Sperling, P. & Heinz, E. Identification and characterization of a sphingolipid delta 4-desaturase family. *J. Biol. Chem.* **277,** 25512–8 (2002).

158. Hanada, K. *et al.* Molecular machinery for non-vesicular trafficking of ceramide. *Nature* **426,** 803–9 (2003).

159. Yamaoka, S., Miyaji, M., Kitano, T., Umehara, H. & Okazaki, T. Expression cloning of a human cDNA restoring sphingomyelin synthesis and cell growth in sphingomyelin synthase-defective lymphoid cells. *J. Biol. Chem.* **279,** 18688–93 (2004).

160. Oshida, K. *et al.* Effects of dietary sphingomyelin on central nervous system myelination in developing rats. *Pediatr. Res.* **53,** 589–93 (2003).

161. Schulte, S. & Stoffel, W. Ceramide UDPgalactosyltransferase from myelinating rat brain: purification, cloning, and expression. *Proc. Natl. Acad. Sci. U. S. A.* **90,** 10265–9 (1993).

162. Sandhoff, K. & Kolter, T. Biosynthesis and degradation of mammalian glycosphingolipids. *Philos. Trans. R. Soc. Lond. B. Biol. Sci.* **358,** 847–61 (2003).

163. Mao, C. & Obeid, L. Ceramidases: regulators of cellular responses mediated by ceramide, sphingosine, and sphingosine-1-phosphate. *Biochim Biophys Acta* **1781,** 424–434 (2008).

164. Kohama, T. *et al.* Molecular Cloning and Functional Characterization of Murine Sphingosine Kinase. *J. Biol. Chem.* **273,** 23722–23728 (1998).

165. Bandhuvula, P. & Saba, J. D. Sphingosine-1-phosphate lyase in immunity and cancer: silencing the siren. *Trends Mol. Med.* **13,** 210–7 (2007).

166. Alewijnse, A. E. & Peters, S. L. M. Sphingolipid signalling in the cardiovascular system: good, bad or both? *Eur. J. Pharmacol.* **585,** 292–302 (2008).

167. Cowart, L. A. Sphingolipids: players in the pathology of metabolic disease. *Trends Endocrinol. Metab.* **20,** 34–42 (2009).

168. Bertea, M. *et al.* Deoxysphingoid bases as plasma markers in diabetes mellitus. *Lipids Health Dis.* **9,** 84 (2010).

169. Othman, a *et al.* Plasma deoxysphingolipids: a novel class of biomarkers for the metabolic syndrome? *Diabetologia* **55,** 421–31 (2012).

170. Penno, A. *et al.* Hereditary sensory neuropathy type 1 is caused by the accumulation of two neurotoxic sphingolipids. *J. Biol. Chem.* **285,** 11178–87 (2010).

171. Zitomer, N. C. *et al.* Ceramide synthase inhibition by fumonisin B1 causes accumulation of 1-deoxysphinganine: a novel category of bioactive 1-deoxysphingoid bases and 1-deoxydihydroceramides biosynthesized by mammalian cell lines and animals. *J. Biol. Chem.* **284,** 4786–95 (2009).

172. Cuadros, R. *et al.* The marine compound spisulosine, an inhibitor of cell proliferation, promotes the disassembly of actin stress fibers. *Cancer Lett.* **152,** 23–29 (2000).

173. Salcedo, M. *et al.* The marine sphingolipid-derived compound ES 285 triggers an atypical cell death pathway. *Apoptosis* **12,** 395–409 (2007).

174. Sánchez, A. M. *et al.* Spisulosine (ES-285) induces prostate tumor PC-3 and LNCaP cell death by de novo synthesis of ceramide and PKCzeta activation. *Eur. J. Pharmacol.* **584,** 237–45 (2008).

175. Zuellig, R. *et al.* Deoxysphingolipids, a novel biomarker for type 2 diabetes, are cytotoxic for insulin-producing cells. *Diabetes* **Epub ahead,** (2013).

176. Verhoeven, K. *et al.* SPTLC1 mutation in twin sisters with hereditary sensory neuropathy type I. *Neurology* **62,** 1001–1002 (2004).

177. Houlden, H. *et al.* Clinical, pathological and genetic characterization of hereditary sensory and autonomic neuropathy type 1 (HSAN I). *Brain* **129,** 411–25 (2006).

178. Eichler, F. S. *et al.* Overexpression of the wild-type SPT1 subunit lowers desoxysphingolipid levels and rescues the phenotype of HSAN1. *J. Neurosci.* **29,** 14646–51 (2009).

179. Weiss, S. *et al.* Synaptogenesis of cultured striatal neurons in serum-free medium: a morphological and biochemical study. *Proc. Natl. Acad. Sci. U. S. A.* **83,** 2238–42 (1986).

180. Zhang, S. *et al.* Hypoxia induces an autocrine-paracrine survival pathway via platelet-derived growth factor (PDGF)-B/PDGF- β receptor/phosphatidylinositol 3-kinase/Akt signaling in RN46A neuronal cells. *FASEB J.* **17,** 1709–1711 (2003).

181. Joseph, J. *et al.* Copernicus revisited : amyloid beta in Alzheimer ' s disease. *Neurobiol. Aging* **22,** 131–146 (2001).

182. Jellinger, K. a & Attems, J. Prevalence and pathogenic role of cerebrovascular lesions in Alzheimer disease. *J. Neurol. Sci.* **229-230,** 37–41 (2005).

183. Ben-Ari, Y. Effects of anoxia and aglycemia on the adult and immature hippocampus. *Biol. Neonate* **62,** 225–30 (1992).

184. Auer, R. Excitotoxic mechanisms, and age-related susceptibility to brain damage in ischemia, hypoglycemia and toxic mussel poisoning. *Neurotoxicology* **12,** 541–6 (1991).

185. Towfighi, J., Mauger, D., Vannucci, R. C. & Vannucci, S. J. Influence of age on the cerebral lesions in an immature rat model of cerebral hypoxia-ischemia: a light microscopic study. *Brain Res. Dev. Brain Res.* **100,** 149–60 (1997).

186. Wright, K. M., Smith, M. I., Farrag, L. & Deshmukh, M. Chromatin modification of Apaf-1 restricts the apoptotic pathway in mature neurons. *J. Cell Biol.* **179,** 825–32 (2007).

187. Yakovlev, a G. *et al.* Differential expression of apoptotic protease-activating factor-1 and caspase-3 genes and susceptibility to apoptosis during brain development and after traumatic brain injury. *J. Neurosci.* **21,** 7439–46 (2001).

188. Polster, B. M., Robertson, C. L., Bucci, C. J., Suzuki, M. & Fiskum, G. Postnatal brain development and neural cell differentiation modulate mitochondrial Bax and BH3 peptide-induced cytochrome c release. *Cell Death Differ.* **10,** 365–70 (2003).

189. Vogelbaum, M. a, Tong, J. X. & Rich, K. M. Developmental regulation of apoptosis in dorsal root ganglion neurons. *J. Neurosci.* **18,** 8928–35 (1998).

190. Donovan, M. & Cotter, T. G. Caspase-independent photoreceptor apoptosis in vivo and differential expression of apoptotic protease activating factor-1 and caspase-3 during retinal development. *Cell Death Differ.* **9,** 1220–31 (2002).

191. Hu, B. R., Liu, C. L., Ouyang, Y., Blomgren, K. & Siesjö, B. K. Involvement of caspase-3 in cell death after hypoxia-ischemia declines during brain maturation. *J. Cereb. Blood Flow Metab.* **20,** 1294–300 (2000).

192. Attucci, S. *et al.* Group I metabotropic glutamate receptor inhibition selectively blocks a prolonged Ca(2+) elevation associated with age-dependent excitotoxicity. *Neuroscience* **112,** 183–94 (2002).

193. Antoniou, X. *et al.* JNK Contributes to Hif-1 α Regulation in Hypoxic Neurons. *Brain Res.* **1381,** 114–127 (2011).

194. Le, S. S. *et al.* Inhibition of Rac GTPase triggers a c-Jun- and Bim-dependent mitochondrial apoptotic cascade in cerebellar granule neurons. *J. Neurochem.* **94,** 1025–1039 (2005).

195. Yamauchi, J., Miyamoto, Y., Sanbe, A. & Tanoue, A. JNK phosphorylation of paxillin , acting through the Rac1 and Cdc42 signaling cascade , mediates neurite extension in N1E-115 cells. *Exp. Cell Res.* **312,** 1954–2961 (2006).

196. Minden, A., Lin, A., Abo, A. & Karin, M. Selective Activation of the JNK Signaling Cascade and c-Jun Transcriptional Activity by the Small GTPases Rac and Cdc42Hs. *Cell* **81,** 1147–1157 (1995).

197. Comerford, K. M., Cummins, E. P. & Taylor, C. T. c-Jun NH 2 -Terminal Kinase Activation Contributes to Hypoxia-Inducible Factor 1α − Dependent P-Glycoprotein Expression in Hypoxia. *Cancer Res*. **64,** 9057–9061 (2004).

198. Michiels, C. *et al.* HIF-1 and AP-1 cooperate to increase gene expression in hypoxia: role of MAP kinases. *IUBMB Life* **52,** 49–53 (2001).

199. Xu, Y. *et al.* The accumulations of HIF-1 α and HIF-2 α by JNK and ERK are involved in biphasic effects induced by different levels of arsenite in human bronchial epithelial cells. *Toxicol. Appl. Pharmacol.* **266,** 187–197 (2013).

200. Seko, Y., Takahashi, N., Tobe, K., Kadowaki, T. & Yazaki, Y. Hypoxia and hypoxia/reoxygenation activate p65PAK, p38 mitogen-activated protein kinase (MAPK), and stress-activated protein kinase (SAPK) in cultured rat cardiac myocytes. *Biochem. Biophys. Res. Commun.* **239,** 840–4 (1997).

201. Zhang, N. *et al.* Neuron-specific phosphorylation of c-Jun N-terminal kinase increased in the brain of hypoxic preconditioned mice. *Neurosci. Lett.* **423,** 219–24 (2007).

202. Mottet, D. *et al.* M Regulation of hypoxia-inducible factor-1alpha protein level during hypoxic conditions by the phosphatidylinositol 3-kinase/Akt/glycogen synthase kinase 3beta pathway in HepG2 cells. *J. Biol. Chem.* **278,** 31277–31285 (2003).

203. Mottet, D. *et al.* Regulation of hypoxia-inducible factor-1alpha protein level during hypoxic conditions by the phosphatidylinositol 3-kinase/Akt/glycogen synthase kinase 3beta pathway in HepG2 cells. *J. Biol. Chem.* **278,** 31277–85 (2003).

204. Loberg, R. D., Vesely, E. & Brosius, F. C. Enhanced glycogen synthase kinase-3beta activity mediates hypoxia-induced apoptosis of vascular smooth muscle cells and is prevented by glucose transport and metabolism. *J. Biol. Chem.* **277,** 41667–73 (2002).

205. Li, Q. *et al.* Lithium reduces apoptosis and autophagy after neonatal hypoxia-ischemia. *Cell Death Dis.* **1,** e56 (2010).

206. Kelly, S. *et al.* Glycogen synthase kinase 3beta inhibitor Chir025 reduces neuronal death resulting from oxygen-glucose deprivation, glutamate excitotoxicity, and cerebral ischemia. *Exp. Neurol.* **188,** 378–86 (2004).

207. Valerio, A. *et al.* Glycogen synthase kinase-3 inhibition reduces ischemic cerebral damage, restores impaired mitochondrial biogenesis and prevents ROS production. *J. Neurochem.* **116,** 1148–59 (2011).

208. Stockmann-Juvala, H. & Savolainen, K. A review of the toxic effects and mechanisms of action of fumonisin B1. *Hum. Exp. Toxicol.* **27,** 799–809 (2008).

209. Imgrund, S. *et al.* Adult ceramide synthase 2 (CERS2)-deficient mice exhibit myelin sheath defects, cerebellar degeneration, and hepatocarcinomas. *J. Biol. Chem.* **284,** 33549–60 (2009).

210. Pewzner-Jung, Y. *et al.* A critical role for ceramide synthase 2 in liver homeostasis: I. alterations in lipid metabolic pathways. *J. Biol. Chem.* **285,** 10902–10 (2010).

211. Silva, L. C. *et al.* Ablation of ceramide synthase 2 strongly affects biophysical properties of membranes. *J. Lipid Res.* **53,** 430–6 (2012).

212. McLean, W. G. The role of axonal cytoskeleton in diabetic neuropathy. *Neurochem. Res.* **22,** 951–6 (1997).

213. Medori, R., Autilio-Gambetti, L., Monaco, S. & Gambetti, P. Experimental diabetic neuropathy: impairment of slow transport with changes in axon cross-sectional area. *Proc. Natl. Acad. Sci. U. S. A.* **82,** 7716–20 (1985).

214. Medori, R., Jenich, H., Autilio-Gambetti, L. & Gambetti, P. Experimental diabetic neuropathy: similar changes of slow axonal transport and axonal size in different animal models. *J. Neurosci.* **8,** 1814–21 (1988).

215. Nitta, a *et al.* Diabetic neuropathies in brain are induced by deficiency of BDNF. *Neurotoxicol. Teratol.* **24,** 695–701 (2002).

216. Kholmanskikh, S. S., Dobrin, J. S., Wynshaw-Boris, A., Letourneau, P. C. & Ross, M. E. Disregulated RhoGTPases and actin cytoskeleton contribute to the migration defect in Lis1-deficient neurons. *J. Neurosci.* **23,** 8673–81 (2003).

217. Bonny, C., Oberson, A., Negri, S., Sauser, C. & Schorderet, D. F. Cell-Permeable Peptide Inhibitors of JNK. *Diabetes* **50,** 77–82 (2001).

218. Mei, Y. *et al.* Activating transcription factor 3 up-regulated by c-Jun NH(2)-terminal kinase/c-Jun contributes to apoptosis induced by potassium deprivation in cerebellar granule neurons. *Neuroscience* **151,** 771–9 (2008).

219. Hess, P., Pihan, G., Sawyers, C. L., Flavell, R. a & Davis, R. J. Survival signaling mediated by c-Jun NH(2)-terminal kinase in transformed B lymphoblasts. *Nat. Genet.* **32,** 201–5 (2002).

220. Yu, C. *et al.* JNK suppresses apoptosis via phosphorylation of the proapoptotic Bcl-2 family protein BAD. *Mol. Cell* **13,** 329–40 (2004).

221. Mollen, K. P. *et al.* Hypoxia activates c-Jun N-terminal kinase via Rac1-dependent reactive oxygen species production in hepatocytes. *Shock* **28,** 270–7 (2007).

222. Yamauchi, J. *et al.* The mood stabilizer valproic acid improves defective neurite formation caused by Charcot-Marie-Tooth disease-associated mutant Rab7 through the JNK signaling pathway. *J. Neurosci. Res.* **88,** 3189–97 (2010).

223. Yang, H.-S. & Hinds, P. W. Phosphorylation of ezrin by cyclin-dependent kinase 5 induces the release of Rho GDP dissociation inhibitor to inhibit Rac1 activity in senescent cells. *Cancer Res.* **66,** 2708–15 (2006).

224. Patrick, G. N. *et al.* Conversion of p35 to p25 deregulates Cdk5 activity and promotes neurodegeneration. *Nature* **402,** 615–22 (1999).

225. Lee, M. S. *et al.* Neurotoxicity induces cleavage of p35 to p25 by calpain. *Nature* **405,** 360–4 (2000).

226. Monyer, H. *et al.* Heteromeric NMDA Receptors : Molecular and Functional Distinction of Subtypes. *Science* **256,** 1217–1221 (1992).

227. Clements, J. D. & Westbrook, G. L. Activation kinetics reveal the number of glutamate and glycine binding sites on the N-methyl-D-aspartate receptor. *Neuron* **7,** 605–13 (1991).

228. Monyer, H., Burnashev, N., Laurie, D. J., Sakmann, B. & Seeburg, P. H. Developmental and regional expression in the rat brain and functional properties of four NMDA receptors. *Neuron* **12,** 529–40 (1994).

229. Sheng, M., Cummings, J., Roland, L., Jan, Y. & Jan, L. Changing subunit composition of heteromeric NMDA receptors during development of rat cortex. *Nature* **368,** 177–147 (1994).

230. Pickard, L., Noël, J., Henley, J. M., Collingridge, G. L. & Molnar, E. Developmental changes in synaptic AMPA and NMDA receptor distribution and AMPA receptor subunit composition in living hippocampal neurons. *J. Neurosci.* **20,** 7922–31 (2000).

231. Gangadharan, V. *et al.* Peripheral calcium-permeable AMPA receptors regulate chronic inflammatory pain in mice. *J. Clin. Invest.* **121,** 1608–23 (2011).

232. McRoberts, J. a. *et al.* Role of peripheral N-methyl-D-aspartate (NMDA) receptors in visceral nociception in rats. *Gastroenterology* **120,** 1737–1748 (2001).

6. Manuscripts

6.1 Rac1 plays a crucial role in the neuronal adaptation to hypoxia

Tanja Güntert, Max Gassmann, Omolara O. Ogunshola

Institute of Veterinary Physiology, Vetsuisse Faculty & Zurich Center of Integrative Human Physiology (ZIHP), University of Zurich, Zurich, Switzerland.

Manuscript is under review (Journal of Cellular Physiology).

Personal contribution: *All experiments and manuscript writing has been done by Tanja Güntert.*

Journal of Cellular Physiology

Journal of Cellular Physiology

Rac1 plays a crucial role in the neuronal adaptation to hypoxia

Journal:	*Journal of Cellular Physiology*
Manuscript ID:	Draft
Wiley - Manuscript type:	Original Research Article
Date Submitted by the Author:	n/a
Complete List of Authors:	Güntert, Tanja; University of Zurich, Veterinary Physiology Gassmann, Max; University of Zurich, Veterinary Physiology Ogunshola, Omolara; University of Zurich, Veterinary Physiology
Key Words:	HIF-1α, JNK, GSK3, neuronal survival, in vitro

John Wiley & Sons, Inc.

Rac1 plays a crucial role in the neuronal adaptation to hypoxia

Tanja Güntert, Max Gassmann, Omolara O. Ogunshola*

Institute of Veterinary Physiology, Vetsuisse Faculty & Zurich Center of Integrative Human Physiology (ZIHP), University of Zurich, Zurich, Switzerland.

Running Title: Rac1 in HIF-1α regulation

Keywords: HIF-1α, JNK, GSK3, neuronal survival, in vitro

* Corresponding author:

Omolara O. Ogunshola, PhD

Institute of Veterinary Physiology and Zurich Center of Integrative Human Physiology (ZIHP),

Vetsuisse Faculty,

University of Zurich,

Winterthurerstrasse 260, CH-8057 Zurich, Switzerland

Tel: +41 44 635 8805, Fax: +41 44 635 8, Email: larao@access.uzh.ch

Total number of figures: 7, total number of tables: 0, supplementary figures: 2.

Contract grant sponsor: Zurich Center for Integrative Human Physiology (ZIHP)

Abstract

Besides its role as a master regulator of the cytoskeleton the Rho GTPase Rac1 has been shown to be involved in cellular processes stimulated by hypoxic stress. In contrast to other brain cells neurons are known to be sensitive to reduced oxygen supply and as a result many neurodegenerative diseases are associated with hypoxic conditions. In this study primary cortical mouse neurons were used as an *in vitro* model to analyze the role of Rac1 in the neuronal hypoxic response. We show that Rac1 is upregulated and activated during hypoxia. Pharmacological inhibition of Rac1 completely abrogated hypoxic HIF-1α stabilization and expression of the HIF-1 targets VEGF and GLUT1. Surprisingly neuronal death was not induced for up to 6h of hypoxia even when Rac1 was inhibited. Additionally regulation of both JNK and GSK3β are highly dependent on Rac1 and mediate neuronal Rac1-driven HIF-1α accumulation. Thus overall we show that hypoxia-activated Rac1 is critical for HIF-1α stabilization during acute oxygen deprivation and that neurons potentially survive short periods of hypoxia in absence of HIF-1 signaling. Furthermore JNK and GSK3 contribute to the full induction of Rac1-driven HIF-1α accumulation during hypoxia.

Introduction

Proper brain function is crucial for whole body physiology and performance. Although the human brain constitutes only 2% of our body weight it consumes 25% of oxygen in rest. Since neurons are highly sensitive to changes in local oxygen tension due to their high oxygen consumption rates (Noh *et al.*, 2012) understanding the neuronal response to hypoxia is essential to develop strategies to prevent injury or improve brain function after hypoxic insult.

Adaption to hypoxia on the cellular level is mainly regulated by the transcription factor hypoxia-inducible factor-1 (HIF-1) (Iyer *et al.*, 1998). HIF-1 is a heterodimer that consists of the constitutively expressed HIF-1β (also known as aryl hydrocarbon receptor nuclear translocation, ARNT) and the oxygen-regulated HIF-1α subunit (Wang and Semenza, 1995). During normoxic conditions HIF-1α is hydroxylated by oxygen-dependent prolyl hydroxylases. This modification leads to the recognition of HIF-1α by Van Hippel-Lindau (VHL) that targets HIF-1α for proteasomal degradation (Cockman *et al.*, 2000). When oxygen levels drop the prolyl hydroxylases are inhibited, HIF-1α accumulates in the cytoplasm and translocates into the nucleus where it dimerizes with its β-subunit (Kallio *et al.*, 1998; Jaakkola *et al.*, 2001). Together with additional co-factors HIF-1 binds to the hypoxia-response element (HRE) of its target genes and initiates their transcription (Jiang *et al.*, 1996). By inducing glycolytic enzymes like phosphofructokinase and angiogenic factors like Erythropoietin and Vascular endothelial growth factor HIF-1 can confer tolerance to hypoxia (Bernaudin *et al.*, 2002). However HIF-1 contributes also to hypoxia-induced cell death by inducing pro-apoptotic Bcl-2 family members or by stabilizing the tumor suppressor p53 (Halterman *et al.*, 1999; Kim *et al.*, 2004). Notably other

post-translational modifications like sumoylation and phosphorylation also influence HIF-1 stability, localization and transcriptional activity showing that its regulation is a complex process (Mylonis *et al.*, 2006; Berta *et al.*, 2007; Flügel *et al.*, 2007) .

Rho GTPases are key regulators of the cytoskeleton but additionally are involved in various cellular processes including cell survival and death (see for review Linseman and Loucks, 2008). Interestingly some family members are regulated by hypoxia similar to HIF-1α. Rac1, RhoA and Cdc42 were shown to be upregulated after a few hours of oxygen deprivation (Turcotte *et al.*, 2003), and it was demonstrated that different Rho GTPases regulate the stabilization of HIF-1α in different cell types during hypoxia (Xue *et al.*, 2006; Zhang *et al.*, 2009). Rac1 appears to be a central player in the regulation of HIF-1 and seems to be associated with HIF-1 in a positive feedback loop. Indeed hypoxia-activated Rac1 is crucial for HIF-1 activity in Hep3B cells (Hirota and Semenza, 2001). In turn HIF-1 binds to the Rac1 promoter and enhances its expression in pulmonary artery smooth muscle cells (Diebold *et al.*, 2010). Particularly in the brain, however, it is unclear whether a similar interaction between Rac1 and HIF-1 exists and/or via which pathways the proteins might be connected.

This study investigated whether Rac1 modulates HIF-1-driven hypoxic adaptation of mature primary cortical neurons and aimed to identify candidates that mediate the crosstalk between those pathways.

Material and Methods

All experiments were performed in accordance with Swiss animal protection laws and University of Zürich institutional guidelines for animal experimentation. Permission approved by the Zurich cantonal animal experimentation committee.

Reagents and Antibodies

If not stated differently chemicals and reagents were purchased from Sigma-Aldrich (Missouri, USA). All cell culture reagents were purchased from Life Technologies (Zug, Switzerland). The following antibodies were used: Anti HIF-1α (NOVUS, Littleton, USA), anti Rac1, anti β-Actin (Sigma), anti TUJ-1 (COVANCE, Berkeley, CA, USA), anti phospho-GSK3β and anti total GSK3α/β (Millipore, Billerica, MA, USA), anti phospho-JNK and anti total JNK (R&D Systems, Minneapolis, MN, USA), anti phospho-p55 and p85 PI3K and total p85 PI3K, anti phospho-AKT and anti total AKT (Cell signaling, Danvers, MA, USA).

Neuronal culture

Primary neuronal cells were obtained from cerebral cortex of C57BL/6 mouse embryos at gestational stage E14 as described previously (Ogunshola *et al.*, 2002). Following dissection cortices were dissociated in Hank`s buffer saline (HBSS) containing trypsin and DNaseI (Roche, Penzberg, Germany) for 5 min at 37°C. Cells were seeded on poly-L-lysine coated plastic petri or on poly-D-lysine coated glass coverslips in 24 well plates (60 000 cells/cm^2). Neurobasal medium was complemented with B27 supplement (1X), AlbuMAXI (0.25g/ml), streptavidin-penicillin (1%), Sodium-Pyruvate 100U/ml and L-Glutamine (0.5

mM). Neurons were maintained at normoxia (21% O_2, 5% CO_2) in a humidified incubator at 37 °C for 17 days (days in vitro=DIV). Half of the media was replaced every 6 days.

Hypoxia experiments and inhibitor treatments

For hypoxic exposure cells were put in a purpose-built hypoxic glove-box chamber (in vivo 400, RUSKINN Technologies, Guiseley, UK) for different time intervals (37°C, 5% CO_2). The oxygen level was maintained at 1%. Rac1 inhibitor (Millipore, Billerica, MA, USA) was added just prior to hypoxic exposure. Inhibitors of GSK3β (SB216763, Cayman chemicals, Ann Arbor, MI, USA; LiCl, Sigma) were added 24h before and JNK inhibitor SP600123 was added 1h before cells were subjected to hypoxia. Control cells were kept under normal conditions (37°C, 21% O_2, 5% CO_2) in the incubator.

Western Blot

Neurons were lysed in ice-cold lysis buffer (150 mM NaCl, 50 mM Tris, 1% Triton X-100, 1% NP-40) for 10 min and centrifuged at 16 000 rcf for 10 min at 4°C. The supernatant was collected and stored at -20°C. Protein concentration was measured using Bio-Rad assay (according manufacturer`s protocol). 40-60 µg of protein were loaded on SDS-polyacrylamide gels then transferred to nitrocellulose membrane. After blocking in 0.1% TBS-Tween with 5% milk powder or 5 % BSA membranes were incubated overnight at 4°C with primary antibody. Membranes were washed before being incubated with an HRP-conjugated secondary antibody for 1h at room temperature. All blots were

normalized to TUJ-1 or to β-Actin and quantified by densitometry using imageJ software.

Quantitative real-time PCR (qRT-PCR)

Total RNA was extracted using TRIzol reagent (Invitrogen, AG, Switzerland) according to the manufacturer`s protocol. For subsequent cDNA synthesis ImProm-II Reverse Transcription System (Promega, Madison, WI, USA) was used. Mouse-specific Taq-man-based gene expression assays were utilized to preform real-time PCR (HIF-1α [Mm00468869_m1], VEGF [Mm00437304_m1], Glut1 [Mm00441473_m1], GAPDH [Mm99999915_g1], Applied Biosystems). All reactions were run in duplicates using ABI 7500 RT-PCR thermocycler (Applied Biosystems, Foster City, CA, USA). Data were analyzed using the ΔΔCt-Method.

Immunocytochemistry

Cells on glass coverslips were fixed for 5 min in 4% paraformaldehyde in PBS, permeabilized 3 to 5 minutes with 0.1% Triton X-100 in PBS and then blocked in 10% normal goat serum. Antibodies were applied overnight at 4°C. Cells were incubated with fluorescent secondary antibody (AlexaFluor488, AlexaFluor594, Molecular Probes, Leiden, Netherlands) for 1h at room temperature. After washing with PBS cells were counterstained with 10 μM DAPI in H_2O for 5 min. For F-actin staining cells were incubated in Phalloidin-TRITC for 40 min at room temperature after the fixation. Coverslips were mounted in fluorescent mounting medium (Dako, Glostrup, Denmark) then viewed and analyzed with an Axiovert inverted fluorescent microscope (Zeiss, Germany).

Rac1 activity assay (G-LISA)

The activation of Rac1 was assessed using the colorimetric G-LISA Activation Assay Biochem Kit (BK125, Cytoskeleton, Denver, CO, USA). Briefly lysates were collected, protein concentrations were determined and samples were snap-frozen until the assay was prepared. All steps were performed according to the manufacturers protocol.

Cell death assays:

1. LDH assay: For quantification of cell death the release of lactate dehydrogenase from cells into the culture medium was detected using Cytotoxicity Detection Kit (Roche, Penzberg, Germany) according to the manufacturer`s instructions.

2. MTT assay: Thiazolyl blue tetrazolium bromide (Sigma) was dissolved in PBS and added to the cells in a 96 well format (final concentration 0.5 mg/ml). After 1h incubation at 37°C media was removed and 100 µL DMSO was added to measure absorption at 595 nm (subtract background at 670 nm).

Statistical analysis

All graphs were created from at least 3 independent experiments and analyzed using GraphPad Prism software. Error bars represent the mean ± standard deviation. For comparison between different timepoints within a group one-way ANOVA was used to assess statistical significance. For comparisons between different groups we performed two-way ANOVA. In both cases Bonferroni post-hoc test was done. For simple comparison between two groups we used paired, two-tailed Student`s t-test. A value of $p<0.05$ was considered significant.

Results

Rac1 is upregulated and activated upon hypoxic exposure

It has been shown in different cancer cell lines like Caki-1, MKN-45 and HepG2 (Turcotte *et al.*, 2003; Xue *et al.*, 2006) that Rac1 is upregulated by acute hypoxia. Neurons are exquisitely sensitive to reduced oxygen concentrations. Thus we exposed mature primary cortical mouse neurons to 1% of oxygen for short periods of time to investigate if Rac1 is similarly modulated by hypoxia. Western blot analysis showed that after 4h and 6h of hypoxia Rac1 protein levels were increased compared to normoxic control samples (Fig. 1A). By immunocytochemistry we could confirm this observation. Normoxic cells showed very weak staining for Rac1 whereas hypoxic cells showed a bright and clear signal (Fig. 1B). To determine if Rac1 activity is altered under hypoxia we used Rac G-LISA. Hypoxic exposure strongly increased Rac activity after 2h (142.8 ± 7.2; $p<0.01$) and remained elevated up to 6h (147.9 ± 18.5; $p<0.01$) compared to the normoxic control (Fig. 1C). Our results show that in acute hypoxia not only elevates neuronal Rac1 protein levels but also increases its activity.

Rac1 is crucial for HIF-1-driven adaptive hypoxic response

Since Rac1 is strongly regulated by decreased oxygen concentrations we investigated whether Rac1 plays a role in the neuronal hypoxic response. In retinal pigment epithelium cells (Zhang *et al.*, 2009) it has been shown that hypoxia-inducible factor-1α (HIF-1α) is induced during hypoxia in Rac1-dependent manner. As expected hypoxic HIF-1α protein stabilization was detected by Western blot after 4h and 6h. However treatment of cells with a

specific inhibitor of Rac1 resulted in a complete abrogation of hypoxic HIF-1α accumulation (Fig. 2A). Immunocytochemical analyis confirmed these results. Normoxic cells showed a basal HIF-1α signal while hypoxic exposure led to an increased HIF-1α staining mainly located in the nucleus. Similar to the Western blot results Rac1 inhibition strongly suppressed HIF-1α basal levels in normoxic and nuclear accumulation in hypoxic cells (Fig. 2B). To confirm that Rac1 is needed for the HIF-1-driven cellular adaptation to hypoxia we analyzed the expression of HIF-1 as well as its target genes GLUT1 and VEGF and of HIF-1α itself in both normoxic and hypoxic cells by quantitative real-time PCR. Neither hypoxia nor Rac1 blockade altered HIF-1α mRNA levels. However as expected mRNA levels of both GLUT1 and VEGF were increased by hypoxia (Fig. 2C). The highest fold change increase of VEGF levels compared to normoxic control sample was observed after 4h 8.71 ± 0.97 ($p< 0.01$), but after 6h hypoxia expression levels were still highly elevated (5.4 ± 2.37; $p<0.01$). GLUT1 mRNA levels were raised to a similar extent after 4h and 6h of hypoxia compared to normoxia (4h: 3.37 ± 0.36; 6h: 3,53 ± 0.92, both $p<0.01$). Normoxic expression of either target gene was not altered by Rac1 inhibitor treatment (50 μM and 100 μM). However inhibitor treatment significantly reduced hypoxia-induced GLUT1 and VEGF expression to a degree similar to normoxic samples. Thus Rac1 induces HIF-1α protein stabilization and downstream signaling without altering HIF-1α mRNA levels. Taken together Rac1 is a potent regulator of the HIF-1-driven cellular hypoxic response in neurons.

Neurons survive acute hypoxia without HIF-1-driven adaptive response

Without Rac1 neurons fail to induce genes that are important for hypoxic adaptation. To assess whether Rac1 inhibition affects neuronal survival during acute hypoxia MTT and LDH assays were performed to measure cell death. MTT results showed that blockade of Rac1 in normoxia or during 4h of hypoxia did not affect enzyme activity (Fig. 3A). After 6h of hypoxia we observed a trend towards reduced enzymatic activity when Rac1 was inhibited (50 μM Rac1 inhibitor: 81.6 ± 12.6; 100 μM Rac1 inhibitor: 71.6 ± 12.6). However changes were not significant. Similar to MTT data, LDH levels were neither altered by hypoxia nor by Rac1 inhibition (Fig. 3B) confirming that acute hypoxia alone does not induce cell death in neurons as shown in both assays. Overall neurons survive acute hypoxia in the absence of Rac1 and thus without HIF-1- driven adaptive gene expression.

JNK is involved in Rac1-dependent HIF-1α regulation

We show that in primary cortical neurons Rac1 is critical for hypoxic HIF-1α stabilization und subsequent cellular adaptation by inducing gene expression. It has been reported that JNK is phosphorylated during hypoxia, an occurence important for HIF-1 transcriptional activity (Comerford *et al.*, 2004). Furthermore Minden and colleagues (Minden *et al.*, 1995b) showed that Rac1 activates JNK signaling cascades. Thus Rac1-driven HIF-1α stabilization could be mediated by JNK. We analyzed JNK phosphorylation levels by Western blot using TUJ-1, a neuron-specific β-Tubulin, as loading control. After 4h of hypoxia phospho/total JNK levels were significantly increased (120.6 ± 4.6, $p<0.05$). However neurons treated with Rac1 inhibitor (50 μM or 100 μM) showed a

dramatic decrease in JNK phosphorylation in normoxia (50.8 ± 6.5; $p<0.01$) and hypoxia (4h: 76.0 ± 7.0, $p<0.05$ and 37.8 ± 17.5, $p<0.0001$; 6h: 72.3 ± 13.5 and 46.7 ± 14.8, $p<0.01$) while total levels were unchanged (Fig. 4A). Thus JNK activity in neurons highly depends on Rac1. To determine if JNK is involved in HIF-1α induction we exposed neurons to the JNK-specific inhibitor SP600125 prior to hypoxic treatment. Indeed hypoxic accumulation of HIF-1α was significantly reduced in cells treated with 50 μM JNK inhibitor after 4h (72.0 ± 3.3, $p<0.05$) and 6h (69.6 ± 14.6, $p<0.05$) in comparison to the untreated controls (Fig. 4B). Immunocytochemistry confirmed these findings. After 6h of hypoxia HIF-1α staining was less intense when JNK was blocked in comparison to untreated cells similar to the Rac1 inhibition effects (Fig. 4C). Taken together the results show that in neurons JNK contributes to Rac1-driven HIF-1α induction during acute hypoxia.

Active GSK3 is critical for hypoxic HIF-1α accumulation in neurons

It has been reported that Glycogen synthase kinase 3 (GSK3) regulates HIF-1α levels in HepG2 cells (Flügel *et al.*, 2007). Since GSK3 can be linked with Rac1 via PI3K/AKT cascade we investigated if neuronal Rac1-dependent HIF-1α accumulation is mediated by GSK3. GSK3 is expressed in two isoforms GSK3α and GSK3β, the later beeing highly expressed in CNS neurons. To assess if GSK3β is dependent on Rac1 signaling we performed Western blot to analyze the phosphorylated (Ser9), inactive form of GSK3β and total protein levels of cells treated with and without Rac1 inhibitor (Fig. 5A). TUJ-1 was used as loading control. After 6h of hypoxia GSK3β phospho/total level was significantly decreased (73.8 ± 4.1, $p<0.05$) compared to normoxia. In contrast Rac1

inhibition led to a strong increase of phosphorylated GSK3β und thus inactivation of the kinase in both normoxic (208.9 ± 68.3) and hypoxic conditions (4h: 277.4 ± 24.3 and 272.3 ± 84.2; both $p<0.01$, 6h: 289.6 ± 61.5 and 353.6 ± 98.7; both $p<0.0001$) compared to untreated control. Thus neuronal activity of GSK3β is highly dependent on Rac1. Next, to investigate whether Rac1-dependent modulation of GSK3β is involved in hypoxic HIF-1α induction we directly targeted GSK3. Cells were treated with either lithium chloride (LiCL) or SB216763, both compounds shown to effectively inhibit GSK3 activity, prior to hypoxic exposure. Western blot (Fig. 5B, C) showed that at 10 mM LiCl significantly reduced HIF-1α levels after 4h ($p<0.05$) and 6h ($p<0.001$) of hypoxia. Similarly 10 μM of the specific GSK3 inhibitor SB216763 also suppressed hypoxia-induced HIF-1α accumulation at 4h and 6h (both $p<0.05$). In agreement LiCL also reduced neuronal HIF-1α localization in hypoxia in comparison to the untreated control (Fig. 5D). Our results demonstrate that active GSK3 is crucial for full hypoxic induction of HIF-1α in neurons.

Rac1 regulates PI3K/AKT pathway

GSK3 is a direct target of AKT (Protein kinase B) that in turn is regulated by Phosphatidylinositol 3-kinase (PI3K) (Cross *et al.*, 1995). PI3K itself has been shown to be associated with Rac1 signaling (Lin *et al.*, 2011; Zhu and Nelson, 2013). To determine if Rac1-dependent GSK3β regulation could be mediated by PI3K/AKT pathway we investigated if Rac1 inhibition changes phosphorylation and thus activity of PI3K and AKT similar to GSK3β. Phosphorylation of the p85 regulatory subunit of PI3K, widely used to determine PI3K activity was not altered by Rac1 blockage or decreased oxygen levels (Supplementary figure 2).

However phosphorylation of p55, another regulatory subunit of PI3K, was dose-dependently enhanced in cells treated with Rac1 inhibitor in both normoxia and hypoxia (Fig. 6A). In normoxia levels of phosphorylated p55 levels increased more than 2 fold ($p<0.05$) when Rac1 was inhibited. In hypoxia 100 μM Rac1 inhibitor enhanced phospho-p55 levels by up to 3 fold after 4h and 6h ($p<0.05$) compared to the untreated control (Fig 6A). Similarly AKT phosphorylation was strongly elevated after inhibitor treatment in normoxia (177.2 ± 57.1; $p<0.001$) and hypoxia (4h: 197.5 ± 13.3 and 196.5 ± 10.1; both $p<0.001$, 6h: 163.7 ± 10.7 and 224.1 ± 35.6; $p<0.0001$) whereas total levels of AKT remained unchanged (Fig 6B). These data show that Rac1 controls the activity state of p55 PI3K and AKT and provide a possible mechanism by which Rac1 might regulate GSK3β and thus HIF-1α stabilization.

Discussion

Neurons are highly sensitive to oxygen deprivation and hypoxic injury causes significant dysfunction. This study demonstrates for the first time that Rac1 is crucial for stabilizing HIF-1α and thus for the induction of the adaptive response to acute hypoxia in fully differentiated primary cortical neurons. Unexpectedly, we observed that mature neurons survive acute hypoxia without Rac1 and thus even without HIF-1-mediated adaptation. Furthermore the Rac1 effects are mediated by both JNK and GSK3 to accomplish full HIF-1α induction.

After the first report showing that Rac1 controls hypoxic HIF-1α protein accumulation in HEK293 (Hirota and Semenza, 2001), many studies followed reporting the involvement of Rho GTPase Rac1 in HIF-1 regulation in different

cancer cell lines (Görlach *et al.*, 2003; Turcotte *et al.*, 2003; Xue *et al.*, 2006). However little is known about the involvement of Rac1 in the hypoxic response of the brain although it is of special interest to fully understand how this organ reacts to reduced oxygen concentration to prevent hypoxia-associated brain injury. Primary cortical neurons responded to oxygen deprivation with increase of Rac1 protein levels and activity after acute exposure (2h-6h). Similar to our data Turcotte (Turcotte *et al.*, 2003) reported significantly elevated Rac1 levels at same exposures of hypoxia in Caki-1 cells. It was also shown that hypoxia regulates Rac1 protein levels very similarly to HIF-1α levels in retinal pigment epithelial cells (Zhang *et al.*, 2009), and 30 minutes of hypoxia already activates Rac1 in HEK293 cells (Hirota and Semenza, 2001). We now show that Rac1 is absolutely crucial for HIF-1α accumulation in neurons since its inhibition completely abrogated HIF-1α stabilization. Contrary to the study in HEK293 of Hirota and Semenza (Hirota and Semenza, 2001) neuronal Rac1 inhibition did not alter HIF-1α mRNA levels. In our study hypoxic expression of the HIF-1 target genes GLUT1 and VEGF were strongly suppressed by Rac1 inhibition suggesting that neuronal Rac1 controls HIF-1α on the protein level and is needed for full induction of the cellular response to acute hypoxia.

We did not observe any alterations in neuronal survival up to 6h of hypoxia. This might be surprising at a first glance but several studies demonstrate that even sensitive cells like neurons do not undergo cell death when oxygen levels are above 0.5 % (see for review (Snyder and Chandel, 2009)). Zhang and colleagues (Zhang *et al.*, 2003) showed hat differentiated RN46A neuronal cells exposed to 1% oxygen for 48h also did not significantly undergo apoptosis. Other studies suggest that anoxic conditions are necessary to induce apoptosis (Papandreou *et*

al., 2005) or that apoptosis is induced only in combination with glucose deprivation (Wohnsland *et al.*, 2010). In primary cortical rat neurons anoxic cell death was induced only when glucose concentration was decreased (Wohnsland *et al.*, 2010) and similarly glucose supplementation protected DRG neurons from hypoxia-induced death (Honma *et al.*, 2003). The role of HIF-1 in cell survival during hypoxia is still debated. As opposed to the discussed negative effects of long-term HIF-1 stabilization, in acute and mild hypoxia HIF-1α is believed to be protective. In the brain moderate and brief hypoxic insults can induce a protective regulation that is called preconditioning (Bruer *et al.*, 1997). Neuroprotective effects of HIF-1 are mainly mediated via the expression of HIF targets genes like VEGF and EPO (Jin *et al.*, 2000; Liu *et al.*, 2005). However it is discussed more and more that the protective adaptation can be independent of HIF-1. Li and colleagues (Li and Brorson, 2013) showed that cortical neurons continuously exposed to 1% oxygen were protected against ischemia-reperfusion and excitotoxicity, surprisingly independent of HIF-1α. In our model mature cortical neurons seem to survive acute hypoxia even when HIF-1 signaling and thus expression of adaptive genes was blocked by Rac1 inhibition. However there is a difference between the acute response to hypoxia and the adaptation to prolonged hypoxic exposure. We have evidence that during prolonged hypoxia neuronal survival is impaired and that the absence of Rac1 and HIF-1α indeed increase hypoxia-induced cell death (data not shown).

Since JNK activity is regulated by hypoxia and dependent on Rac1 (Minden *et al.*, 1995a; Chen *et al.*, 2010) we hypothesized that Rac1 regulates HIF-1α via JNK in neurons. Indeed significantly elevated neuronal phosphorylation of JNK after 4h

of hypoxia was similar to other *in vitro* studies in HepG2 cells (Minet *et al.*, 2001). In accordance with a study in N1E-115 neuroblastoma cells (Yamauchi *et al.*, 2006) JNK phosphorylation was strongly decreased by Rac1 inhibition suggesting hypoxia-mediated Rac1 induction of JNK activity. Indeed another study demonstrated hypoxic JNK activation to be Rac1 dependent in hepatocytes (Mollen *et al.*, 2007). In contrast to our findings it was published that JNK is a negative factor for HIF-1α accumulation in primary rat neurons (Antoniou *et al.*, 2011), however the majority of studies suggest a positive correlation between active JNK and HIF-1 signaling similar to our findings. In agreement inhibition of JNK diminished HIF-1 transcriptional activity in HeLa cells and reduced HIF-1α protein levels in human bronchial epithelia cells (Comerford *et al.*, 2004; Xu *et al.*, 2013) . Our data shows a similar mechanism in neuronal cells and suggests overall that JNK activation during hypoxia is a Rac1-driven process that effects HIF-1α stabilization in mature neurons.

We identified GSK3β as a further candidate that mediates Rac1-driven HIF-1α stabilization It has been shown that GSK3β is particularly abundant in the CNS (Jin *et al.*, 2006) and has been demonstrated to directly phosphorylate HIF-1α and thus target it for ubiquitinylation and subsequent proteasomal degradation (Flügel *et al.*, 2007). Furthermore, GSK3 is a direct target of the PI3K/AKT pathway which itself is involved in HIF-1 regulation during hypoxia (Zhong *et al.*, 2000) and was tightly associated with Rac1 signaling in COS 7 and natural killer cells (Jiang *et al.*, 2001; Murga *et al.*, 2002). Similar to such studies we demonstrate a positive correlation between GSK3 activity and hypoxia and thus HIF-1α induction. We observed a significant decrease in serine phosphorylation levels und thus activation of GSK3β after 6h of hypoxia. In HepG2 cells prolonged

hypoxia was demonstrated to activate GSK3 (Mottet *et al.*, 2003) and in vivo rapid activation of GSK3α and GSK3β during hypoxia has been reported (Roh *et al.*, 2005). Indeed Rac1 blockade strongly increased neuronal GSK3β serine phosphorylation and thus simultaneously abrogated HIF-1α accumulation and inactivated GSK3β. Furthermore direct inhibition of neuronal GSK3 by both lithium chloride and SB216763 decreased HIF-1α stabilization. However till now increased serine-phosphorylation and thus inactivation of GSK3 has been correlated with enhanced HIF-1α levels (Schnitzer *et al.*, 2005; Flügel *et al.*, 2012). Thus we demonstrate for the first time that active GSK3 contributes to HIF-1α stabilization during acute hypoxia. Future studies will be necessary to explore the molecular mechanisms of this probably cell type specific signaling event.

A major regulatory pathway of GSK3 activity is PI3K/AKT (Cross *et al.*, 1995). In various cell types and experimental conditions Rac1 has been associated with PI3K signaling. PI3K influences Rac1 activity (Zhu and Nelson, 2013) and conversely represents a downstream target of Rac1 (Lin *et al.*, 2011). Rac1 inhibition led to a concentration-dependent increase of neuronal p55 PI3K phosphorylation in normoxia and hypoxia. P55 is an isoform of the regulatory p85 subunit of PI3K enriched in mouse brain and testis as well as in rat muscle and brain (Pons *et al.*, 1995; Inukai *et al.*, 1996). After phosphorylation it regulates PI3K activity similar to p85 (Pons *et al.*, 1995). Thus we hypothesize that in our neuronal model phosphorylation of the regulatory p55 subunit may modulate PI3K activity and in accordance AKT was greatly activated when Rac1 was blocked in both normoxia and hypoxia. Taken together our data indicate that strong inactivation of GSK3β due to Rac1 blockade could be mediated by the

hyper-activation of PI3K/AKT signaling. Several reports suggest that activation of PI3K and AKT leads to neuroprotection (Zhang *et al.*, 2010; Kim *et al.*, 2012) and we hypothesize such activation can confer hypoxic tolerance during acute hypoxia by compensating the absence of Rac1 and HIF-1α. The potential neuroprotective role of PI3K/AKT especially during prolonged hypoxia needs to be investigated in more detail.

Importantly our study highlights that the effects of Rac1 inhibition on JNK, PI3K/AKT and GSK3β activity are independent of oxygen concentrations and therefore represent a general mechanism of Rac1 action (Fig. 7A). However it is also clear that hypoxia-induced Rac1-dependent activation of JNK and GSK3 is required for HIF-1α stabilization in primary neurons. Rac1 inhibition resulted in a strong activation of PI3K/AKT thus we hypothesize that hypoxia-activated Rac1 prevents this over-activation thereby promoting active GSK3 that contributes to HIF-1α stabilization (Fig. 7B).

In conclusion regulation of HIF-1α during hypoxia is a highly complex phenomenon that involves cell type-specific processes. Rac1 has a pivotal role in the neuronal hypoxic response being crucial for HIF-1α accumulation particularly via JNK and GSK3 pathways. To the best of our knowledge this is the first time that active GSK3 has been shown to mediate HIF-1α stabilization during acute hypoxia in primary neurons. Furthermore loss of Rac1 and HIF-1 during acute hypoxia is accompanied by a strong activation of PI3K/AKT but does not induce cell death. Our findings give important insights into neuronal HIF-1α modulation and cellular adaptation to hypoxia. This gain of knowledge will surely be beneficial to develop novel therapeutic strategies to prevent neuronal loss due to hypoxic injury.

Acknowledgements

This work was supported by the Zurich Center for Integrative Human Physiology (ZIHP), University of Zurich. We thank Sabrina Sonda for providing the JNK inhibitor. The authors declare no conflict of interest.

REFERENCES:

Antoniou, X., Sclip, A., Ploia, C., Colombo, A., Moroy, G., and Borsello, T. (2011). JNK Contributes to Hif-1 α Regulation in Hypoxic Neurons. Brain Res. *1381*, 114–127.

Bernaudin, M., Nedelec, A., Divoux, D., Mackenzie, E. T., Petit, E., and Schumann-bard, P. (2002). Normobaric Hypoxia Induces Tolerance to Focal Permanent Cerebral Ischemia in Association With an Increased Expression of Hypoxia-Inducible Factor-1 and Its Target Genes , Erythropoietin and VEGF , in the Adult Mouse Brain. J. Cereb. Blood Flow Metab. *22*, 393–403.

Berta, M. a, Mazure, N., Hattab, M., Pouysségur, J., and Brahimi-Horn, M. C. (2007). SUMOylation of hypoxia-inducible factor-1alpha reduces its transcriptional activity. Biochem. Biophys. Res. Commun. *360*, 646–652.

Bruer, U., Weih, M. K., Isaev, N. K., Meisel, a, Ruscher, K., Bergk, A, Trendelenburg, G., Wiegand, F., Victorov, I. V, and Dirnagl, U. (1997). Induction of tolerance in rat cortical neurons: hypoxic preconditioning. FEBS Lett. *414*, 117–121.

Chen, X., Tian, Y., Yao, L., Zhang, J., and Liu, Y. (2010). Hypoxia stimulates proliferation of rat neural stem cells with influence on the expression of cyclin D1 and c-Jun N-terminal protein kinase signaling pathway in vitro. Neuroscience *165*, 705–714.

Cockman ME., Masson N., Mole DR., Jaakkola P., Chang GW., Clifford SC., Maher ER., Pugh CW., Ratcliffe PJ., Maxwell PH. (2000). Hypoxia inducible factor-alpha binding and ubiquitylation by the von Hippel-Lindau tumor suppressor protein. J. Biol. Chem. *175*, 25733–25741.

Comerford, K. M., Cummins, E. P., and Taylor, C. T. (2004). c-Jun NH2-terminal kinase activation contributes to hypoxia-inducible factor 1alpha-dependent P-glycoprotein expression in hypoxia. Cancer Res. *64*, 9057–9061.

Cross, D., Alessi, D., and Cohen, P. (1995). Inhibition of glycogen synthase kinase-3 by insulin mediated by protein kinase B. Nature *378*, 785–789.

Diebold, I., Petry, A., Djordjevic, T., Fineman, J., Black, S., Schreiber, C., Fratz, S., Hess, J., Kietzmann, T., and Go, A. (2010). Reciprocal Regulation of Rac1 and PAK-1 by HIF-1 a : A Positive-Feedback Loop Promoting. Antioxid. Redox Signal. *13*, 399–412.

Flügel, D., Görlach, A., and Kietzmann, T. (2012). GSK-3β regulates cell growth, migration, and angiogenesis via Fbw7 and USP28-dependent degradation of HIF-1α. Blood *119*, 1292–1301.

Flügel, D., Görlach, A., Michiels, C., and Kietzmann, T. (2007). Glycogen synthase kinase 3 phosphorylates hypoxia-inducible factor 1alpha and mediates its destabilization in a VHL-independent manner. Mol. Cell. Biol. *27*, 3253–3265.

Görlach, A., Berchner-Pfannschmidt, U., Wotzlaw, C., Cool, R. H., Fandrey, J., Acker, H., Jungermann, K., and Kietzmann, T. (2003). Reactive oxygen species modulate HIF-1 mediated PAI-1 expression : involvement of the GTPase Rac1. J. Thromb. Haemost. *89*, 926–935.

Halterman, M. W., Miller, C. C., and Federoff, H. J. (1999). Hypoxia-inducible factor-1alpha mediates hypoxia-induced delayed neuronal death that involves p53. J. Neurosci. *19*, 6818–6824.

Hirota, K., and Semenza, GL. (2001). Rac1 activity is required for the activation of hypoxia-inducible factor 1. J. Biol. Chem. *276*, 21166–21172.

Honma, H., Podratz, J. L., and Windebank, A. J. (2003). Acute glucose deprivation leads to apoptosis in a cell model of acute diabetic neuropathy. J. Peripher. Nerv. Syst. *8*, 65–74.

Inukai K., Anai M., Van Breda E., Hosaka T., Katagiri H., Funaki M., Fukushima Y., Ogihara T., Yazaki Y., Kikuchi., Oka Y., Asano T. (1996). A Novel 55-kDa Regulatory Subunit for Phosphatidylinositol 3-Kinase Structurally Similar to p55PIK Is Generated by Alternative Splicing of the p85 Gen. J. Biol. Chem. *271*, 1–5.

Iyer NV., Kotch LE., Agani F., Leung SW., Laughner E., Wenger RH., Gassmann M., Gearhart JD., Lawler AM., Yu AY., Semenza GL. (1998). Cellular and developmental control of O2 homeostasis by hypoxia-inducible factor 1 alpha. Genes Dev. *12*, 149–162.

Jaakkola P., Mole DR., Tian YM., Wilson MI., Gielbert J., Gaskell SJ., von Kriegsheim A., Hebestreit HF., Mukherji M., Schofield CJ., Maxwell PH., Pugh CW., Ratcliffe PJ. (2001). Targeting of HIF-alpha to the von Hippel-Lindau ubiquitylation complex by O2-regulated prolyl hydroxylation. Science *292*, 468–472.

Jiang, B. H., Jiang, G., Zheng, J. Z., Lu, Z., Hunter, T., and Vogt, P. K. (2001). Phosphatidylinositol 3-kinase signaling controls levels of hypoxia-inducible factor 1. Cell Growth Differ. *12*, 363–369.

Jiang, B., Rue, E., Guang, L., Roe, R., Semenza, G. L., and Wang, G. L. (1996). Dimerization , DNA Binding , and Transactivation Properties of Dimerization , DNA Binding , and Transactivation Properties of Hypoxia-inducible Factor 1. J. Biol. Chem. *271*, 17771–17778.

Jin, H. G., Yamashita, H., Nagano, Y., Fukuba, H., Hiji, M., Ohtsuki, T., Takahashi, T., Kohriyama, T., Kaibuchi, K., and Matsumoto, M. (2006). Hypoxia-induced upregulation of endothelial small G protein RhoA and Rho-kinase/ROCK2 inhibits eNOS expression. Neurosci. Lett. *408*, 62–67.

Jin, K. L., Mao, X. O., Nagayama, T., Goldsmith, P. C., and Greenberg, D. A. (2000). Induction of vascular endothelial growth factor and hypoxia-inducible factor-1alpha by global ischemia in rat brain. Neuroscience *99*, 577–585.

Kallio, P. J., Okamoto, K., Brien, S. O., Carrero, P., Makino, Y., Tanaka, H., and Poellinger, L. (1998). Signal transduction in hypoxic cells : inducible nuclear translocation and recruitment of the CBP / p300 coactivator by the hypoxia-inducible factor-1 α. EMBO *17*, 6573–6586.

Kim, J.-Y., Ahn, H.-J., Ryu, J.-H., Suk, K., and Park, J.-H. (2004). BH3-only protein Noxa is a mediator of hypoxic cell death induced by hypoxia-inducible factor 1alpha. J. Exp. Med. *199*, 113–124.

Kim, S., Lee, K.-Y., Koh, S.-H., Park, H.-H., Yu, H.-J., and Lee, Y. J. (2012). Role of the phosphatidylinositol 3-kinase and extracellular signal-regulated kinase pathways in the neuroprotective effects of cilnidipine against hypoxia in a primary culture of cortical neurons. Neurochem. Int. *61*, 1172–1182.

Li, D., and Brorson, J. (2013). Adaptation to moderate hypoxia protects cortical neurons against ischemia-reperfusion injury and excitotoxicity independently of HIF-1α. Exp. Neurol. *230*, 302–310.

Lin, C., Cheng, H., Ma, H., Wu, C., and Hong, C. (2011). Thrombin Induces NF- κ B Activation and IL-8 / CXCL8 Expression in Lung Epithelial Cells by a Rac1-dependent PI3K / Akt Pathway. J. Biol. Chem. *286*, 10483–10494.

Linseman, D., and Loucks, F. (2008). Diverse roles of Rho family GTPases in neuronal development, survival, and death. Front. Biosci. *13*, 657–676.

Liu, J., Narasimhan, P., Yu, F., and Chan, P. H. (2005). Neuroprotection by Hypoxic Preconditioning Involves Oxidative Stress-Mediated Expression of Hypoxia-Inducible. Stroke *36*, 1264–1269.

Minden, A., Lin, A., Abo, A., and Karin, M. (1995). Selective Activation of the JNK Signaling Cascade and c-Jun Transcriptional Activity by the Small GTPases Rac and Cdc42Hs. Cell *81*, 1147–1157.

Minet, E., Michel, G., Mottet, D., Piret, JP., Barbieux, A, Raes, M., and Michiels, C. (2001). c-JUN gene induction and AP-1 activity is regulated by a JNK-dependent pathway in hypoxic HepG2 cells. Exp. Cell Res. *265*, 114–124.

Mollen, KP., McCloskey, CA., Tanaka, H., Prince, JM., Levy, RM., Zuckerbraun, BS., and Billiar, TR. (2007). Hypoxia activates c-Jun N-terminal kinase via Rac1-dependent reactive oxygen species production in hepatocytes. Shock *28*, 270–277.

Mottet, D., Dumont, V., Deccache, Y., Demazy, C., Ninane, N., Raes, M., and Michiels, C. (2003). Regulation of hypoxia-inducible factor-1alpha protein level

during hypoxic conditions by the phosphatidylinositol 3-kinase/Akt/glycogen synthase kinase 3beta pathway in HepG2 cells. J. Biol. Chem. *278*, 31277–31285.

Murga, C., Zohar, M., Teramoto, H., and Gutkind, J. S. (2002). Rac1 and RhoG promote cell survival by the activation of PI3K and Akt, independently of their ability to stimulate JNK and NF-κB. Oncogene *21*, 207–216.

Mylonis, I., Chachami, G., Samiotaki, M., Panayotou, G., Paraskeva, E., Kalousi, A., Georgatsou, E., Bonanou, S., and Simos, G. (2006). Identification of MAPK phosphorylation sites and their role in the localization and activity of hypoxia-inducible factor-1alpha. J. Biol. Chem. *281*, 33095–33106.

Noh, K., Hwang, J., Follenzi, A., Athanasiadou, R., and Miyawaki, T. (2012). Repressor element-1 silencing transcription factor (REST) -dependent epigenetic remodeling is critical to ischemia-induced neuronal death. PNAS *109*, E962–E971.

Ogunshola, OO., Antic, A., Donoghue, MJ., Fan, SY., Kim, H., Stewart, WB., Madri, JA, and Ment, LR. (2002). Paracrine and autocrine functions of neuronal vascular endothelial growth factor (VEGF) in the central nervous system. J. Biol. Chem. *277*, 11410–11415.

Papandreou, I., Krishna, C., Kaper, F., Cai, D., Giaccia, A. J., and Denko, N. C. (2005). Anoxia Is Necessary for Tumor Cell Toxicity Caused by a Low-Oxygen Environment Anoxia Is Necessary for Tumor Cell Toxicity Caused by a Low-Oxygen Environment. Cancer Res. *65*, 3171–3178.

Pons, S., Asano, T., Glasheen, E., Zhang, Y., Fisher, T. L., Myers, M. G., Sun, X. J., and White, M. F. (1995). The Structure and Function of p55 PIK Reveal a New Regulatory Subunit for Phosphatidylinositol 3-Kinase. Mol. Cell. Biol. *15*, 4453–4465.

Roh, MS., Eom, TY., Zmijewska, A., De Sarno, P., Roth, KA, and Jope, RS. (2005). Hypoxia activates glycogen synthase kinase-3 in mouse brain in vivo: protection by mood stabilizers and imipramine. Biol. Psychiatry *57*, 278–286.

Schnitzer, E., Schmid, T., Zhou, J., Eisenbrand, G., and Brüne, B. (2005). Inhibition of GSK3 b by indirubins restores HIF-1 a accumulation under prolonged periods of hypoxia / anoxia. FEBS Lett. *579*, 529–533.

Snyder, C. M., and Chandel, N. S. (2009). Mitochondrial Regulation of Cell Survival and Death During Low-Oxygen Conditions. Antioxid. Redox Signal. *11*, 2673–2683.

Turcotte, S., Desrosiers, R. R., and Béliveau, R. (2003). HIF-1alpha mRNA and protein upregulation involves Rho GTPase expression during hypoxia in renal cell carcinoma. J. Cell Sci. *116*, 2247–2260.

Wang, G., and Semenza, G. (1995). Purification and characterization of hypoxia-inducible factor 1. J. Biol. Chem. *270*, 1230–1237.

Wohnsland, S., Bürgers, H. F., Kuschinsky, W., and Maurer, M. H. (2010). Neurons and neuronal stem cells survive in glucose-free lactate and in high glucose cell culture medium during normoxia and anoxia. Neurochem. Res. *35*, 1635–1642.

Xu, Y., Li, Y., Li, H., Pang, Y., Zhao, Y., Jiang, R., and Shen, L. (2013). The accumulations of HIF-1 α and HIF-2 α by JNK and ERK are involved in biphasic effects induced by different levels of arsenite in human bronchial epithelial cells. Toxicol. Appl. Pharmacol. *266*, 187–197.

Xue, Y., Bi, F., Zhang, X., Zhang, S., Pan, Y., Liu, N., Shi, Y., Yao, X., Zheng, Y., and Fan, D. (2006). Role of Rac1 and Cdc42 in hypoxia induced p53 and von Hippel-Lindau suppression and HIF1alpha activation. Int. J. Cancer *118*, 2965–2972.

Yamauchi, J., Miyamoto, Y., Sanbe, A., and Tanoue, A. (2006). JNK phosphorylation of paxillin , acting through the Rac1 and Cdc42 signaling cascade , mediates neurite extension in N1E-115 cells. Exp. Cell Res. *312*, 1954–2961.

Zhang, L., Qu, Y., Tang, J., Chen, D., Fu, X., Mao, M., and Mu, D. (2010). PI3K/Akt signaling pathway is required for neuroprotection of thalidomide on hypoxic – ischemic cortical neurons in vitro. Brain Res. *1357*, 1357–165.

Zhang, P., Zhang, X., Hao, X., Wang, Y., Hui, Y., Wang, H., Hu, D., and Zhou, J. (2009). Rac1 activates HIF-1 in retinal pigment epithelium cells under hypoxia. Graefes Arch. Clin. Exp. Ophthalmol. *247*, 633–639.

Zhang, S., Gozal, D., Sachleben, L., Rane, M., Klein, J., and Gozal, E. (2003). Hypoxia induces an autocrine-paracrine survival pathway via platelet-derived growth factor (PDGF)-B/PDGF- β receptor/phosphatidylinositol 3-kinase/Akt signaling in RN46A neuronal cells. FASEB J. *17*, 1709–1711.

Zhong, H., Chiles, K., Feldser, D., Laughner, E., Hanrahan, C., Georgescu, M., Simons, J. W., and Semenza, G. L. (2000). Modulation of Hypoxia-inducible Factor 1 α Expression by the Epidermal Growth Factor /Phosphatidylinositol 3-kinase/PTEN/AKT/FRAP Pathway in Human Prostate Cancer Cells : Implications for Tumor Angiogenesis and Therapeutics Advances in Brief Prosta. J. Cancer Res. *60*, 1541–1545.

Zhu, W., and Nelson, C. M. (2013). PI3K regulates branch initiation and extension of cultured mammary epithelia via Akt and Rac1 respectively. Dev. Biol. *379*, 235–245.

Figure 1

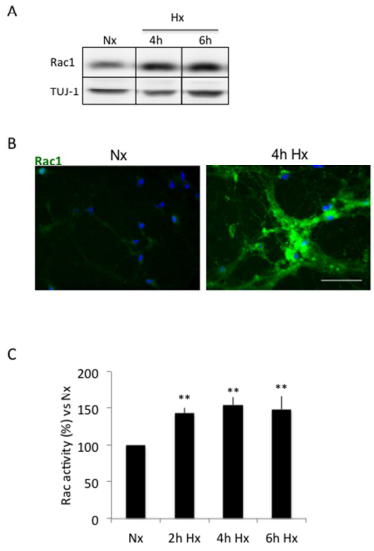

Figure 1. Rac1 is upregulated and activated during hypoxia.
Cells were incubated for 4h and 6h under normoxic (Nx) or hypoxic (Hx) conditions. Cell lysates were used to detect total Rac1 protein levels by Western blot. TUJ-1 was used as loading control (A). Cellular Rac1 levels were additionally analyzed by Immunocytochemistry (B) green: Rac1, blue: DAPI, scale bar: 50 µm. Rac1 activity was determined by G-LISA (C). ** $p<0.01$ versus normoxia. Data were analyzed using one-way ANOVA followed by Bonferroni post-hoc test.

254x338mm (72 x 72 DPI)

Figure 2

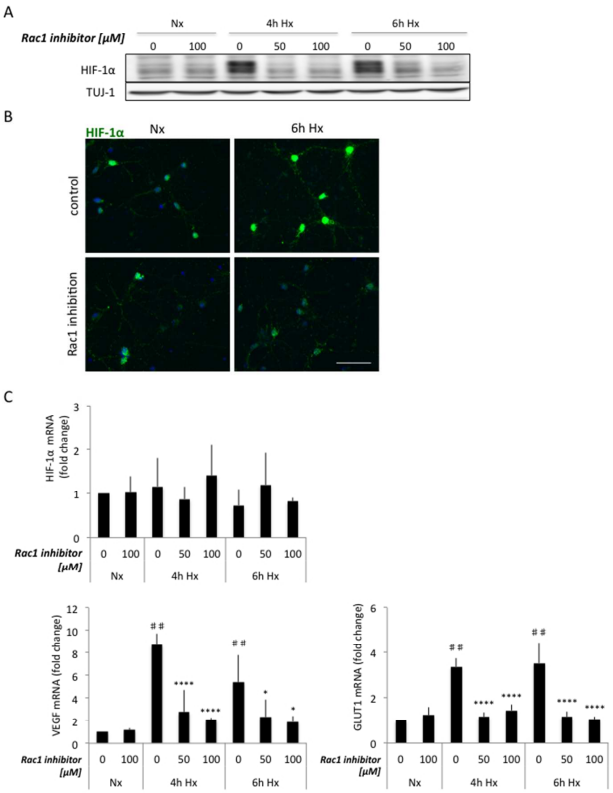

Figure 2: Rac1 is crucial for HIF-1α-mediated signaling in neurons.
Cells were treated with 50 or 100 μM Rac1 inhibitor just prior to normoxic (Nx) or hypoxic (Hx) exposure. A, extracts were resolved by SDS-PAGE and HIF-1α protein levels were determined by Western blot. TUJ-1 was used as loading control. B, Normoxic and hypoxic cells with or without 100 μM Rac1 inhibitor were fixed and immunolabeled for HIF-1α (green) and counterstained with DAPI (blue). Scale bar: 50 μm. C, Rac1 treated and untreated cells were put into Trizol after normoxic and hypoxic exposure. RNA was extracted and the cDNA was used to analyze the expression of HIF-1α and HIF-1 target genes VEGF and GLUT1 by TaqMan-based RT-PCR. Data were normalized to GAPDH and fold change is compared to normoxic control sample. # # p<0.01 versus normoxic control, * p<0.05, **** p<0.0001, comparison within the group. Data were analyzed using two-way ANOVA followed by Bonferroni post-hoc test.
254x338mm (72 x 72 DPI)

Figure 3

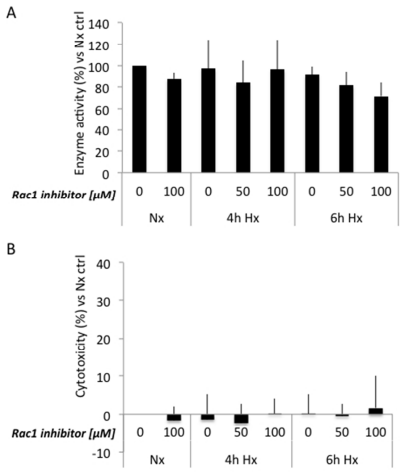

Figure 3: Neurons survive acute hypoxia without Rac1 and HIF-1α.
Cells were treated with Rac1 inhibitor and kept under normoxic (Nx) or hypoxic conditions (Hx). Untreated neurons were used as control. The effect of short hypoxic insults and the inhibition of Rac1 on cell death were determined by two methods. A, MTT assay was used as an indicator for cell survival. B, LDH release into the culture medium was measured to detect cytotoxicity. Data analysis was performed using two-way ANOVA followed Bonferroni post-hoc test.

254x338mm (72 x 72 DPI)

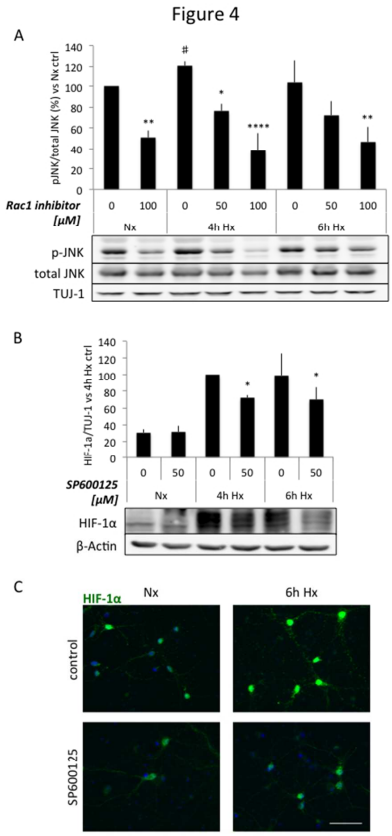

Figure 4: JNK is involved in Rac1-dependent HIF-1α regulation.
A, The Effect of Rac1 inhibition on JNK activity was assessed by Western blot using antibodies that detect phosphorylated or total JNK protein. Cells were treated with 50μM or 100 μM Rac1 inhibitor and kept under normal conditions (Nx) or were exposed to hypoxia (Hx). Untreated neurons were used as controls. Results display the ratio of phosphorylated to total protein levels normalized to the loading control TUJ-1 and compared to the normoxic control sample. B, Neurons were pretreated with 50 μM of JNK inhibitor SP600125 for 1h prior to hypoxic or normoxic exposure and HIF-1α levels were compared to untreated samples by Western blot. The graph shows HIF-1α protein levels normalized to the loading control β-Actin. The 4h hypoxic samples were set to 100%. # $p<0.05$ versus Nx, *$p<0.05$, **$p<0.01$, ****$p<0.0001$ comparison within the groups. Data were analyzed using two-way ANOVA followed by Bonferroni post-hoc test. For comparison between hypoxia and normoxia effects only we used paired, two-tailed Student`s t-test. C, Immunocytochemistry was performed to asses cellular HIF-1α levels in normoxia and hypoxia in the presence or absence of 50 μM JNK inhibitor SP600125. Green: HIF-1α, blue: DAPI, Scale bar: 50 μM.

Figure 5

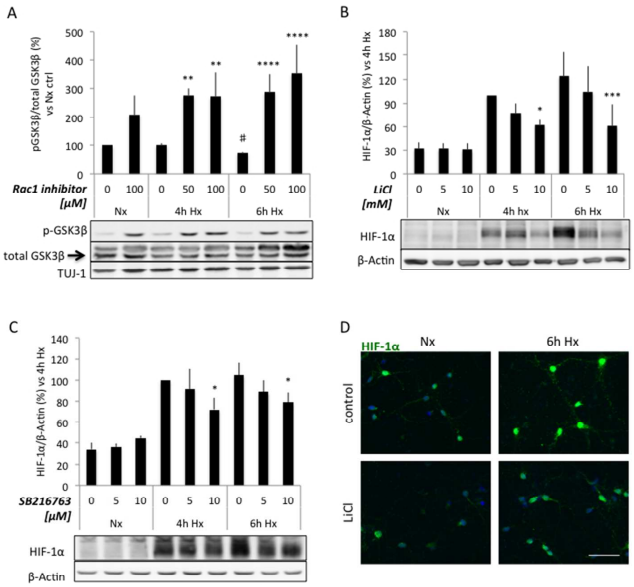

Figure 5: Active GSK3β is critical for HIF-1a accumulation in neurons during hypoxia. Cells were treated with 50 or 100 μM Rac1 inhibitor und exposed to 4h and 6h of hypoxia (Hx) or kept under normoxia (Nx). Untreated neurons were used as controls. A, Western blots were performed to first detect the phosphorylated form and then the total protein of GSK3β. TUJ-1 was used as loading control. B,C Western blots were used to analyze the effect of GSK3 blockade on HIF-1α levels. GSK3 was inhibited by treatment with 5 mM and 10 mM LiCl or 5 μM and 10 μM SB216763 24h prior to hypoxic exposure. Graphs show quantification of normalized HIF-1α levels of cells treated with LiCL (B) or SB216763 (C). The 4h hypoxic control sample was set to 100% and β-Actin was used as loading control. Error bars represent SD. * p<0.05, ** p<0.01, *** p<0.001 and **** p< 0.0001, comparison within the group. Data were analyzed using two-way ANOVA followed by Bonferroni post-hoc test. For comparison between hypoxia and normoxia effects only we used paired, two-tailed Student`s t-test. # p<0.05 versus Nx control. D, Immunocytochemistry was used to demonstrate cellular HIF-1α levels in normoxia and hypoxia in the presence or absence of 10 mM LiCl (C). Green: HIF-1α, blue: DAPI, Scale bar: 50 μM.

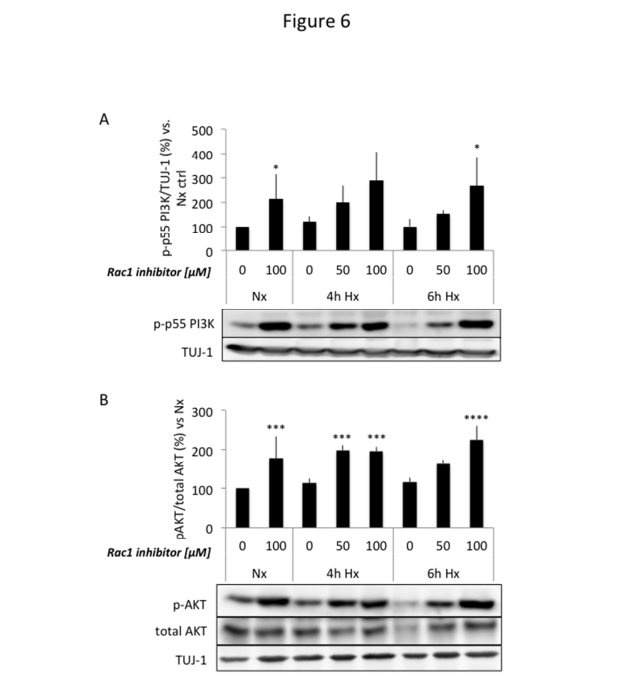

Figure 6: Rac1 may regulate GSK3β activity via PI3K/AKT pathway
Lysates of cells treated with or without Rac1 inhibitor (50 and 100 μM) were used for Western blot to detect phosphorylated and total protein levels of PI3K p55 (A) and AKT (B) in normoxia (Nx) and hypoxia (Hx). Results are expressed as the ratio of phosphorylated to total protein and data is normalized to the loading control TUJ-1. Error bars represent SD. * p<0.05, *** p<0.001, **** p< 0.0001, comparison within the group. Data analysis was performed using two-way ANOVA followed by Bonferroni post-hoc test.
254x338mm (72 x 72 DPI)

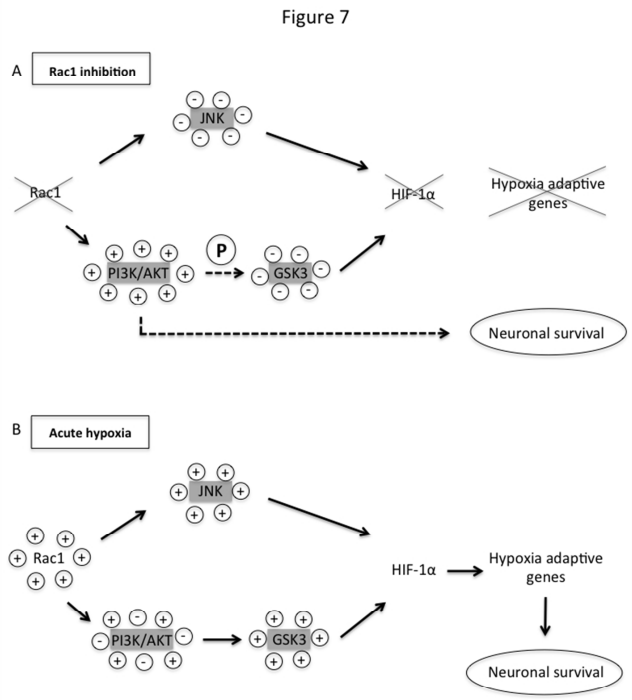

Figure 7: Rac1-dependent regulation of HIF-1α in neurons.
The scheme summarizes our data. B, Shows the effect of Rac1 inhibition. The dashed lines remain to be further investigated. P: phosphorylation. A, Schematic representation of the conclusions from our results. (+): activation, (-): inactivation.

254x338mm (72 x 72 DPI)

Supplementary figure 1

A

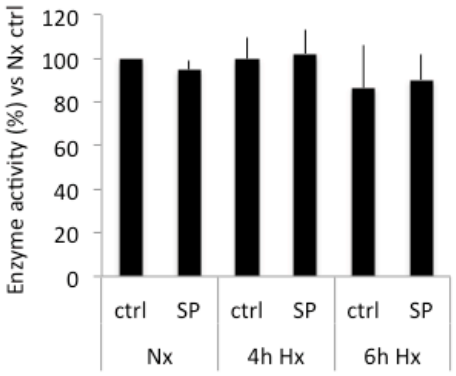

B

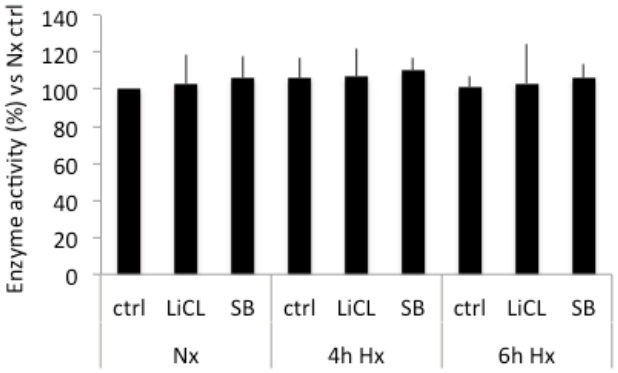

Supplementary figure 2

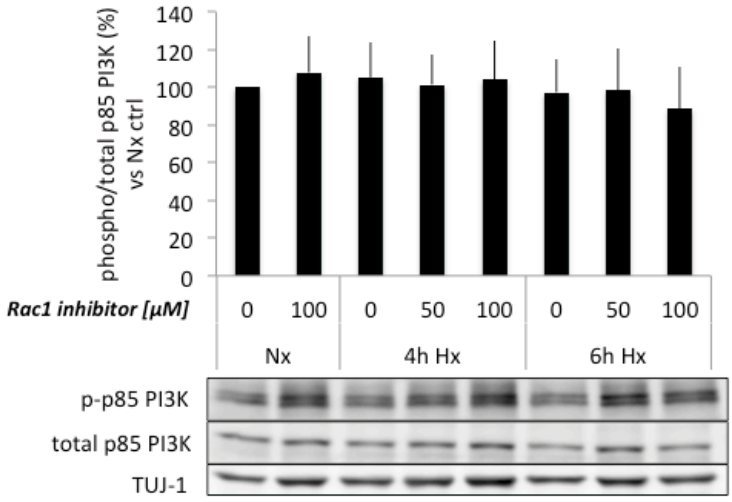

Supplementary Figure 1: Inhibition of JNK and GSK3 does not affect neuronal survival.

A, MTT assay was used to determine the effect of 50 μM JNK inhibitor SP600125 (SP) on cell survival during normoxia (Nx) and hypoxia (Hx) compared to Nx control (ctrl). B, Cells were pretreated for 24h with 10 mM LiCl or 10 μM SB216763 (SB) and then exposed to hypoxia or kept under normoxic conditions before cell survival was measured by MTT assay. Results were compared to normoxic control. Error bars represent SD.

Supplementary Figure 2: Rac1 inhibition does not alter PI3K p85 subunit.

Lysates of normoxic (Nx) and hypoxic (Hx) cells with or without Rac1 inhibitor treatment were used to detect phosphorylated and total levels of PI3K p85 by Western blot. The graph shows the ratio of phosphorylated to total p85 subunit compared to normoxic control (ctrl). TUJ-1 was used as loading control. Error bars represent SD.

6.2 1-Deoxysphingolipid-induced neurotoxicity involves N-methyl-D-aspartate receptor signaling

Tanja Güntert[1,5], Alaa Othman[2,5], Sabrina Sonda[3], Richard A. Zuellig[4], Thorsten Hornemann[2,5], Omolara O. Ogunshola[1,5]

[1] Institute of Veterinary Physiology, Vetsuisse Faculty, University of Zurich,

[2] Institute for Clinical Chemistry, University Hospital Zurich,

[3] Swiss Hepato-Pancreato-Biliary Center, Department of Visceral and Transplantation Surgery, University Hospital, Zurich

[4] Division of Endocrinology, Diabetes and Clinical Nutrition, University Hospital, Zurich,

[5] Zurich Center of Integrative Human Physiology (ZIHP), Zurich, Switzerland.

Manuscript submitted to Neurobiology of Disease

Personal contribution: *All experiments (with exception of the experiments for figure 1C and supplementary figure A) and manuscript writing has been done by Tanja Güntert.*

1-Deoxysphingolipid-induced neurotoxicity involves N-methyl-D-aspartate receptor signaling.

Tanja Güntert[A,E], Alaa Othman[B,E], Sabrina Sonda[C], Richard A. Zuellig[D,E], Thorsten Hornemann[B,E], Omolara O. Ogunshola[A,E *]

[A] Institute of Veterinary Physiology, Vetsuisse Faculty, University of Zurich,

[B] Institute for Clinical Chemistry, University Hospital Zurich,

[C] Swiss Hepato-Pancreato-Biliary Center, Department of Visceral and Transplantation Surgery, University Hospital, Zurich

[D] Division of Endocrinology, Diabetes and Clinical Nutrition, University Hospital, Zurich,

[E] Zurich Center of Integrative Human Physiology (ZIHP), Zurich, Switzerland.

Running Title: Deoxysphingolipid-induced neurotoxicity

* Corresponding author:
Omolara O. Ogunshola, PhD
Institute of Veterinary Physiology & Zurich Center of Integrative Human Physiology (ZIHP),
Vetsuisse Faculty,
University of Zurich,
Winterthurerstrasse 260, CH-8057 Zurich, Switzerland
Tel: +41 44 635 8805, Fax: +41 44 635 8, Email: larao@access.uzh.ch

Total number of figures: 7, total number of tables: 0, supplementary figures: 4.

Abstract

The formation of 1-deoxysphingolipids, including 1-deoxysphinganine has been identified as major pathological player in hereditary sensory and autosomal neuropathy type 1. However the molecular mechanisms by which 1-deoxysphingolipids induce neurotoxicity is unknown. To get a handle on their action, we treated primary neurons with the atypical sphingoid base 1-deoxysphinganine or its canonical counterpart C_{18}sphinganine and studied the outcome on cell survival and cytoskeleton integrity. Here we demonstrate that 1-deoxysphinganine is internalized and metabolized to 1-deoxydihydroceramide species that mediate the neurotoxic effects since inhibition of ceramide synthase protected neurons from 1-deoxysphinganine-mediated cell death. Treatment with 1-deoxysphinganine led to alterations of multiple components of the neuronal cytoskeleton and deregulation of cytoskeleton-regulating proteins like Rac1, Ezrin and insulin receptor substrate 53. Furthermore, 1-deoxysphinganine triggered changes in protein levels of N-methyl-D-aspartate receptor subunit NR2B, the postsynaptic density protein 95 and induced cleavage of p35 to p25. Notably, blocking the N-methyl-D-aspartate receptor by MK-801 or memantine significantly prevented the 1-deoxysphinganine-induced effects. Overall, our results show that mechanisms of 1-deoxysphinganine-induced neurotoxicity target cytoskeletal rearrangements and N-methyl-D-aspartate receptor signaling. This suggests that besides the stabilization of cytoskeletal structures the inhibition of glutamate receptors could be a potential therapeutic approach to prevent 1-deoxysphingolipid-induced neurodegeneration.

Keywords: Hereditary sensory and autosomal neuropathy type 1, lipid metabolism, cytoskeleton, Rac1, glutamate receptor

Introduction

Sphingolipids not only participate in plasma membrane formation but are also important signaling molecules involved in several cellular processes (Ghosh et al., 1990; Lépine et al., 2011; Obeid et al., 1993; Sim-Selley et al., 2009). The first step of the *de novo* sphingolipid biogenesis is catalyzed by the serine-palmitoyltransferase (SPT) that conjugates palmitoyl-CoA with L-serine. Recently it was shown that SPT can also use other amino acids as alternative substrates such as alanine or glycine to a certain extent. This forms a class of atypical 1-deoxy-long chain bases (1-deoxy-LCBs), (Zitomer et al., 2009) that lack the C1-hydroxyl group of the canonical substrate sphinganine (C18SA). The conjugation with alanine forms 1-deoxysphinganine (1-deoxySA) whereas the use of glycine results in 1-deoxymethylsphinganine. Thus deoxyLCBs can be metabolized to 1-deoxy(dihydro)ceramides and 1-deoxysphingosine but not further to complex sphingolipids nor canonically degraded as the catabolic intermediate sphigosine-1-phosphate cannot be formed. In consequence they accumulate and were shown to induce cell death in different cells types (Cuadros et al., 2000; Salcedo et al., 2007; Sánchez et al., 2008; Zuellig et al., 2013). In isolated dorsal root ganglion neurons a neurotoxic effect of deoxyLCBs was highlighted and associated with alterations in neurofilament structure and neurite numbers (Penno et al., 2010).

Hereditary sensory and autosomal neuropathy type 1 (HSNA1) is a dominantly inherited axonal neuropathy that is clinically characterized by a progressive loss of pain and temperature sensation and possible neuropathic pain attacks and skin ulcers (Houlden et al., 2006). HSAN1 is associated with several missense mutations in the SPT genes SPTLC1 and SPTLC2. These mutations greatly increase the activity of SPT with alanine and glycine and results in a pathologically enhanced deoxyLCB

generation which underlies the HSAN1 pathology (Eichler et al., 2009; Gable et al., 2010; Penno et al., 2010). Elevated plasma levels of deoxyLCBs were also found in an HSAN1 mouse model (Eichler et al., 2009). Clinically, HSAN1 is very similar to diabetic sensory neuropathy (DSN), the most common chronic complication in diabetes. Recently deoxyLCBs were reported to be elevated in plasma of patients with metabolic syndrome and diabetes mellitus type 2 (Bertea et al., 2010; Othman et al., 2012). This suggests that deoxyLCBs may be novel therapeutic targets for the treatment of T2DM and DSN. It is therefore important to get a better insight on the mechanisms by which deoxyLCBs mediate their neurotoxic activity. The objective of this study was to investigate the impact of 1-deoxySA on cell survival and cytoskeletal integrity in cultured neurons and to unravel the underlying molecular mechanisms that drive 1-deoxySA-induced cell death and cytoskeletal alterations.

Material and Methods

All experiments were performed in accordance with Swiss animal protection laws and University of Zürich institutional guidelines for animal experimentation.

Reagents and Antibodies

If not stated differently chemicals and reagents were purchased from Sigma-Aldrich (Missouri, USA). All cell culture reagents were purchased from Life Technologies (Zug, Switzerland). The following antibodies were used: anti Rac1 (BD Biosciences, San Jose, CA, USA), anti RhoA and anti p35/25 (Santa Cruz, CA, USA), anti β-Actin (Sigma), anti TUJ-1 (COVANCE, Berkeley, CA, USA), anti phospho JNK and anti total JNK (R&D Systems, Minneapolis, MN, USA), anti NF-H and anti NF-L

(NOVUS, Littleton, USA), anti phospho Ezrin (Thr567) and anti total Ezrin, anti PSD-95, anti IRSp53, anti MAP2, anti NMDAR2B (all Cell signaling, Danvers, MA, USA). InSolution Rac1 inhibitor (Millipore, Billerica, MA, USA), Rho inhibitor (Cytoskeleton, Denver, CO, USA), JNK inhibitor SP600125 (Sigma).

Neuronal culture

Primary neuronal cells were obtained from cerebral cortex of C57Bl/6 mouse embryos at gestational stage E14 as described previously (Ogunshola et al., 2002). Following dissection cortices were dissociated in Hank`s buffer saline containing trypsin and DNaseI for 5 min at 37°C. Cells were seeded on poly-L-lysine coated plastic petri dishes or on poly-D-lysine coated glass coverslips in 24 well plates (60 000 cells/cm^2). Neurobasal medium was complemented with B27 supplement (1X), AlbuMAXI (0.25g/ml), streptavidin-penicillin (1%), Sodium-Pyruvate 100U/ml and L-Glutamine (0.5 mM). Neurons were maintained at normal atmosphere (21% O_2, 5% CO_2) in a humidified incubator at 37 °C for 6 or 17 days (days in vitro=DIV). Half the media was replaced every 6 days.

Lipid and inhibitor treatment

Lipids were synthesized as BSA complex as described in (Penno et al., 2010) and added to the cells for 24 or 48 hours. BSA was used as control. Fumonisin B1 and inhibitors of Rac1, RhoA and JNK were added 30 min prior cells were exposed to the lipids. MK-801 and memantine were added 1h prior lipid treatment.

Analysis of sphingoid bases and ceramides by LC–MS/MS

Ceramide species were extracted by adding 1 ml methanol/chloroform (2:1) (including 200 pmole of C_{12} ceramide or C_{12} 1-deoxydihydroceramide internal standards (Avanti Polar Lipids) to 100 µl of re-suspended cells followed by the addition of 0.5 ml of chloroform and 200 µl alkaline water. Interfering phospholipids were hydrolyzed by re-extracting the dried lipids with methanol-KOH:chloroform (4:1) as described earlier (Penno 2010). Lipids were separated on a C18 column (Uptispere 120 Å, 5µm, 125 × 2 mm, Interchim, France) and analyzed on a TSQ Quantum Ultra (Thermo, Reinach, Switzerland) using atmospheric pressure chemical ionization (APCI) (10). Ceramides and 1-deoxydihydroceramides were identified by precursor ion scan (20mV collision energy) with fragments of (m/z 264.3) and (m/z 268.3) respectively

Western Blot

Neurons were lysed in ice-cold lysis buffer (150 mM NaCl, 50 mM Tris, 1% Triton X-100, 1% NP-40) for 10 min and centrifuged at 16 000 rcf for 10 min at 4°C. The supernatant was collected and stored at -20°C. Protein concentration was measured using Bio-Rad assay (according manufacturers protocol). 40-60 µg of protein were loaded on SDS-polyacrylamide gels then transferred to nitrocellulose membrane. After blocking in 0.1% TBS-Tween with 5% milk powder or 5 % BSA membranes were incubated overnight at 4°C with primary antibody. Membranes were washed before being incubated with an HRP-conjugated secondary antibody for 1h at room temperature. All blots were normalized to TUJ-1 or to β-Actin and quantified by densitometry using imageJ software.

RNA isolation and PCR Array

Total neuronal RNA was extracted using TRIzol reagent (Invitrogen, AG, Switzerland) according to the manufacturer`s protocol and RNA concentration and quality was detected using NanoDrop spectrophotometer (Thermo Scientific, Walthman, MA, USA). Equivalent amounts of RNA were used for subsequent cDNA synthesis with the RT^2 First Strand (SABiosciences). Together with the RT^2 qPCR Master Mix the obtained cDNA was loaded into each well of the 96-well Mouse Cytoskeleton Regulators RT^2 Profiler PCR Array System (SABiosciences, Hombrechtikon, Switzerland). The PCR was run according to the manufacturer`s protocol using an ABI 7500 RT-PCR thermocycler (Applied Biosystems, Foster City, CA, USA) and obtained data were analyzed using the Excel template provided by SABiosciences based on the ΔΔCt-Method.

Immunocytochemistry

Cells on glass coverslips were fixed for 5 min in 4% paraformaldehyde in PBS, permeabilized 3 to 5 minutes with 0.1% Triton X-100 in PBS and then blocked in 10% normal goat serum. Antibodies were applied overnight at 4°C. Cells were incubated with fluorescent secondary antibody (AlexaFluor488, AlexaFluor594, Molecular Probes, Leiden, Netherlands) for 1h at room temperature. After washing with PBS cells were counterstained with 10 nM DAPI in H_2O for 5 min. For F-actin staining cells were incubated in Phalloidin-tetramethylrhodamine for 40 min at room temperature after fixation. Coverslips were mounted in fluorescent mounting medium (Dako, Glostrup, Denmark) then viewed and analyzed with an Axiovert inverted fluorescent microscope (Zeiss, Germany).

Rho GTPase activity assay (G-LISA)

The activation of Rac1 and RhoA was assessed by using the colorimetric G-LISA Activation Assay Biochem Kits (BK125, BK124, Cytoskeleton, Denver, CO, USA). Briefly lysates were collected, protein concentrations were determined and samples were snap-frozen until the assay was prepared. All steps were performed according to the manufacturer's protocol.

Cell death assays

1) LDH assay: To quantify cell death the release of lactate dehydrogenase from cells into the culture medium was detected using Cytotoxicity Detection Kit (Roche, Penzberg, Germany) according to the manufacturer's instructions.

2) MTT assay: Thiazolyl blue tetrazolium bromide was dissolved in PBS and added to the cells in a 96 well format (final concentration 0.5 mg/ml). After 1h incubation at 37°C media was removed and 100 µL dimethyl sulfoxide was added to cells to measure absorption at 595 nm (subtract background at 670 nm).

Statistical analysis

All graphs represent at least 3 independent experiments and analyzed using GraphPad Prism software. In all graphs error bars represent the mean ± standard deviation. Data were analyzed using one-way or two-way ANOVA and subsequent Bonferroni post-hoc testing was done. A value of $p<0.05$ was considered significant with * used to designate comparison between the lipid treatments and $ for comparison of inhibitor treatments with the lipid-only control within the group.

Results

1-deoxySA is toxic for cortical neurons.

We first analyzed the effect of 1-deoxysphinganine (1-deoxySA) on the survival of cortical neurons. Neurons were cultured for 17 days after isolation and then treated for 24h and 48h with either 1-deoxySA, C18SA or C18SO. C18SA and C18SO are the canonical LCBs. Since the lipids were complexed to BSA, lipid-free BSA was used as control. Cell death was monitored using MTT assay and LDH cytotoxicity assays (Fig. 1). The addition 0.5 µM of 1-deoxySA for 24h showed a marked decrease of cell survival in the MTT assay (52.7% ± 24.0, $p<0.001$) compared to controls and was significantly further decreased after 48h (15.0% ± 5.7, $p<0.001$ versus 24h sample) (Fig. 1A). Higher concentration, 2 µM, of 1-deoxySA induced significant cell death already after 24h (6.9% ± 0.1, $p<0.0001$). No toxic effect was seen for C18SO or BSA whereas 2 µM C18SA showed some minor impact on survival when added for 48h. (69.4% ± 12.2; $p<0.01$). A similar picture, although not as striking, was seen with the LDH assay (Fig. 1B). At 2 µM 1-deoxySA induced cell death by approximately 20% (19.5% ± 9.7, $p<0.05$) and 30 % (31.7% ± 8.5, $p<0.01$) compared to BSA alone. At 0.5 µM 1-deoxySA induced significant cell death only after 48h (17.4% ± 2.3, $p<0.05$ versus BSA). Neither C18SO nor C18SA had a negative effect on cell survival.

Ceramide is the downstream product of sphinganine and an important signaling molecule which was shown to induce cell death in various cell types including neurons (Medler et al., 2008; Obeid et al., 1993; Stoica et al., 2005). In analogy also 1-deoxySA is metabolized further downstream to 1-deoxy(dihydro)ceramide. Intracellular ceramide species in 1-deoxySA treated neurons were observed in a concentration-dependent accumulation of 1-deoxydihydroceramide which was

primarily conjugated with a C18 fatty acid (m18:0,18:0). No 1-deoxydihydroceramides was seen in C18SA or BSA treated controls (Fig. 1C). Normal ceramide levels were not altered by 1-deoxySA-treatment (Supplementary figure A). In parallel to the accumulation of 1-deoxydihydroceramide we observed the accumulation of another lipid species that matched the theoretical mass and in source fragmentation signature of deoxyceramides. However, the retention time of this metabolite was shifted compared to the synthetic standards which is why the exact nature of this metabolite was not fully confirmed yet. To investigate whether neurotoxicity is mediated by 1-deoxydihydroceramide we blocked its formation by inhibiting ceramide synthase with Fumonisin B1 (FB1) at different concentrations. Cells were treated with 0.5 µM or 2 µM of 1-deoxySA for 24h and cell survival was assessed by MTT (Fig. 1D). Again, 1-deoxySA significantly impaired cell survival in a concentration-dependent manner but survival was significantly improved when neurons were pretreated with FB1. The survival of cells that were treated with 0.5 µM 1-deoxySA and 15 µM FB1 was comparable to the controls (96.7% ± 10.0) whereas cells treated with 2 µM of 1-deoxySA were rescued by FB1 in a concentration-dependent manner and showed a survival comparable to controls at 70 µM FB1 (94.5% ± 12.8).

Thus 1-deoxySA is internalized by neurons and further metabolized to deoxy(dihydro)ceramide species that mediate neurotoxic effects in a concentration and time-dependent manner.

1-deoxySA leads to disruption of cytoskeleton structures.

It was reported that 1-deoxySA induced alterations in neurofilament structure and loss of neurites in cultured sensory neurons (Penno et al., 2010). Therefore we tested the effect of 1-deoxySA on the cytoskeleton in our model (Fig. 2). Exposure to 0.5 µM of

C18SA or 1-deoxySA for 24h did not alter neurofilament structures, whereas at 2 µM we observed a strongly reduced staining for NF-L and NF-H compared to the BSA control. BSA and C18SA-treated samples showed a tightly connected neuronal actin network whereas 0.5 µM 1-deoxySA was associated with a loss of stained neurites. At higher 1-deoxySA-concentrations the intensity of the staining was further reduced. At 2 µM 1-deoxySA clearly induced F-actin alterations whereby the neurite structures looked less distinct and the staining appeared fuzzy. Similar effects were observed in samples that were stained for MAP2, a dendritic microtubule marker. 1-deoxySA treated cells showed less neurites and an increasingly punctuated staining. Hence 1-deoxySA induces alterations in neurofilament, actin and microtubule structures and results in the loss of neurites.

1-deoxySA-induced neurotoxicity is associated with decreased Rac1 activity.

Rho GTPases are not only key players in regulating cytoskeletal organization but can also regulate neuronal survival via their downstream cascades. We investigated whether inhibition of the Rho GTPases Rac1 and RhoA affects neuronal survival and whether Rho GTPase deregulation is associated with 1-deoxySA-induced cytoskeleton alterations. Inhibition of RhoA did not alter neuronal survival but blocking of Rac1 induced significant cell death (Supplementary figure B.3). We then used G-LISA assays to assess activity states of Rac1 and RhoA and indeed observed that the activity of both GTPases was reduced in cells treated with 2 µM 1-deoxySA (67.1% ± 12.0, $p<0.01$ and 65.6% ± 26.3 respectively), although RhoA activity results did not reach significance. Total levels of both proteins were unchanged (Supplementary figure B.1, B.2). One of the downstream targets of Rac1 is JNK, which is involved in the regulation of cell survival and cell death. Neuronal JNK

activity is strongly dependent on Rac1 (Güntert el al., unpublished) and similarly to Rac1 inhibition of JNK significantly impaired neuronal survival (Supplementary figure B.3). We thus explored whether 1-deoxySA treatment leads alters JNK activity using Western blot (Fig. 3C). Indeed 2 µM 1-deoxySA significantly diminished JNK phosphorylation ($p<0.01$ versus BSA) while total JNK levels remained constant. Taken together this data suggest that part of the neurotoxic effects of 1-deoxySA may be associated with reduced activation of Rac1 and its downstream target JNK.

1-deoxySA deregulates the cytoskeleton-associated proteins IRSp53 and Ezrin.

Since 1-deoxySA leads to distinct cytoskeletal changes we hypothesized that cytoskeletal regulators other than Rho GTPases could also be modulated by the deoxy-lipid. Therefore we used a specific qRT-PCR array to screen for expression of 84 genes that encode for cytoskeleton regulating proteins comparing cells treated with 2 µM 1-deoxySA or with 2 µM C18SA. We observed significant changes in expression of predominantly 6 genes (Supplementary figure C). Interestingly the expression of *baiap2* was 3.64 fold higher in 1-deoxySA-treated cells. This gene encodes for insulin receptor substrate 53 (IRSp53), a downstream target of Rho GTPases and part of a protein complex with postsynaptic density protein 95 (PSD-95) and N-methyl-D-aspartate receptor (NMDAR) that is involved in synaptogenesis and dendritic spine morphogenesis (Choi et al., 2005). Immunocytochemistry in contrast to RNA levels showed 1-deoxySA decreased IRSp53-specific staining compared to C18SA and BSA-treatment (Fig. 4A). Western blot analysis of cells pre-incubated with the NMDAR antagonists MK-801 and memantine (10 µM for 1h) in addition to the lipid treatment was used to confirm involvement of NMDAR in 1-deoxySA-induced neurotoxicity. Consistent with the staining we found that the presence of 2

µM 1-deoxySA reduced IRSp53 protein levels by 60 % (41.9% ± 11.9, $p<0.05$) compared to controls (Fig. 4B). Interestingly both NMDAR inhibitors could reverse this effect (Mema: 80.2% ± 32.2; MK-801: 89.7% ± 25.2, $p<0.05$ versus 2 µM 1-deoxySA only) suggesting a role for NMDAR in 1-deoxySA-induced toxicity.

The qRT-PCR panel also indicated a 2.61 fold upregulation of Erzin, a cytoplasmic peripheral membrane protein belonging to the ERM protein family. Ezrin links the plasma membrane with the actin cytoskeleton and is involved in adhesion, membrane ruffling and microvilli formation (Tsukita, 1999). Phosphorylation of Ezrin has been shown to be involved in cytoskeletal rearrangements (Belkina et al., 2009). Similar to IRSp53 we performed immunocytochemistry for Ezrin and analyzed phosphorylated as well as total protein levels (Fig. 4C). We detected elevated phospho-ezrin staining in 1-deoxySA-treated cells compared to controls. An enhanced phospho/total Ezrin ratio was confirmed by Western blot in 2 µM 1-deoxySA-treated neurons (174.5% ± 20.3, $p<0.05$) whereas total Ezrin levels remained stable (Fig. 4D). Similar to IRSp53, blocking the NMDAR with MK-801 and memantine significantly prevented the 1-deoxySA-induced changes ($p<0.05$ and $p<0.01$, respectively).

In summary 2 µM 1-deoxySA deregulates the cytoskeleton-associated proteins IRSp53 and Ezrin on both protein and expression level in cortical neurons that can be prevented by inhibition of NMDAR.

1-deoxySA decreases protein levels of NMDAR NR2B subunit and the NMDAR-associated protein PSD95.

Since the effects of 1-deoxySA on cytoskeletal proteins could be reversed by NMDAR inhibition we evaluated if the lipid directly influences NMDAR. Using qRT-PCR we detected a high expression of NMDA receptor subunits NR2B and NR1

NMDAR (data not shown). We selected NR2B subunit for further analysis since it connects with PSD-95 (Kornau et al., 1995) that in turn forms a complex with IRSp53 (Choi et al., 2005). Like before we treated neurons with BSA, C18SA, 1-deoxySA with or without MK-801 or memantine and detected NR2B by Western blot (Fig. 5A). The presence of 2 µM 1-deoxySA resulted in a significant loss of NR2B protein (23.6% ± 8.8, $p<0.01$) compared to C18SA or BSA treated cells. Again pre-incubation with both NMDAR inhibitors significantly prevented the 1-deoxySA-induced effect. MK-801 recovered NR2B levels to more than 80% (82.9% ± 15.2, $p<0.01$ versus 2 µM 1-deoxySA) and memantine elevated it to 75% (73.0% ± 11.2, $p<0.05$ versus 2 µM 1-deoxySA). As expected the effect of 1-deoxySA on PSD-95 was very similar to NR2B. The presence of 2 µM 1-deoxySA led to a strong decrease of PSD-95 protein levels ($p<0.05$) compared to BSA (Fig. 5B). However inhibition of NMDAR could only partly prevent the reduction in PSD-95 levels and did not reach significance.

NMDAR inhibition reduces 1-deoxySA-induced cleavage of p35 to p25 and neurotoxicity.

It has been shown that in hippocampal neurons NMDAR activation can induce cleavage of the CDK5-activator p35 (Kerokoski et al., 2004). The cleavage of p35 to p25 and the subsequent deregulation of CDK5 is associated with neurodegeneration and cytoskeletal abnormalities (Lee et al., 2000; Patrick et al., 1999). Next we investigated if 1-deoxySA induces cleavage of p35 and if this can be prevented by NMDAR inhibition. Furthermore we tested if blocking the NMDAR can prevent 1-deoxySA-induced neuronal death. The presence of 2 µM 1-deoxySA reduced p35 protein levels by more than 60 % ($p<0.0001$) compared to BSA. Both NMDAR

antagonists could prevent this decline although the pretreatment with memantine did not reach significance (Fig. 6A). Accordingly 2 µM of 1-deoxySA induced a strong accumulation of p25 (443.6% ± 58.9, $p<0.0001$) that, again, could be significantly reduced by a pre-treatment with both MK-801 and memantine (141.1% ± 13.1, $p<0.001$ and 261.5% ± 70.3, $p<0.01$ versus 2 µM 1-deoxySA, respectively); (Fig.6B). The influence of the NMDAR antagonists on cell survival was assessed by LDH (Fig. 6C) and MTT assay (Fig. 6D). The LDH assay showed that pretreatment with both MK-801 and memantine could significantly reduce 1-deoxySA-induced cell death ($p<0.0001$). The same tendency was observed in the MTT assay (Fig. 7D) although the effects were not as pronounced. Both MK-801 and memantine-pretreated cells showed an increased survival compared to 1-deoxySA-treatment in the absence of the inhibitors (21.6% ± 1.8 and 22.9% ± 4.0, both $p<0.0001$) although survival was still reduced compared to BSA-treated controls. Additional brightfield images also showed the effect of NMDAR antagonists on cell morphology (Supplementary figure D).

In conclusion, 1-deoxySA induces cleavage of p35 and accumulation of p25, both of which can be strongly reversed by NMDAR antagonists. In addition 1-deoxySA-mediated neuronal death can be partly reversed by NMDAR inhibition.

Discussion

Deoxy-long chain bases are neurotoxic lipids involved in the pathology of HSAN1 and may also contribute to the progression of T2DM and DSN. HSAN1 and DSN are clinically similar and both associated with increased deoxyLCB formation (Bertea et al., 2010; Othman et al., 2012; Zuellig et al., 2013). Since the mechanisms of

deoxyLCBs-mediated neurotoxicity are largely unknown we aimed to elucidate the effects of 1-deoxySA on cultured neurons. We show that 1-deoxySA-induced neuronal death is mediated by deoxy-ceramide species and identified several cytoskeleton-associated factors that are modulated by 1-deoxySA. Moreover we demonstrated that 1-deoxySA modulates NMDAR subunit NR2B and inhibition of NMDAR activation greatly prevented 1-deoxySA-induced neuronal death. Based on these finding we propose a model of how 1-deoxySA might mediate neurotoxicity (Fig 7).

It has been shown previously that deoxysphingolipids induce cell death in different cells types (Cuadros et al., 2000; Salcedo et al., 2007; Sánchez et al., 2008; Zuellig et al., 2013). Similarly we observed a time and concentration dependent neurotoxic effect of 1-deoxySA on primary cortical neurons. Internalization and further metabolism of 1-deoxSA to deoxyceramide species appeared to be responsible for the observed toxicity since the inhibition of ceramide synthase rescued neurons from cell death. Similar results were recently reported in pancreatic β-cells suggesting a more general mode of action of deoxyLCBs (Zuellig et al., 2013). However, ceramide synthesis is essential and FB1 is toxic in vivo [see for review (Stockmann-Juvala and Savolainen, 2008)] and genetic deletion of ceramide synthase has been shown to results in detrimental phenotypes (Imgrund et al., 2009; Pewzner-Jung et al., 2010; Silva et al., 2012). Thus inhibition of ceramide synthase cannot be considered as therapeutic approach to prevent 1-deoxySA-induced toxicity.

In response to 1-deoxySA we observed structural alteration for all three cytoskeleton components, actin filaments, neurofilaments and microtubules in cultured neurons. Indeed 1-deoxySA induced actin rearrangements in insulin-producing cells (Zuellig et al., 2013) and the disassembly of stress fibers in Vero cells has been reported

previously (Cuadros et al., 2000). In contrast to our data these studies did not report alterations in microtubule structures indicating that the potential of 1-deoxySA to affect microtubules might be neuron-specific. Indeed, gene expression for CLIP1 was 5 fold reduced in 1-deoxySA treated neurons compared to control. CLIP1 controls microtubule growth and bundling and utilizes Rac1 to bind to microtubules (Arnal et al., 2004; Fukata et al., 2002; Nakano et al., 2010). Although CLIP1 was not further analyzed in this work disruption/reduction of its function might also contribute to altered neuronal microtubule structures upon 1-deoxySA-treatment. The lipid-induced cytoskeletal alterations are unlikely a consequence of neuronal death but rather a direct effect of 1-deoxySA that might contribute to cell death. Indeed it was shown earlier that 1-deoxySA at concentrations of up to 1 µM were not directly cytotoxic to cultured dorsal root ganglion neurons despite induced neurofilaments retraction and disturbed actin-neurofilament interactions (Penno et al., 2010). Similarly, 1-deoxySA induced alterations in pancreatic beta-cells before apoptotic markers were upregulated (Zuellig et al., 2013). Notably, cytoskeleton alterations, especially impaired axonal transport, have been described for DSN (McLean, 1997). Furthermore Medori and colleagues demonstrate impairment of axonal transport of neurofilament, actin and tubulin and described distal axonal atrophy accompanied by a great loss of neurofilaments in a rat diabetes model (Medori et al., 1985, 1988). Hence 1-deoxySA-treatment induces cytoskeleton alterations very similar to those described in peripheral neuropathies, thus confirming the usefulness of our model system.

Rho GTPases have been proposed to be involved in lipid-induced cytoskeleton rearrangements (Cuadros et al., 2000). Our data suggest that a significantly reduced Rac1 activity underlies 1-deoxySA-induced cytoskeletal rearrangements. A cell-type specific regulation seems evident since earlier data from beta cells showed that 1-

deoxySA increased Rac1 activity and actin accumulation whereas we observed a disassembly of neuronal microfilaments together with decreased in Rac1 activity. JNK, a general downstream target of Rac1 (Minden et al., 1995) is also in our own neuronal model highly dependent on Rac1 (Güntert et al. unpublished). Thus we suggest that 1-deoxySA triggers JNK inactivation via the inactivation of Rac1 correlating with the fact that inhibition of both has negative effects on neuronal survival. This agrees with studies by Le and colleagues (Le et al., 2005) that demonstrated that Rac1 inhibition triggers apoptosis in cerebellar granule neurons. In contrast other studies report that JNK inhibition is beneficial for the survival of cerebellar granule neurons and beta cells (Bonny et al., 2001; Mei et al., 2008). However in BCR/ABL-transformed leukemic cells and B-lymphoma cells JNK promoted survival (Gururajan et al., 2005; Hess et al., 2002). Moreover it was demonstrated that JNK is crucial for interleukin-3 induced survival through phosphorylation and thus inactivation of the pro-apoptotic protein BAD (Yu et al., 2004). Thus the role of JNK in cell death and survival remains controversial and may be highly dependent on cell type and stimulus. In our model 1-deoxySA-induced reduction of Rac1 activity and the subsequent lowered activity of its downstream target JNK might contribute to the observed neuronal death.

In addition to Rho GTPases, deregulation of Ezrin via 1-deoxySA-triggered phosphorylation might contribute directly or indirectly to cytoskeleton rearrangements. It has been shown that phospho-Ezrin links the actin cytoskeleton to the plasma membrane and interacts with integral membrane proteins to participate in signaling processes (Neish and Fehon, 2011). Interestingly Yang and colleagues (Yang and Hinds, 2006) demonstrated that CDK5 phosphorylates Ezrin that in turn inhibits Rac1 in senescent cells. We also observed p25 accumulation in 1-deoxySA-

treated cells suggesting a hyperactivation of CDK5. Thus we speculate that CDK5 may increase Ezrin phosphorylation and thereby suppress Rac1 activity, although further studies on this are required. Another protein that seems to be involved in 1-deoxySA-induced cytoskeletal alterations is IRSp53. IRSp53 forms a complex with Rac1 and Wave2 to promote membrane ruffling and dendritic spine morphogenesis. (Choi et al., 2005; Miki et al., 2000). Since the formation of the Rac1/IRSp53/WAVE2 complex is dependent on Rac1 activity, lipid-induced reduction of Rac1 activity may lead to a disruption of this pathway.

IRSp53 is highly abundant in the postsynaptic density (PSD) where it is associated with other signaling partners via scaffolding proteins (Abbott et al., 1999; Bockmann et al., 2002; Soltau et al., 2004). One of those signaling partners is PSD-95 that in turn interacts with the NMDA receptor, both having a very similar expression pattern (Kornau et al., 1995). Indeed, our data demonstrate comparable effects on IRSP53, PSD-95 and NMDA receptor subunit NR2B since all proteins were strongly decreased in 1-deoxySA-treated neurons. NMDAR degradation is dependent on its activity (Kato et al., 2005) and inhibition of the NMDAR prevented 1-deoxySA-induced loss of NR2B, IRSp53 and to a lesser extent the decrease of PSD-95 levels. Thus activation of the NMDAR signaling cascades could mediate the 1-deoxySA induced effects. The overactivation of NMDA and AMPA glutamate receptors leads to excitotoxicity via increased intracellular calcium and the subsequent cleavage of the CDK5-activator p35 to p25 in hippocampal neurons (Kerokoski et al., 2004), an outcome tightly associated with neurodegeneration (Lee et al., 2000; Patrick et al., 1999). Accordingly we noted decreased p35 levels and strong p25 accumulation in 1-deoxySA-treated neurons that again could be reversed by NMDAR inhibition. This suggests that 1-deoxySA-induced neurotoxicity is at least partly mediated by NMDA

receptor however further investigations need to elucidate whether 1-deoxySA or its further metabolites can directly interact with the receptor. Since AMPA receptor activation may also mediate part of the neurotoxic effects of 1-deoxySA it remains to be tested whether parallel inhibition of both glutamate receptors could completely prevent the cytoskeleton alterations and protect neurons from deoxysphingolipid-induced death. Notably, both NMDA and AMPA receptors are also expressed in the peripheral nervous system (Gangadharan et al., 2011; Ma and Hargreaves, 2000; McRoberts et al., 2001) further supporting the validity of our study. Overall a multifaceted impact of 1-deoxySA on the cytoskeleton, cytoskeleton regulators and associated proteins contributes to neuronal death.

In conclusion this study underlines various intracellular factors that are modulated by 1-deoxySA. 1-deoxySA-treatment induces massive changes in neuronal cytoskeleton organization and deregulation of a number of cytoskeleton regulating proteins like Rac1, Ezrin and IRSp53. Furthermore 1-deoxySA-induced neuronal death is mediated by NMDAR NR2B signaling and can be partly prevented by NMDAR antagonists. Thus we show for the first time a molecular mechanism by which 1-deoxysphingolipids can induce neurotoxicity. We therefore hypothesize that glutamate receptors may be a potential therapeutic target to prevent deoxysphingolipid induced neurodegeneration.

Acknowledgement

We thank Anna Bogdanova for the NMDAR antagonists and Thomas Lutz and Heiko Bode for valuable discussions. The authors declare no conflict of interest.

Funding

This work was financed by grants from Zurich Center of Integrated Human Physiology, University of Zurich (ZIHP); the 7th Framework Program of the European Commission ("RESOLVE", Project number 305707) and "radiz"—Rare Disease Initiative Zurich, University of Zurich

References:

Abbott M a, Wells DG, Fallon JR. The insulin receptor tyrosine kinase substrate p58/53 and the insulin receptor are components of CNS synapses. J. Neurosci. 1999; 19: 7300–8.

Arnal I, Heichette C, Diamantopoulos GS, Chre D. CLIP-170/tubulin-curved oligomers coassemble at microtubule ends and promote rescues. Curr. Biol. 2004; 14: 2086–2095.

Belkina N V, Liu Y, Hao J-J, Karasuyama H, Shaw S. LOK is a major ERM kinase in resting lymphocytes and regulates cytoskeletal rearrangement through ERM phosphorylation. Proc. Natl. Acad. Sci. U. S. A. 2009; 106: 4707–12.

Bertea M, Rütti MF, Othman A, Marti-Jaun J, Hersberger M, von Eckardstein A, et al. Deoxysphingoid bases as plasma markers in diabetes mellitus. Lipids Health Dis. 2010; 9: 84.

Bockmann J, Kreutz MR, Gundelfinger ED, Böckers TM. ProSAP/Shank postsynaptic density proteins interact with insulin receptor tyrosine kinase substrate IRSp53. J. Neurochem. 2002; 83: 1013–7.

Bonny C, Oberson A, Negri S, Sauser C, Schorderet DF. Cell-Permeable Peptide Inhibitors of JNK. Diabetes 2001; 50: 77–82.

Choi J, Ko J, Racz B, Burette A, Lee J-R, Kim S, et al. Regulation of dendritic spine morphogenesis by insulin receptor substrate 53, a downstream effector of Rac1 and Cdc42 small GTPases. J. Neurosci. 2005; 25: 869–79.

Cuadros R, Montejo de Garcini E, Garcini D, Wandosell F, Faircloth G, Fernandez-Sousa J, et al. The marine compound spisulosine, an inhibitor of cell proliferation, promotes the disassembly of actin stress fibers. Cancer Lett. 2000; 152: 23–29.

Eichler FS, Hornemann T, McCampbell A, Kuljis D, Penno A, Vardeh D, et al. Overexpression of the wild-type SPT1 subunit lowers desoxysphingolipid levels and rescues the phenotype of HSAN1. J. Neurosci. 2009; 29: 14646–51.

Fukata M, Watanabe T, Noritake J, Nakagawa M, Yamaga M, Kuroda S, et al. Rac1 and Cdc42 capture microtubules through IQGAP1 and CLIP-170. Cell 2002; 109: 873–85.

Gable K, Gupta SD, Han G, Niranjanakumari S, Harmon JM, Dunn TM. A disease-causing mutation in the active site of serine palmitoyltransferase causes catalytic promiscuity. J. Biol. Chem. 2010; 285: 22846–52.

Gangadharan V, Wang R, Ulzhöfer B, Luo C, Bardoni R, Bali KK, et al. Peripheral calcium-permeable AMPA receptors regulate chronic inflammatory pain in mice. J. Clin. Invest. 2011; 121: 1608–23.

Ghosh TK, Bian J, Gill DL. Intracellular calcium release mediated by sphingosine derivatives generated in cells. Science 1990; 248: 1653–6.

Gururajan M, Chui R, Karuppannan AK, Ke J, Jennings CD, Bondada S. c-Jun N-terminal kinase (JNK) is required for survival and proliferation of B-lymphoma cells. Blood 2005; 106: 1382–91.

Hess P, Pihan G, Sawyers CL, Flavell R a, Davis RJ. Survival signaling mediated by c-Jun NH(2)-terminal kinase in transformed B lymphoblasts. Nat. Genet. 2002; 32: 201–5.

Houlden H, King R, Blake J, Groves M, Love S, Woodward C, et al. Clinical, pathological and genetic characterization of hereditary sensory and autonomic neuropathy type 1 (HSAN I). Brain 2006; 129: 411–25.

Imgrund S, Hartmann D, Farwanah H, Eckhardt M, Sandhoff R, Degen J, et al. Adult ceramide synthase 2 (CERS2)-deficient mice exhibit myelin sheath defects, cerebellar degeneration, and hepatocarcinomas. J. Biol. Chem. 2009; 284: 33549–60.

Kato A, Rouach N, Nicoll R a, Bredt DS. Activity-dependent NMDA receptor degradation mediated by retrotranslocation and ubiquitination. Proc. Natl. Acad. Sci. U. S. A. 2005; 102: 5600–5.

Kerokoski P, Suuronen T, Salminen A, Soininen H, Pirttilä T. Both N-methyl-D-aspartate (NMDA) and non-NMDA receptors mediate glutamate-induced cleavage of the cyclin-dependent kinase 5 (cdk5) activator p35 in cultured rat hippocampal neurons. Neurosci. Lett. 2004; 368: 181–5.

Kornau HC, Schenker LT, Kennedy MB, Seeburg PH. Domain interaction between NMDA receptor subunits and the postsynaptic density protein PSD-95. Science 1995; 269: 1737–40.

Le SS, Loucks FA, Udo H, Richardson-burns S, Phelps A, Bouchard RJ, et al. Inhibition of Rac GTPase triggers a c-Jun- and Bim-dependent mitochondrial apoptotic cascade in cerebellar granule neurons. J. Neurochem. 2005; 94: 1025–1039.

Lee MS, Kwon YT, Li M, Peng J, Friedlander RM, Tsai LH. Neurotoxicity induces cleavage of p35 to p25 by calpain. Nature 2000; 405: 360–4.

Lépine S, Allegood JC, Park M, Dent P, Milstien S, Spiegel S. Sphingosine-1-phosphate phosphohydrolase-1 regulates ER stress-induced autophagy. Cell Death Differ. 2011; 18: 350–61.

Ma QP, Hargreaves RJ. Localization of N-methyl-D-aspartate NR2B subunits on primary sensory neurons that give rise to small-caliber sciatic nerve fibers in rats. Neuroscience 2000; 101: 699–707.

McLean WG. The role of axonal cytoskeleton in diabetic neuropathy. Neurochem. Res. 1997; 22: 951–6.

McRoberts J a., Coutinho S V., Marvizón JCG, Grady EF, Tognetto M, Sengupta JN, et al. Role of peripheral N-methyl-D-aspartate (NMDA) receptors in visceral nociception in rats. Gastroenterology 2001; 120: 1737–1748.

Medler TR, Petrusca DN, Lee PJ, Hubbard WC, Berdyshev E V, Skirball J, et al. Apoptotic sphingolipid signaling by ceramides in lung endothelial cells. Am. J. Respir. Cell Mol. Biol. 2008; 38: 639–46.

Medori R, Autilio-Gambetti L, Monaco S, Gambetti P. Experimental diabetic neuropathy: impairment of slow transport with changes in axon cross-sectional area. Proc. Natl. Acad. Sci. U. S. A. 1985; 82: 7716–20.

Medori R, Jenich H, Autilio-Gambetti L, Gambetti P. Experimental diabetic neuropathy: similar changes of slow axonal transport and axonal size in different animal models. J. Neurosci. 1988; 8: 1814–21.

Mei Y, Yuan Z, Song B, Li D, Ma C, Hu C, et al. Activating transcription factor 3 up-regulated by c-Jun NH(2)-terminal kinase/c-Jun contributes to apoptosis induced by potassium deprivation in cerebellar granule neurons. Neuroscience 2008; 151: 771–9.

Miki H, Yamaguchi H, Suetsugu S, Takenawa T. IRSp53 is an essential intermediate between Rac and WAVE in the regulation of membrane ruffling. Nature 2000; 408: 732–5.

Minden a, Lin a, Claret FX, Abo a, Karin M. Selective activation of the JNK signaling cascade and c-Jun transcriptional activity by the small GTPases Rac and Cdc42Hs. Cell 1995; 81: 1147–57.

Nakano A, Kato H, Watanabe T, Min K-D, Yamazaki S, Asano Y, et al. AMPK controls the speed of microtubule polymerization and directional cell migration through CLIP-170 phosphorylation. Nat. Cell Biol. 2010; 12: 583–90.

Neish A, Fehon R. Ezrin, Radixin and Moesin: key regulators of membrane-cortex interactions and signaling. Curr. Opin. Cell Biol. 2011; 23: 377–382.

Obeid LM, Linardic CM, Karolak L a, Hannun Y a. Programmed cell death induced by ceramide. Science 1993; 259: 1769–71.

Ogunshola OO, Antic A, Donoghue MJ, Fan S-Y, Kim H, Stewart WB, et al. Paracrine and autocrine functions of neuronal vascular endothelial growth factor (VEGF) in the central nervous system. J. Biol. Chem. 2002; 277: 11410–5.

Othman a, Rütti MF, Ernst D, Saely CH, Rein P, Drexel H, et al. Plasma deoxysphingolipids: a novel class of biomarkers for the metabolic syndrome? Diabetologia 2012; 55: 421–31.

Patrick GN, Zukerberg L, Nikolic M, de la Monte S, Dikkes P, Tsai LH. Conversion of p35 to p25 deregulates Cdk5 activity and promotes neurodegeneration. Nature 1999; 402: 615–22.

Penno A, Reilly MM, Houlden H, Laurá M, Rentsch K, Niederkofler V, et al. Hereditary sensory neuropathy type 1 is caused by the accumulation of two neurotoxic sphingolipids. J. Biol. Chem. 2010; 285: 11178–87.

Pewzner-Jung Y, Park H, Laviad EL, Silva LC, Lahiri S, Stiban J, et al. A critical role for ceramide synthase 2 in liver homeostasis: I. alterations in lipid metabolic pathways. Biol. Chem. 2010; 285: 10902–10.

Salcedo M, Cuevas C, Alonso JL, Otero G, Faircloth G, Fernandez-Sousa JM, et al. The marine sphingolipid-derived compound ES 285 triggers an atypical cell death pathway. Apoptosis 2007; 12: 395–409.

Sánchez AM, Malagarie-Cazenave S, Olea N, Vara D, Cuevas C, Díaz-Laviada I. Spisulosine (ES-285) induces prostate tumor PC-3 and LNCaP cell death by de novo synthesis of ceramide and PKCzeta activation. Eur. J. Pharmacol. 2008; 584: 237–45.

Silva LC, Ben David O, Pewzner-Jung Y, Laviad EL, Stiban J, Bandyopadhyay S, et al. Ablation of ceramide synthase 2 strongly affects biophysical properties of membranes. J. Lipid Res. 2012; 53: 430–6.

Sim-Selley L, PB G, MU M, Macdonald T, KR L, S M, et al. Sphingosine-1-phosphate receptors mediate neuromodulatory functions in the CNS. J. Neurochem. 2009; 110: 1191–1202.

Soltau M, Berhörster K, Kindler S, Buck F, Richter D, Kreienkamp H-J. Insulin receptor substrate of 53 kDa links postsynaptic shank to PSD-95. J. Neurochem. 2004; 90: 659–65.

Stockmann-Juvala H, Savolainen K. A review of the toxic effects and mechanisms of action of fumonisin B1. Hum. Exp. Toxicol. 2008; 27: 799–809.

Stoica B a, Movsesyan V a, Knoblach SM, Faden AI. Ceramide induces neuronal apoptosis through mitogen-activated protein kinases and causes release of multiple mitochondrial proteins. Mol. Cell. Neurosci. 2005; 29: 355–71.

Tsukita S. Cortical Actin Organization: Lessons from ERM (Ezrin/Radixin/Moesin) Proteins. J. Biol. Chem. 1999; 274: 34507–34510.

Yang H-S, Hinds PW. Phosphorylation of ezrin by cyclin-dependent kinase 5 induces the release of Rho GDP dissociation inhibitor to inhibit Rac1 activity in senescent cells. Cancer Res. 2006; 66: 2708–15.

Yu C, Minemoto Y, Zhang J, Liu J, Tang F, Bui TN, et al. JNK suppresses apoptosis via phosphorylation of the proapoptotic Bcl-2 family protein BAD. Mol. Cell 2004; 13: 329–40.

Zitomer NC, Mitchell T, Voss K a, Bondy GS, Pruett ST, Garnier-Amblard EC, et al. Ceramide synthase inhibition by fumonisin B1 causes accumulation of 1-deoxysphinganine: a novel category of bioactive 1-deoxysphingoid bases and 1-

deoxydihydroceramides biosynthesized by mammalian cell lines and animals. J. Biol. Chem. 2009; 284: 4786–95.

Zuellig R, Hornemann T, Othman A, Hehl A, Saponara E, Grabliauskaite K, et al. Deoxysphingolipids, a novel biomarker for type 2 diabetes, are cytotoxic for insulin-producing cells. Diabetes 2013; Epub ahead

Figure legends

Figure 1: 1-deoxySA and further metabolites are toxic for cortical neurons. Neurons were incubated with 0.5 µM or 2 µM of 1-deoxySA, C18SA or C18SO or BSA control for 24h or 48h and cell death was assessed by two methods. A, MTT assay was used to detect enzymatic activity and BSA was set to 100 %. ** $p<0.01$ versus C18SO and BSA, *** $p< 0.001$ versus 0.5 µM C18SA, C18SO and BSA, **** $p<0.0001$ versus all other treatments. B, LDH assay was applied to detect cytotoxicity and BSA was set to 0%. * $p<0.05$ versus BSA, ** $p<0.01$ versus C18SA and C18SO, *** $p<0.001$ versus BSA. C, Mass spectrometric quantification shows the elevated intracellular 1-deoxy-dh-ceramide levels of different acyl chain length in neurons upon treatment with 0.5 µM or 2 µM of 1-deoxySA for 24h compared with 2 µM C18SA or BSA as control. Levels (pmol) were normalized to protein content of the used cell pellets. * $p<0.05$, **** $p<0.0001$ versus BSA and C18SA. Analysis was done using one-way ANOVA followed by Bonferroni post-hoc test. D, To inhibit ceramide synthesis neurons were exposed to 0.5 and 2 µM 1-deoxySA after pretreatment for 30 min with different concentrations of Fumonisine B1 (FB1) and cell survival was detected by MTT assay. BSA was used as control and set to 100%. $ $p<0.01$, $$ $p<0.001$, $$$ $p<0.0001$ versus control of the same group (0 µM Fumonisine B1). Data were analyzed using two-way ANOVA followed by Bonferroni post-hoc test.

Figure 2: 1-deoxySA leads to disruption of cytoskeleton structures.

Cells were treated with 0.5 and 2 µM C18SA or 1-deoxySA or with the BSA control for 24h prior to immunocytochemistry. We used anti Neurofilament light (NF-L) and anti Neurofilament heavy (NF-H) antibodies to stain neurites. Phalloidin staining was

used to visualize filamentous Actin (F-Actin) and anti MAP2 antibody was used as microtubule marker. Nuclei were counterstained with DAPI (blue). Scale bar: 50 µM.

Figure 3: 1-deoxySA-induced neurotoxicity is associated with decreased Rac1 activity.

Neurons were incubated for 24h with 0.5 µM and 2 µM 1-deoxSA or C18SA or with BSA as a control and Rho GTPase activity was determined in cell lysates via A) Rac G-LISA and B) RhoA G-LISA to determine Rho GTPase activity. ** $p<0.01$ versus all other treatments. C, Western blot of the lipid-treated neurons was performed to detect JNK phosphorylation status. Results are expressed as the ratio of phosphorylated (pJNK) versus total protein and were compared to the BSA control. * $p<0.05$ versus C18SO, 0.5 µM 1-deoxySA and 2 µM C18SA, ** $p<0.01$ versus BSA. Data were analyzed using two-way ANOVA followed by Bonferroni post-hoc test.

Figure 4: 1-deoxySA deregulates the cytoskeleton-associated proteins IRSp53 and Ezrin.

To determine the effect of exposure to 1-deoxySA, C18SA or BSA on cytoskeleton regulating proteins neurons were treated as previously and subjected to immunocytochemistry to visualize IRSp53 (A, green) and E(C, green). Scale bar: 50 µM. B and D, To confirm the staining lipid-treated neurons were used for Western blot to detect IRSp53 (B) and the phosphorylated and total form of Ezrin (D). In addition to 1-deoxySA exposure cells were pre-incubated for 1h with 10 µM of the NMDAR inhibitors MK-801 or Memantine (Mema).* $p<0.05$ versus C18SA and BSA, $ $p<0.05$ versus 2 µM 1-deoxySA (B). D, To assess changes in Ezrin phosphorylation the result are displayed as ratio between the phosphorylated (p-Ezrin)

and the total protein form and compared to BSA. * $p<0.05$ versus C18SA and BSA, $ $p<0.05$ and $$ $p<0.01$ versus 2 µM 1-deoxySA. Data were analyzed using two-way ANOVA. For comparison between MK-801 and memantine with 1-deoxySA only one-way ANOVA was applied. Both analyses were followed by Bonferroni post-hoc test.

Figure 5: 1-deoxySA decreases protein levels of NMDAR NR2B subunit and the NMDAR-associated protein PSD95.

To determine the effect of lipid treatment on NMDAR and PSD-95 neurons were treated with 1-deoxySA, C18SA or BSA in the presence or absence of 10 µM of the NMDAR inhibitors MK-801 and memantine (Mema). Lysates were loaded on polyacrylamide gels and NR2B (A) and PSD95 (B) were detected by Western blot. A, Western blot for NR2B. ** $p<0.01$ versus BSA, C18SA and 0.5 µM 1-deoxySA, $ $p<0.05$ and $$ $p<0.01$ versus 2 µM 1-deoxySA. B, Western blot for PSD-95. * $p<0.05$ versus BSA ** $p<0.01$ versus C18SA. Data were analyzed using two-way ANOVA. For comparison between MK-801 and memantine with 1-deoxySA only one-way ANOVA was applied. Both analyses were followed by Bonferroni post-hoc test.

Figure 6: NMDAR inhibition reduces 1-deoxySA-induced cleavage of p35 to p25 and neurotoxicity.

As previously cells were exposed to 1-deoxySA, C18SA or BSA in the presence or absence of MK-801 and memantine to detect effects on p35 and p25 levels and on cell survival. A,B, Western blot was performed to detect p35 and p25 protein levels using an antibody that detects both of the proteins. A, The graph shows p35 levels. ***

p<0.001 versus 0.5 µM 1-deoxySA, **** p<0.0001 versus BSA and C18SA, $$ p<0.01 versus 2 µM 1-deoxySA. B, The graph shows p25 levels. * p<0.05, ** p<0.01 versus BSA, *** p<0.001 versus 2 µM C18SA, **** p< 0.0001 versus BSA, $$ p<0.01 and $$$ p<0.001 versus 2 µM 1-deoxySA. The effect of lipid treatment and NMDAR inhibition on cell survival was determined using LDH (C) and MTT assay (D). C, Cytotoxicity was detected by measuring LDH in the supernatant. BSA control was set to baseline. *** p<0.001 versus 0.5 µM 1-deoxySA, **** p<0.0001 versus BSA and C18SA, $$$$ p<0.0001 versus 2 µM 1-deoxySA. D, MTT assay was as measurement for cell survival and BSA control was set to 100%. **** p<0.0001 versus BSA, C18SA and versus 0.5 µM and 2 µM 1-deoxySA respectively, $$$$ p<0.0001 versus 2 µM 1-deoxySA. Data were analyzed using two-way ANOVA. For comparison between MK-801 and memantine with 1-deoxySA only one-way ANOVA was applied. Both analyses were followed by Bonferroni post-hoc test.

Figure 7: Possible mechanism of 1-deoxySA-induced neurotoxicity

Schematic representation of our results.

Supplementary figure A: 1-deoxySA does not alter intracellular ceramide levels.

Mass spectrometric quantification of intracellular ceramides of neurons treated for 24h with 0.5 µM or 2 µM of 1-deoxySA, or with 2 µM C18SA or BSA as control. Ceramide levels (pmol) were normalized to protein content of the used cell pellets.

Supplementary figure B: 1-deoxySA does not alter total Rac1 or total RhoA levels.

Neurons were incubated for 24h with 0.5 µM and 2 µM 1-deoxySA, C18SA or C18SO or with BSA as a control and Western blot was performed to detect Rac1 (A) and RhoA (B) with specific antibodies. C, To determine the effect of Rac1, RhoA and JNK inhibition on neuronal survival MTT assay was performed on neurons pretreated with 100 µM of Rac1 or Rho inhibitor (Rac1/Rho inhib) or with 50 µM of SP600125 (SP) for 30 min prior to lipid incubation as above. **** $p<0.0001$ versus BSA and Rho inhib. Data were analyzed using one-way ANOVA followed by Bonferroni post-hoc test.

Supplementary figure C: Cytoskeleton regulator qPCR array.

RNA was extracted from cells treated with 2 µM 1-deoxySA or C18SA for 24h and cDNA was synthesized using an array compatible kit. Together with the compatible qPCR master mix the obtained cDNA was added to each well of the Mouse Cytoskeleton Regulator RT^2 Profiler PCR array plates and analyzed. The table shows the three highest fold up and down regulations of 1-deoxySA-exposed cells versus C18SA. *Baiap2* encoding for insulin receptor substrate p53 (IRSp53) and *Ezr* for Ezrin were selected for further analysis.

Supplementary figure D: Effect of 1-deoxySA-exposure and NMDAR antagonist treatment on cell morphology.

To monitor the effect of 2 µM 1-deoxySA in the presence or absence of 10 µM MK-801 or memantine (Mema) on cell morphology and survival compared to BSA and

C18SA controls we took photographs of our neuronal culture after 24h lipid exposure.

Scale bar: 50 μM.

Figure 1

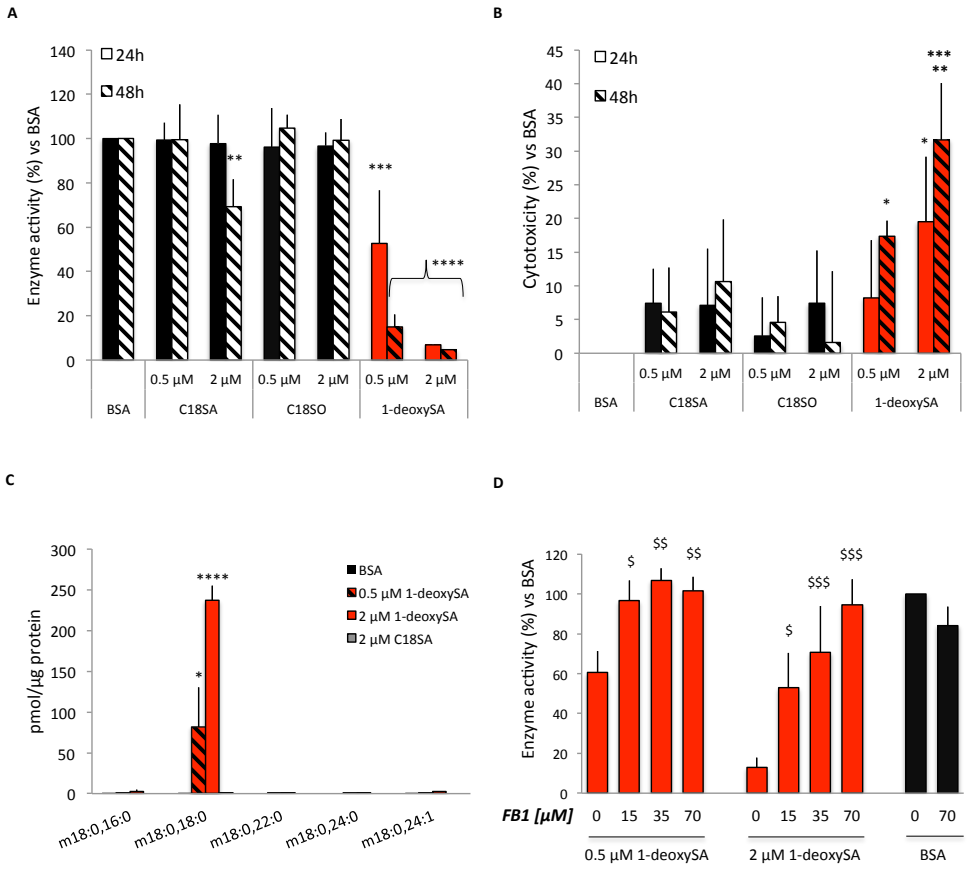
A
Enzyme activity (%) vs BSA
24h
48h
0.5 µM
2 µM
BSA
C18SA
C18SO
1-deoxySA
B
Cytotoxicity (%) vs BSA
C
pmol/µg protein
BSA
0.5 µM 1-deoxySA
2 µM 1-deoxySA
2 µM C18SA
m18:0,16:0
m18:0,18:0
m18:0,22:0
m18:0,24:0
m18:0,24:1
D
Enzyme activity (%) vs BSA
FB1 [µM]
0.5 µM 1-deoxySA
2 µM 1-deoxySA
BSA

Figure 2

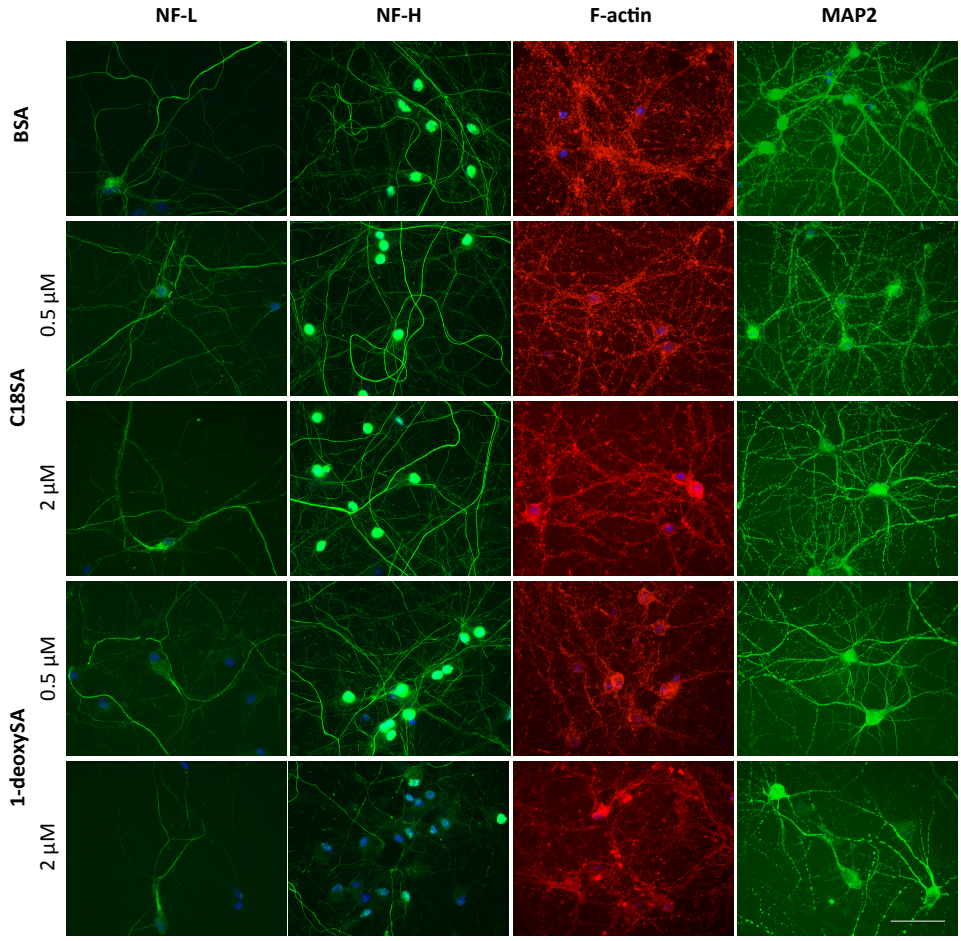

Figure 3

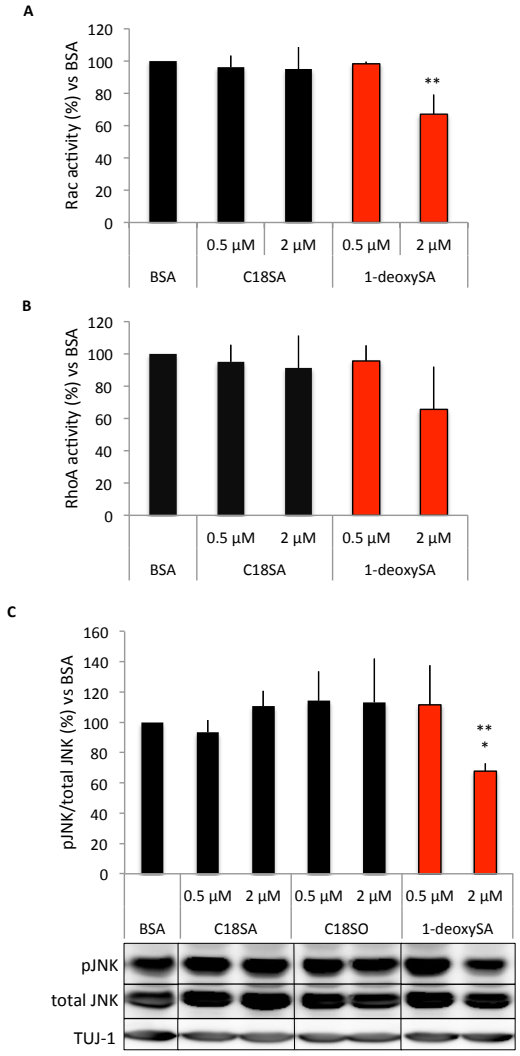
A
Rac activity (%) vs BSA
120
100
80
60
40
20
0
**
0.5 µM
2 µM
0.5 µM
2 µM
BSA
C18SA
1-deoxySA
B
RhoA activity (%) vs BSA
120
100
80
60
40
20
0
0.5 µM
2 µM
0.5 µM
2 µM
BSA
C18SA
1-deoxySA
C
pJNK/total JNK (%) vs BSA
160
140
120
100
80
60
40
20
0
**
*
0.5 µM
2 µM
0.5 µM
2 µM
0.5 µM
2 µM
BSA
C18SA
C18SO
1-deoxySA
pJNK
total JNK
TUJ-1

Figure 4

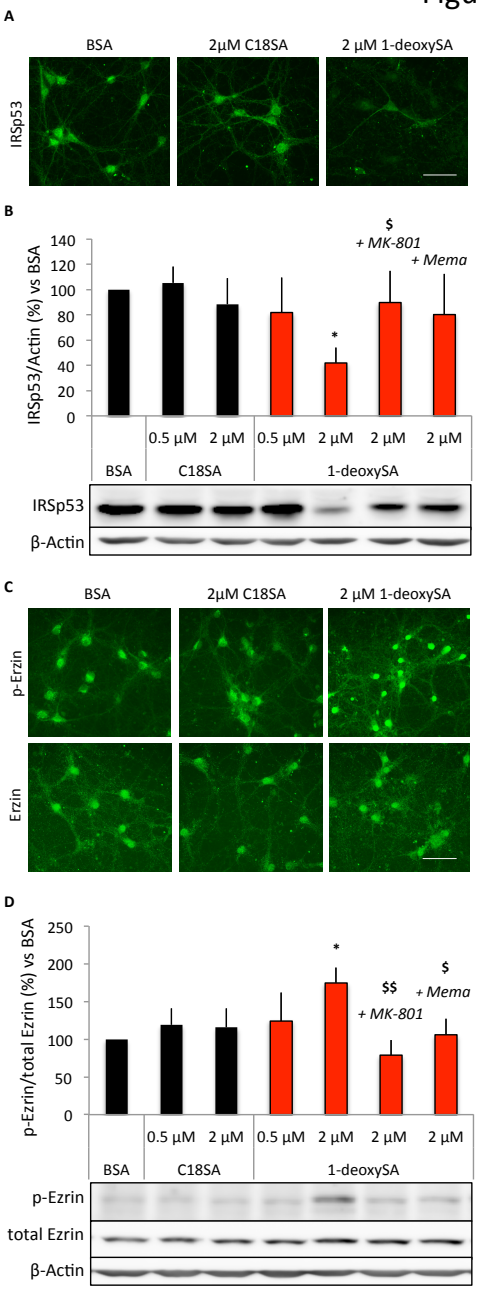
A
BSA
2µM C18SA
2 µM 1-deoxySA
IRSp53
B
IRSp53/Actin (%) vs BSA
140
120
100
80
60
40
20
0
$
+ MK-801
+ Mema
*
0.5 µM
2 µM
0.5 µM
2 µM
2 µM
2 µM
BSA
C18SA
1-deoxySA
IRSp53
β-Actin
C
BSA
2µM C18SA
2 µM 1-deoxySA
p-Erzin
Erzin
D
p-Ezrin/total Ezrin (%) vs BSA
250
200
150
100
50
0
*
$$
$
+ MK-801
+ Mema
0.5 µM
2 µM
0.5 µM
2 µM
2 µM
2 µM
BSA
C18SA
1-deoxySA
p-Ezrin
total Ezrin
β-Actin

Figure 5

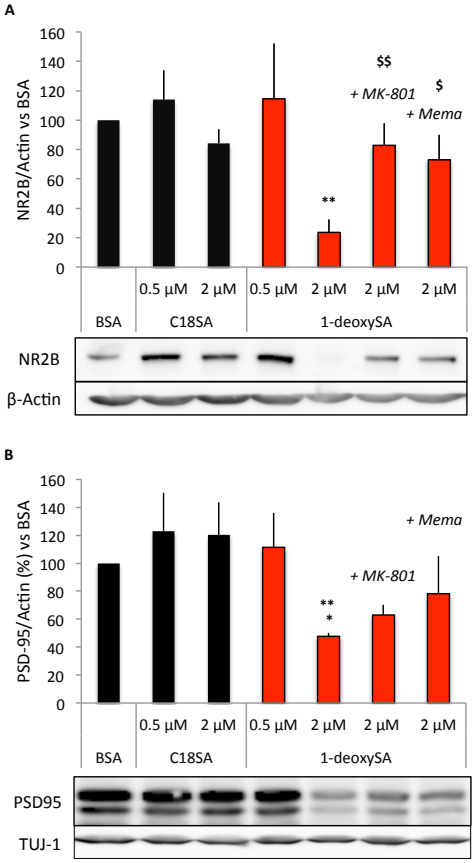
A
NR2B/Actin vs BSA
160
140
120
100
80
60
40
20
0
$$
+ MK-801
$
+ Mema
**
0.5 µM
2 µM
0.5 µM
2 µM
2 µM
2 µM
BSA
C18SA
1-deoxySA
NR2B
β-Actin
B
PSD-95/Actin (%) vs BSA
160
140
120
100
80
60
40
20
0
+ Mema
+ MK-801
**
*
0.5 µM
2 µM
0.5 µM
2 µM
2 µM
2 µM
BSA
C18SA
1-deoxySA
PSD95
TUJ-1

Figure 6

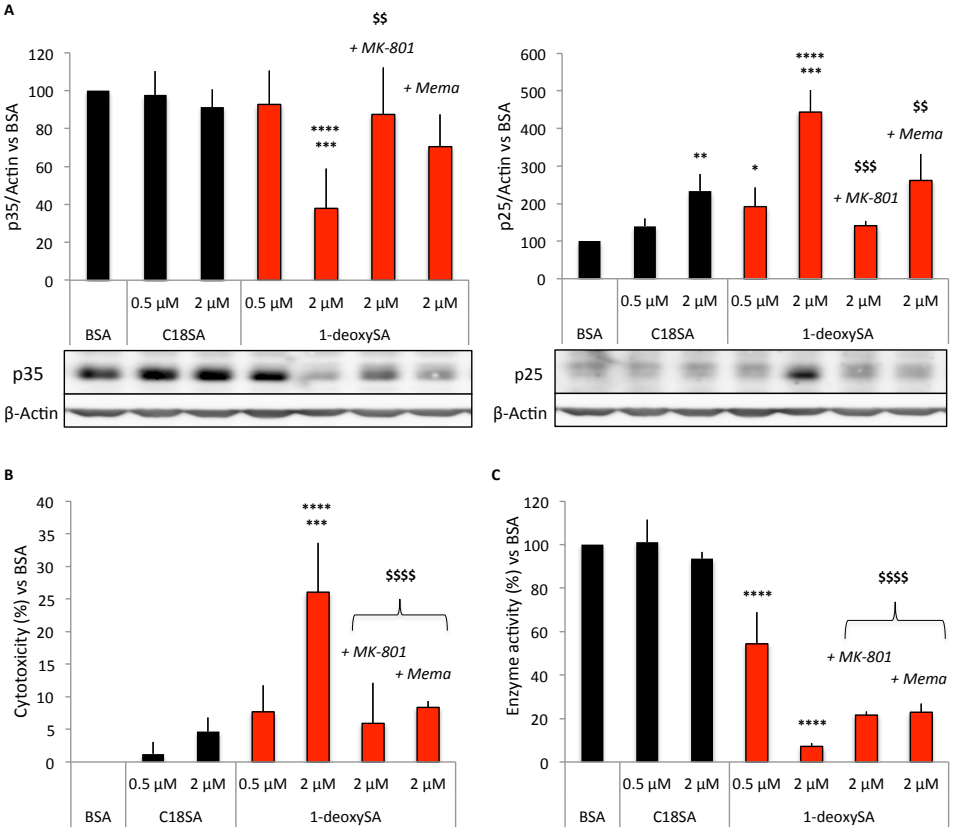
A
p35/Actin vs BSA
p25/Actin vs BSA
BSA
C18SA
1-deoxySA
0.5 µM
2 µM
+ MK-801
+ Mema
p35
p25
β-Actin
B
Cytotoxicity (%) vs BSA
C
Enzyme activity (%) vs BSA

Figure 7

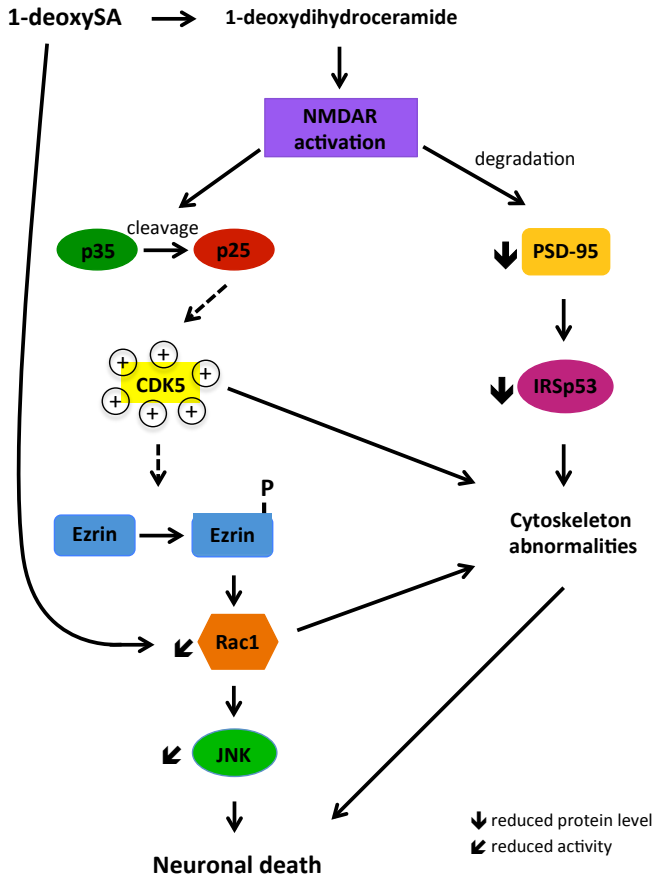
1-deoxySA
1-deoxydihydroceramide
NMDAR activation
degradation
cleavage
p35
p25
PSD-95
CDK5
IRSp53
P
Ezrin
Ezrin
Cytoskeleton abnormalities
Rac1
JNK
Neuronal death
reduced protein level
reduced activity

Supplementary figure A

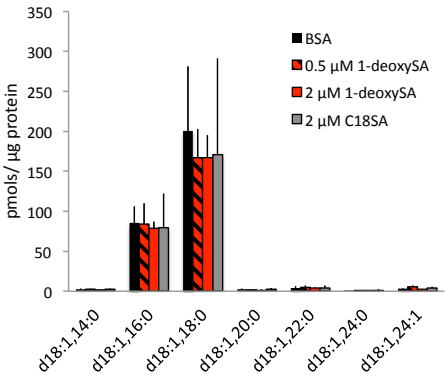

Supplementary figure B

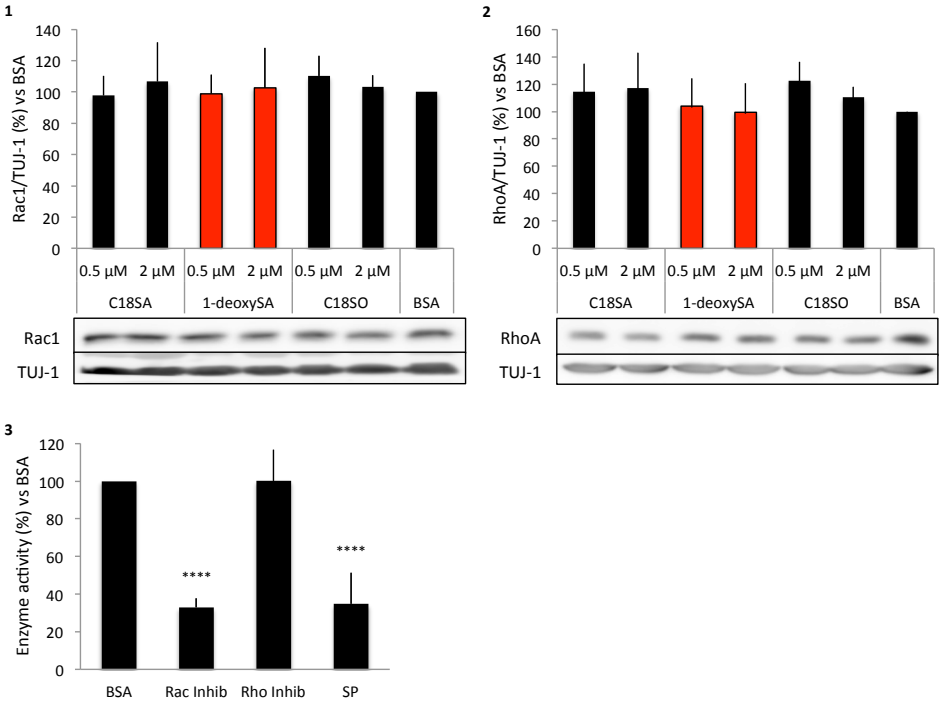

Supplementary figure C

gene	protein	fold up or down regulation
Baiap2	Insulin receptor substrate p53	3.64
Ezr	Ezrin	2.61
Was	Wiskott-Aldrich Syndrome Protein	1.87
Clip1	CAP-GLY domain containing linker protein 1	-5.02
Mtap4	Microtubule-associated protein 4	-2.03
Mylk2	Myosin Light Chain Kinase 2	-2.69

Supplementary figure D

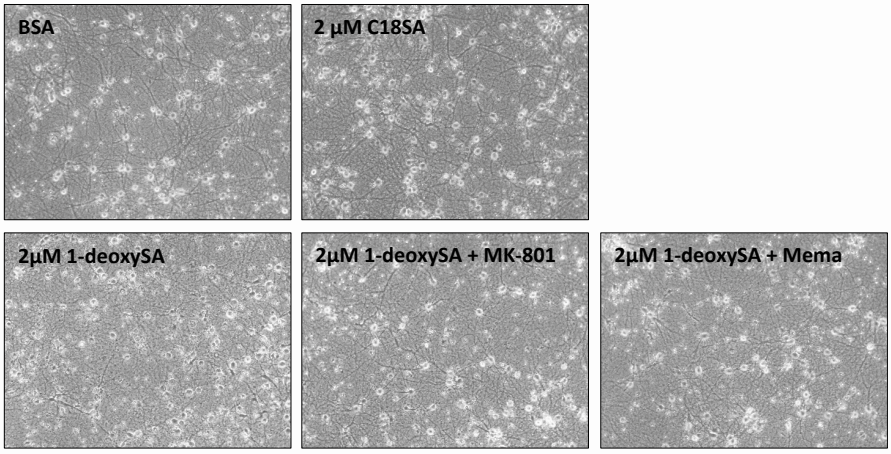

6. 3 Deoxysphingolipids, a novel biomarker for type 2 diabetes, are cytotoxic for insulin- producing cells.

Richard A. Zuellig[1#], Thorsten Hornemann[2,3,4#], Alaa Othman[2,3,4], Adrian B. Hehl[5], Heiko Bode[2,3,4], Tanja Güntert[6], Omolara O. Ogunshola[6], Enrica Saponara[7], Kamile Grabliauskaite[7] Jae-Hwi Jang[7], Udo, Ungethuem[7], Yu Wei[2,3,4], Arnold von Eckardstein[2,3,4], Rolf Graf[7] and Sabrina Sonda[7]

[1]Division of Endocrinology, Diabetes and Clinical Nutrition, University Hospital Zurich, [2]Institute for Clinical Chemistry, University Hospital Zurich, [3]Centre for Integrative Human Physiology, University of Zurich, Zurich, Switzerland, [4]Competence Centre for Systems Physiology and Metabolic Diseases, Zurich, [5] Institute of Parasitology, University of Zurich, [6]Institute of Veterinary Physiology, University of Zurich, [7]Swiss Hepato-Pancreatico-Biliary (HPB)-Center, Division of Surgical Research, Dept.Visceral & Transplantation Surgery, University Hospital Zurich, Switzerland.

[#] Contributed equally to this work

Published in Diabetes, 2013, Epub ahead of print

doi: 10.2337/db13-1042

PMID: 24379346

Personal contribution

- Performed Western blots to investigate involvement of JNK, AKT and p38 MAPK in 1-deoxySA-induced signaling (Fig. 4 A-C)
- Performed Western blots to detect total levels of Rac1 and RhoA in 1-deoxySA-treated cells and control samples (Fig. 5B,C)

Key findings

- 1-deoxySA induces dose-dependently cytotoxicity for Ins-1 cells by triggering senescence and multiple cell death pathways
- 1-deoxySA selectively upregulated ceramide synthase 5 and its metabolite deoxy-dihydroceramide is at least in part mediating the observed toxic effects
- JNK and p38 MAPK are antagonistic effectors of 1-deoxySA-induced cellular senescence
- 1-deoxySA-triggers re-oragnization of the actin cytoskeleton of Ins-1 cells by activating Rac1
- 1-deoxySA reduces metabolic activity, insulin secretion and modulates actin cytoskeleton in primary islets
- Increased glucose levels potentiate 1-deoxySA toxicity

Manuscript

Deoxysphingolipids, a novel biomarker for type 2 diabetes, are cytotoxic for insulin-producing cells.

Richard A. Zuellig[1#], Thorsten Hornemann[2,3,4#], Alaa Othman[2,3,4], Adrian B. Hehl[5], Heiko Bode[2,3,4], Tanja Güntert[6], Omolara O. Ogunshola[6], Enrica Saponara[7], Kamile Grabliauskaite[7], Jae-Hwi Jang[7], Udo, Ungethuem[7], Yu Wei[2,3,4], Arnold von Eckardstein[2,3,4], Rolf Graf[7] and Sabrina Sonda[7*]

[1]Division of Endocrinology, Diabetes and Clinical Nutrition, University Hospital Zurich, [2]Institute for Clinical Chemistry, University Hospital Zurich, [3]Centre for Integrative Human Physiology, University of Zurich, Zurich, Switzerland, [4]Competence Centre for Systems Physiology and Metabolic Diseases, Zurich, [5] Institute of Parasitology, University of Zurich, [6]Institute of Veterinary Physiology, University of Zurich,[7]Swiss Hepato-Pancreatico-Biliary (HPB)-Center, Division of Surgical Research, Departement of Visceral & Transplantation Surgery, University Hospital Zurich, Switzerland.

# Contributed equally to this work

Running title: Deoxysphingolipids and diabetes

** Address correspondence to:*

Sabrina Sonda

Pancreatitis Research Laboratory

Department of Visceral and Transplantation Surgery

University Hospital Zurich

Rämistrasse 100, DL36,8091 Zurich, Switzerland

Diabetes Publish Ahead of Print, published online December 30, 2013

sabrina.sonda@usz.ch

Word count: 3991

Figure and table number: eight figures

Abstract

Irreversible failure of pancreatic β-cells is the main culprit in the pathophysiology of diabetes mellitus, a disease that is now a major global epidemic. Recently, elevated plasma levels of deoxysphingolipids, including 1-deoxysphinganine, have been identified as novel biomarkers for the disease. In this study, we analyzed whether deoxysphingolipids directly compromise the functionality of insulin-producing Ins-1 cells and primary islets. Treatment with 1-deoxysphinganine induced dose-dependent cytotoxicity with senescent, necrotic and apoptotic characteristics and compromised glucose-stimulated insulin secretion. In addition, 1-deoxysphinganine altered cytoskeleton dynamics, resulting in intracellular accumulation of filamentous actin and activation of the RhoGTPase Rac1. Moreover, 1-deoxysphinganine selectively up-regulated ceramide synthase 5 expression and was converted to 1-deoxy-dihydroceramides, without altering normal ceramide levels. Inhibition of intracellular 1-deoxysphinganine trafficking and ceramide synthesis improved the viability of the cells, indicating that the intracellular metabolites of 1-deoxysphinganine contribute to its cytotoxicity. Analyses of signaling pathways identified JNK and p38 MAPK as antagonistic effectors of cellular senescence. Our results revealed that 1-deoxysphinganine is a cytotoxic lipid for insulin-producing cells, suggesting that the increased levels of this sphingolipid observed in diabetic patients may contribute to the reduced functionality of pancreatic β-cells. Thus, targeting deoxy-sphingolipid synthesis may complement the currently available therapies of diabetes.

Introduction

In the last three decades, the prevalence of diabetes has been rising worldwide at a dramatic rate, with incidence projections approaching 8% of the population by 2030 (1; 2). This remarkable increase is largely due to the epidemic spreading of type 2 diabetes mellitus (T2DM), which accounts for 90% of all cases of diabetes mellitus worldwide (reviewed in (3; 4)). Given the level of complexity associated with the pathophysiology of T2DM, understanding the mechanisms underlying this disease is necessary to design alternative strategies to limit its progression. Recently, substantial improvements occurred in the detection of early stage or undiagnosed T2DM, thus allowing appropriate treatments in high risk populations. One of the latest biomarkers identified in patients with diabetes and metabolic syndromes are increased plasma levels of deoxy-sphingolipids (1-deoxySLs) (5; 6), a type of sphingolipid characterized by an initial condensation of alanine or glycine instead of serine with palmitic acid and the resultant absence of the hydroxyl group in position C1. Consequently, although these deoxy-sphingoid bases can be acylated to deoxy-dihydroceramides, they cannot be further metabolized to complex sphingolipids or efficiently degraded by the canonical degradation pathway, and thus tend to accumulate once produced. Importantly, 1-deoxySLs display toxic properties *in vitro* toward several cell lines (7-9) and *in vivo* are thought to impair neuronal functionality in patients with the hereditary sensory and autonomic neuropathy type I (HSAN1) (10).

In light of the increased plasma levels of 1-deoxySLs found in diabetic patients and of the reported cytotoxic effects associated with the exposure to increased 1-deoxySL concentrations, we investigated whether these atypical sphingolipids directly compromise pancreatic β-cells, the dysfunction of which plays an important role in the pathogenesis of both type 1 and type 2 diabetes.

Research Design and Methods

Biochemical reagents

Unless otherwise stated, all chemicals were purchased from Sigma and cell culture reagents from Gibco-BRL. Inhibitor stock solutions were freshly diluted to the concentrations required for the individual experiment indicated in the figure legends. Lipid stock solutions were prepared as a bovine serum albumin (BSA) complex, as described in (10), and added to the cells at the concentrations indicated in the figure legends. BSA was used as control.

In vitro cell culture

The Ins-1 rat insulinoma cell clone 832/13, generously provided by C. Wollheim, was maintained in RPMI 1640 medium, as described (11; 12). Cell metabolic activity was tested with 0.5% tetrazolium salt solution 3-(4,5-dimethylthiazol-2-yl)-2,5-diphenyltetrazolium bromide (MTT), or WST-1 (Roche), according to the manufacturer's instructions. Cell death was quantified by trypan blue exclusion or lactate dehydrogenase (LDH) release in the medium (Roche). Cellular senescence was quantified with the β-galactosidase assay kit (Cell Biolabs). Adp21 (rat) and AdGFP adenovirus were purchased from Vector Biolabs, Philadelphia, USA. Rac1 activity was measured with G-LISA Rac1 activation assay (Cytoskeleton, Denver, USA).

Animal experiments

Wistar rats, leptin deficient ob/ob mice on C57BL/6J background (B6.V-*Lep*/OlaHsd) and wild type (WT) C57BL/6J (Harlan Laboratories) were kept under a light-dark regime (16:8 h), constant temperature, and free access to food and water. All animal experiments were performed

in accordance with swiss federal animal regulations and approved by the cantonal veterinary office of Zurich.

Islets were harvested from pancreata of male Wistar rats (250 to 300 g) by collagenase (NB8 collagenase, Serva, Heidelberg, Germany) followed by trypsin digestion to dissociate them into single cells, according to (13).

Insulin secretion

Dissociated islets cells were seeded in 12-well ECM coated plates (Novamed, Jerusalem, Israel), treated for 24 h with 5 μM sphinganine, 1-deoxysphinganine or BSA and incubated in RPMI medium containing 3.3 mM glucose for 1 h. Following sequential 1 h incubations with low (3.3 mM), high (16.7 mM), low (3.3 mM) glucose concentrations, insulin secretion was measured by radioimmunoassay (Insulin-CT, CIS, Biointernational, Schering AG, Baar, Switzerland), according to the manufacturer's instructions.

qRT-PCR

Total RNA was extracted from Ins-1 cells cultured in 1 μM sphinganine or 1-deoxysphinganine for 24 h. Quality of RNA was assessed by 2100 bioanalyzer (Agilent Technologies, Basel, Switzerland). cDNA was obtained with the RT2 First Strand Kit and profiled using the Rat Cell Death Pathway Finder PCR Array (both from SABiosciences, Hombrechtikon, Switzerland), according to the manufacturer's instructions. CerS primers for SYBR green qPCR are listed in Supplementary Materials and Methods.

Immunohistochemistry and flow cytometry analyses

Pancreas specimens were fixed in 4% formalin and paraffin embedded according to standard procedures (14). Ins-1 cells were fixed in 3.6% formaldehyde and permeabilized with 0.2% Triton X-100 in PBS. Primary antibodies used in this study are listed in Supplementary Materials

and Methods. Apoptosis detection was performed with an ApopTag peroxidase Kit (MP Biomedicals, Illkirch, France). Immunofluorescence analysis and image data collection were performed on a Zeiss Axioplan 2 Imaging fluorescence microscope (Carl Zeiss Microimaging, Göttingen, Germany), or on a Leica SP2 AOBS confocal laser-scanning microscope (Leica Microsystems, Wetzlar, Germany) using a glycerol immersion objective lens (Leica, HCX PL APO CS 63x 1.3 Corr). Image z-stacks were collected with a pinhole setting of Airy 1 and twofold oversampling. Image stacks of optical sections were processed using the Huygens deconvolution software package version 2.7 (Scientific Volume Imaging, Hilversum, NL). Three-dimensional reconstruction, volume rendering, and quantification of signal overlap in the 3D volume model were done with the Imaris software suite (Version 7.2.1, Bitplane, Zurich, Switzerland). The degree of signal overlap in the 3D volume models is shown graphically as scatterplots by plotting the intensity of two fluorescent signals in each voxel of the 3D model. Voxels with similar signal intensity for both signals appear in the area of the diagonal.

Single-cell quantification of stained cells by flow cytometry was performed using a FACSDiva flow cytometer (BD Bioscences, Allschwil, Switzerland).

Western blotting

Ins-1 cells cultured in 1 μM sphinganine, 1-deoxysphinganine or BSA for 24 h were lysed as described (15). Aliquots corresponding to 35 μg of proteins were separated by SDS-PAGE electrophoresis, blotted and probed over night at 4°C. Primary antibodies used in this study are listed in Supplementary Materials and Methods. Immunoreactive bands from at least 3 independent experiments were quantified by densitometry and normalized to β-actin or GAPDH levels.

Analysis of sphingoid bases and ceramides by LC–MS/MS

The sphingoid base profile was analyzed as described earlier (5). Ceramide species were extracted by adding 1 ml methanol/chloroform (2:1) (including 200 pmole of C12 ceramide internal standard (Avanti Polar Lipids) to 100 µl of re-suspended cells followed by the addition of 0.5 ml of chloroform and 200 µl alkaline water (10). Interfering phospholipids were hydrolyzed by re-extracting the dried lipids with methanol-KOH:chloroform (4:1) as described earlier (10). Lipids were separated on a C18 column (Uptispere 120 Å, 5µm, 125 × 2 mm, Interchim, France) and analyzed on a TSQ Quantum Ultra (Thermo, Reinach, Switzerland) using atmospheric pressure chemical ionization (APCI) (10). Ceramides and deoxy-Ceramides were identified by precursor ion scan (20mV collision energy) with fragments of (m/z 264.3) and (m/z 268.3) respectively. Levels were normalized to ISTD and cell numbers.

Statistical analyses

Results are expressed as means ± SEM. Significance was assessed using Student's unpaired, two-tailed *t* tests or one-way analysis of variance. A probability value <0.05 was considered significant. When the overall probability value was <0.05, the Bonferroni multiple-comparison test was used to determine whether there was a significant difference between values of control (reference sample) and samples of interest.

Results

1-deoxySL treatment is cytostatic and cytotoxic for Ins-1 cells

As 1-deoxySLs were found elevated in the plasma of diabetic patients in the low µM range (5; 6), we analyzed whether 1-deoxySLs can directly affect the viability of insulin-secreting cells. To this aim, the rat insulinoma cell line Ins-1 was treated at 50% confluence (Fig. 1A, L: low density) for 24 h with 1-deoxysphinganine or sphinganine as control. 1-deoxysphinganine incubation reduced both the metabolic activity, as measured by MTT (Fig.1A) and WST-1

reduction (Fig. S1A), and the number of live cells (Fig.1B) in a dose-dependent manner. Treatment with 5 μM caused cell round up (Fig. 1C) and death, as shown by robust trypan blue inclusion (Fig.1D) and LDH release (Fig.1E). However, cells treated with 1 μM 1-deoxysphinganine did not increase in number compared with the initial seeding but showed modest levels of lethality (Fig.1D, E), or up-regulation of genes involved in cell death pathways (Fig. S1B-D), suggestive of a cytostatic effect of the lipid at this concentration (Fig. 1B). When the lipid treatment was performed on 90% confluent cells (Fig. 1A, H: high density), the metabolic activity was reduced only at the highest concentration of 1-deoxysphinganine tested, further indicating that 5 μM 1-deoxysphinganine is cytotoxic for both dividing and quiescent cells, while lower lipid concentrations are cytostatic. In addition, treatment for only one hour, followed by washout and subsequent 23 h incubation was sufficient to reduce the metabolic activity of the cells comparably to a continuous 24 h incubation with 1-deoxysphinganine (Fig. 1F), suggesting a rapid effect of the lipid.

1-deoxysphinganine triggers p21-mediated senescence and multiple cell death pathways in Ins-1 cells

We then investigated whether the reduction of replication following low 1-deoxysphinganine concentration is mediated by induction of senescence. 1 μM 1-deoxysphinganine increased β-galactosidase activity (Fig. 2A) and nuclear $p21^{WAF1/Cip1}$ expression (Fig. 2B, C), a hallmark (16) and inducer of senescence (17), respectively. To investigate if increased p21 expression was sufficient to trigger the senescence pathway in Ins-1 cells, we used adenovirus infection overexpressed p21 (Adp21) or GFP (AdGFP) as a control (Fig 2D). Adp21 infection decreased Ins-1 cell replication and increased β-galactosidase activity, while both parameters were unchanged following AdGFP incubation (Fig 2E, F). In addition, the increased β-galactosidase

activity following 1 μM 1-deoxysphinganine treatment or Adp21 infection was accompanied by increased MTT reduction/cell (Fig. S2), suggesting increased mitochondrial dehydrogenase activity, a parameter associated with cellular senescence (18). These data suggest that up-regulation of p21 induced by 1 μM 1-deoxysphinganine treatment contributes to the decreased Ins-1 replication by activating a senescence program.

Next, we further explored the cytotoxic effect of high 1-deoxysphinganine concentrations. Five μM 1-deoxysphinganine abrogated the expression of p21 and induced cells with condensed pyknotic nuclei and high levels of activated caspase-3, hallmarks for the execution phase of apoptosis (Fig. 3A, S3A). In addition, FACS analyses of cells co-stained with annexin V and propidium iodide (PI) revealed that 5 μM 1-deoxysphinganine treatment increased the amount of both apoptotic and necrotic cells (Fig. 3B, C, S3B), and induced the cells to arrest in the G0/G1 phase of the cell cycle (Fig. S4), suggesting that the lipid triggers multiple cell death pathways in Ins-1 cells.

1-deoxysphinganine intracellular metabolites contribute to cytotoxicity in Ins-1 cells

As treatment with exogenous 1-deoxy-dihydroceramides (m18:0,24:1 and m18:0,16:0) and 1-deoxy-methylsphinganine, where alanine is replaced by glycine, reduced the cell replication similarly to 1-deoxysphinganine treatment (Fig. 4A), we then tested whether exogenous 1-deoxysphinganine was also metabolized by the cells to the deoxy forms of ceramide. Incubation with 1-deoxysphinganine significantly increased the cellular levels of deoxy-dihydroceramide with different acyl chain length (Fig. 4B) without altering normal ceramide levels (Fig. S5A), and selectively up-regulated the expression of ceramide synthase 5 (Fig. 4C), suggesting that 1-deoxysphinganine is readily metabolized in Ins-1 cells and accumulates in the acylated form. In addition, pre-treatment of Ins-1 cells with the class 2 amphiphile U-18666A, a well-established

inhibitor of NPC1 (Niemann–Pick C) protein that prevents intracellular trafficking of sphingolipids and cholesterol (19; 20), partially rescued 1-deoxysphinganine-mediated cytotoxicity (Fig. 4D, S5B). Moreover, pharmacological inhibition of ceramide synthesis with fumonisin B1 was unique in reducing the toxicity of 5 μM 1-deoxysphinganine (Fig.4D, S5C), while inhibition of either the first step of sphingolipid synthesis with myriocin or glucosylceramide synthesis with 1-phenyl-2-palmitoylamino-3-morpholino-1-propanol (PPMP) had no effect on cell viability (not shown). Collectively, these data indicate that intracellular uptake followed by metabolic conversion to 1-deoxy-dihydroceramides is responsible, at least in part, for 1-deoxysphinganine toxicity.

1-deoxysphinganine increases the phosphorylation of selected kinases in Ins-1 cells

To further characterize the biochemical components of 1-deoxysphinganine-induced cytotoxicity, we analyzed the phosphorylated status of key proteins involved in major signaling pathways. Western blot quantification revealed increased phosphorylation of JNK and p38 MAPK in 1-deoxysphinganine treated Ins-1 cells. In addition, the ratio of AKT phosphorylation was unchanged upon lipid treatment but the total protein amount increased in presence of 1-deoxysphinganine (Fig. 5A-C). As kinase activation by phosphorylation suggests a possible role of these proteins in 1-deoxysphinganine-mediated phenotype, we tested this hypothesis by treating the cells with specific kinase inhibitors. Pre-treatment with the p38 MAPK inhibitor Birb796 partially rescued cell replication (Fig. 5D) and reduced 1-deoxysphinganine-induced senescence (Fig. 5E). Conversely, the JNK inhibitor SP600125 potentiated cytotoxicity and senescence (Fig. 5D, E), and the combined treatment partially rescued the JNK inhibitor effect at 1 μM 1-deoxysphinganine incubation. These data suggest that p38 MAPK activation is an effector of 1-deoxysphinganine cytotoxicity and senescence, while JNK activation plays a protective role in Ins-1 cells.

1-deoxysphinganine treatment promotes re-organization of the actin cytoskeleton in Ins-1 cells

The observed changes in cell morphology observed following 1-deoxysphinganine treatment (Fig. 1C) prompted us to further analyze whether the lipid induced cytoskeletal alterations. To detect early cytoskeletal re-arrangements, cells were imaged after 5 h of treatment. Phalloidin-stained actin filaments were mainly concentrated in the cortical area and in filopodia following control BSA or sphinganine treatment. However, upon 1-deoxysphinganine incubation, actin staining accumulated in punctated structures mainly located in the peri-nuclear area of the cells. Different from the actin phenotype, tubulin staining showed a similar microtubule pattern in all treatments, suggesting that 1-deoxysphinganine preferentially interferes with the organization of actin cytoskeleton in Ins-1 cells (Fig. 6A). Quantitative analysis of members of the Rho family of GTPases that regulate intracellular actin dynamics (reviewed in (21)), showed increased levels of Rac1 activity (Fig. 6B) and expression of Rac1 and Rho, albeit the latter did not reach significance, upon 1-deoxysphinganine treatment (Fig. 6C), suggesting that Rho family GTPases may be involved in 1-deoxysphinganine-mediated changes in actin cytoskeleton re-organization. Of note, actin alterations were not accompanied by apoptosis at this time point (data not shown). In addition, pre-treatment with JNK, p38 MAPK and ceramide synthase inhibitors did not prevent actin remodeling (Fig. S6A), suggesting that cytoskeletal and cell cycle effects are modulated by different signaling pathways.

To further characterize whether aberrantly localized actin may intersect with the secretory apparatus of the cells, we performed co-staining for actin and insulin. FACS-based single cell quantification revealed that the lipid treatment did not alter the cellular content of actin and insulin (Fig. S6B). However, confocal analyses showed that filamentous actin accumulated

intracellularly in close proximity to and partially co-localized with insulin-containing vesicles (Fig. 6D).

1-deoxysphinganine reduces metabolic activity, insulin secretion and modulates actin cytoskeleton in primary islets

To confirm the relevance of our results in primary cells, we tested whether 1-deoxysphinganine affects the functionality of isolated islets. Lipid delivery to the cells was improved by dissociation of 1400 islets from 6 Wistar rats into single cells, these were seeded in ECM-coated plates and treated for 24 h with 5 μM sphinganine, 1-deoxysphinganine, or BSA as control. Of note, dissociated islets plated on ECM are virtually quiescent (R. Zuellig, personal communication). Under these experimental conditions, 1-deoxysphinganine treatment induced cellular vacuolization (Fig. 7A), and reduced the metabolic activity (Fig. 7B) and, to a lesser extent, the number of live cells (Fig. 7C). However, senescence was not observed, as indicated by comparable βgal activities (Fig. S7A) and absence of p21 staining (not shown). Similarly to the effect in Ins-1 cells, 1-deoxysphinganine treatment induced re-arrangement of actin cytoskeleton with the resulting accumulation of actin in intracellular punctated structures (Fig. 7D). 1-deoxysphinganine did not alter the cellular content of insulin (Fig. S7B) or selectively reduce the number of insulin-producing cells (Fig. S7C). However, following incubation with the lipid, isolated β cells were unable to regulate insulin secretion in response to glucose stimulation (Fig. 7E, S7D). Collectively, these data indicate that 1-deoxysphinganine is cytotoxic to isolated primary islets and compromises both functionality and cyto-architecture of β cells.

Increased glucose levels potentiate 1-deoxysphinganine toxicity

Our *in vitro* results showed 1-deoxySL-mediated cytotoxicity in insulin-producing cells, suggesting that raised levels of these lipids may contribute to the failure of β-cells during the

development of diabetes. However, elevated 1-deoxySLs levels were also found in the plasma of patients with metabolic syndrome that did not present hyperglycemia and overt diabetes (5), raising the question that increased amount of 1-deoxySLs are not the sole cause of β-cell toxicity and that additional factors contribute to the diabetic phenotype. To further investigate the causal network of atypical sphingolipids and β-cell toxicity, we analyzed pancreatic islets in leptin deficient ob/ob mice. Kept on a normal chow diet, these mice develop obesity and a mild hyperglycemia that reverts with aging, as pancreatic β-cell compensation occurs and increased insulin levels improve glucose homeostasis (22; 23). 60 week old ob/ob mice had only slightly higher plasma glucose levels compared with age matched WT animals, but a robust increase in plasma HDL, cholesterol and ALT levels (Fig. S8A), the latter reflecting steatotic liver damage (Fig. S8B). As previously shown (23), ob/ob pancreata were characterized by pronounced islet hyperplasia, vascularization and robust insulin production (Fig. S8B), suggesting that β-cells could compensate for the increased insulin demand without reaching exhaustion. Despite the evident hyperplasia, islets did not show active replication at the analyzed age (Fig. S8B). Interestingly, quantification of the plasma lipid profiles in ob/ob mice revealed a moderate but significant increase of 1-deoxysphinganine levels (Fig. 8A), which was not associated with increased senescence or apoptosis (Fig. S8B). In addition, like in human samples (5), sphingosine was the most abundant species in the mouse plasma and significantly increased in ob/ob mice (Fig. S8C). While it is likely that plasma 1-deoxySLs did not reach a critical concentration threshold to induce β-cell failure, absence of other pathological parameters, including hyperglycemia, may account for the normal viability of β-cells. To test this hypothesis, we incubated Ins-1 cells with 1-deoxysphinganine in presence or absence of glucose. Treatment with 30mM glucose for 24 h potentiated 1-deoxysphinganine-induced toxicity (Fig. 8B, S8D),

suggesting that hyperglycemia and 1-deoxySLs synergize to induce glucolipotoxicity in insulin-producing cells.

Discussion

Elevated levels of 1-deoxySLs have been found in the blood of patients suffering from metabolic syndrome and diabetes mellitus (5; 6), raising the question of the role of atypical lipids in the development of these pathologies. Our results showed that exposure to 1-deoxySLs in the low μM range compromised insulin secretion and triggered senescence and cell death in insulin-producing cells, indicating that 1-deoxySLs are indeed toxic for these cells. In our experimental approach we elucidated 1-deoxysphinganine toxicity at three distinct levels, namely i) changes in cellular structure, ii) engagement of signaling molecules and iii) activation of effector proteins. A major finding of our study is that 1-deoxysphinganine-mediated toxicity is a complex phenomenon and triggers multiple pathways, including cytoskeletal remodeling, senescence, necrosis and apoptosis.

1-deoxysphinganine triggers the re-organization of actin cytoskeleton in insulin-producing cells

1-deoxysphinganine treatment selectively altered cytoskeleton organization both in Ins-1 cells and primary islets, inducing accumulation of filamentous actin in intracellular punctated structures juxtaposed to insulin-containing vesicles. Similar but transient actin fiber alterations have been observed previously in 1-deoxysphinganine-treated Vero cells (7). In addition, 1-deoxysphinganine impaired cytoskeleton dynamics in sensory and motoneurons without inducing cell death (10). Our study showed not only that the lipid induced actin rearrangements before the appearance of apoptotic markers, but also that inhibitors shown to mitigate cytotoxicity did not prevent cytoskeletal remodeling. These data suggest that cytoskeleton rearrangements are a direct effect of 1-deoxysphinganine incubation rather than a consequence of cell lethality and that

cytoskeleton and cell cycle effects are regulated by distinct signaling pathways. In this context, it is currently under investigation whether alterations in Rho GTPase activation, reported by (7) and our study, are the key conserved molecular mechanism also behind cytoskeletal alteration in neurons.

In the case of β-cells, the early cellular morphological alterations may impair cellular functionality, including insulin secretion. Indeed, earlier studies demonstrated that insulin secretion in pancreatic β-cells is coupled with re-organization of the filamentous actin web located beneath the plasma membrane, thus allowing docking of insulin-containing granules to the cell membrane and consequent secretion. Importantly, glucose stimulation directly induces re-arrangement of the actin web (24; 25), to which insulin-containing granules are in tight contact (26). Thus impaired remodeling of actin cytoskeleton resulting from 1-deoxysphinganine treatment may contribute to the defective insulin secretion observed in our primary β-cells cultures. However, we cannot exclude that additional lipid-induced changes, including altered gene transcription, may contribute to the phenotype.

1-deoxy-dihydroceramide contributes to 1-deoxysphinganine-induced cytotoxicity

Ceramide is a key intracellular signaling molecule involved in several cellular functions, including cell death (reviewed in (27)). Importantly, both cell-permeant analogues of ceramide (28) and *de novo* ceramide synthesis (29) impair insulin secretion and mitogenesis in pancreatic *β*-cells and induce apoptosis (reviewed in (30)), supporting a critical regulatory role for ceramide in the metabolic dysfunction of these cells. In the search for the molecular signaling generated by 1-deoxysphinganine treatment, we explored the hypothesis that 1-deoxysphinganine uptake and conversion to 1-deoxy-dihydroceramide is necessary to exert its toxicity. Our mass spectrometry and inhibitor analyses supported this hypothesis. In addition, 1-deoxysphinganine increased the expression of ceramide synthase 5 (CerS5), while β-cell lipotoxicity resulting from palmitate

treatment stimulated the synthesis of CerS4 (31), suggesting that different lipids stimulate specific CerS isoforms. Collectively, our results suggest that some of the cytotoxic effects of 1-deoxysphinganine occur after its intracellular uptake and metabolism to 1-deoxy-dihydroceramide. However, we cannot exclude that 1-deoxysphinganine triggers death receptors on the cell surface. Given the similarity of the molecular structure of 1-deoxysphinganine and sphingosine, it is worthy of further investigation to determine if 1-deoxysphinganine can engage or antagonize the same membrane receptors, as previously suggested (8).

1-deoxysphinganine activates multiple intracellular pathways

In addition to cytoskeletal remodeling, 1-deoxysphinganine treatment induced a complex dose-dependent pattern of toxicity in Ins-1 cells, characterized by the appearance of p21-induced senescence at low doses and apoptosis and necrosis at high doses. Of note, the senescence growth arrest was limited to replicating cells, as demonstrated previously (32-34), and quiescent primary islets were devoid of senescence markers upon lipid treatment. These data imply that 1-deoxysphinganine triggers multiple signaling pathways. Indeed, the lipid was shown to selectively activate JNK, MAPK, Erk1/2, PKC but not AKT in NIH-3T3, RH-7777, PC-3 and LNCaP cell lines (8; 9), while we showed that JNK, p38 MAPK phosphorylation and AKT levels increased in Ins-1 cells, indicating that the intracellular signaling effectors stimulated by 1-deoxysphinganine depend on the cellular context. As JNK and MAPK are known to be activated by intracellular ceramide (35), it is possible that the increased 1-deoxy-dihydroceramide synthesis observed in Ins-1 cells activates these kinases. In addition, the fact that the CerS inhibitor FB1 was the only compound able to rescue the toxicity of high 1-deoxysphinganine doses, suggests that increased ceramide (or its deoxy form) synthesis is upstream of or a prerequisite for the activation of different signaling effectors.

While a more in depth analysis of the set of kinases activated by 1-deoxysphinganine is needed to elucidate the precise downstream signaling cascade, our inhibitor studies revealed an intriguing antagonistic role of JNK and p38 MAPK in the context of 1-deoxysphinganine-induced senescence. Interestingly, a similar dose-dependent senescence-apoptosis transition and opposite effect of p38 MAPK and JNK on senescence has been reported in endothelial progenitor cells upon doxorubicin treatment (36), further confirming that different kinases activated by the same stimulus may exert opposite cellular effects.

In conclusion, our work shows that 1-deoxysphinganine treatment and its conversion to 1-deoxy-dihydroceramide compromises the viability of insulin-producing cells via multiple pathways. This indicates that, similar to free fatty acids (reviewed in (30)), 1-deoxySLs induce lipotoxicity but with higher efficiency (low μM for 1-deoxySLs versus low mM for free fatty acids (31; 37; 38)). However, our *in vivo* study, together with the fact that HSAN1 and metabolic syndrome patients have elevated 1-deoxysphinganine levels without overt diabetes, suggests that the raised amount of 1-deoxysphinganine observed *in vivo* is not sufficient to directly induce β-cell failure but would require additional pathological parameters, for instance an established chronic hyperglycemic state, to promote β-cell toxicity (39). In this context, targeting 1-deoxySL synthesis as a combination therapeutic strategy for diabetes mellitus warrants further investigations.

Acknowledgments

We thank Heidi Seiler for excellent technical assistance and Amedeo Caflisch for providing the Birb796 inhibitor. This research was supported by the Zurich Center for Integrative Human Physiology (ZIHP) and Rare Disease Initiative Zurich (radiz), Clinical Research Priority Program

for Rare Diseases, University of Zurich. No potential conflicts of interest relevant to this article were reported. All the authors of this manuscript contributed in the study design, acquisition, analysis, interpretation of data, drafting and critical revision of the manuscript. R.A.Z., T.H., A.O., A.B.H., E.S., K. G., H.B., Y.W., T.G., O.O.O., J-H.J., U.U. researched data and reviewed/edited manuscript, A.v.E., R.G. contributed to discussion, reviewed/edited manuscript. S.S. wrote manuscript, researched data. S.S. is the guarantor of this work and, as such, had full access to all the data in the study and takes responsibility for the integrity of the data and the accuracy of the data analysis.

References

1. Chen L, Magliano DJ, Zimmet PZ: The worldwide epidemiology of type 2 diabetes mellitus--present and future perspectives. *Nat Rev Endocrinol* 8:228-236, 2012
2. Ashcroft FM, Rorsman P: Diabetes mellitus and the beta cell: the last ten years. *Cell* 148:1160-1171, 2012
3. Prentki M, Nolan CJ: Islet beta cell failure in type 2 diabetes. *J Clin Invest* 116:1802-1812, 2006
4. Donath MY, Ehses JA, Maedler K, Schumann DM, Ellingsgaard H, Eppler E, Reinecke M: Mechanisms of beta-cell death in type 2 diabetes. *Diabetes* 54 Suppl 2:S108-113, 2005
5. Othman A, Rutti MF, Ernst D, Saely CH, Rein P, Drexel H, Porretta-Serapiglia C, Lauria G, Bianchi R, von Eckardstein A, Hornemann T: Plasma deoxysphingolipids: a novel class of biomarkers for the metabolic syndrome? *Diabetologia* 55:421-431, 2012
6. Bertea M, Rutti MF, Othman A, Marti-Jaun J, Hersberger M, von Eckardstein A, Hornemann T: Deoxysphingoid bases as plasma markers in diabetes mellitus. *Lipids Health Dis* 9:84, 2010
7. Cuadros R, Montejo de Garcini E, Wandosell F, Faircloth G, Fernandez-Sousa JM, Avila J: The marine compound spisulosine, an inhibitor of cell proliferation, promotes the disassembly of actin stress fibers. *Cancer Lett* 152:23-29, 2000
8. Salcedo M, Cuevas C, Alonso JL, Otero G, Faircloth G, Fernandez-Sousa JM, Avila J, Wandosell F: The marine sphingolipid-derived compound ES 285 triggers an atypical cell death pathway. *Apoptosis* 12:395-409, 2007
9. Sanchez AM, Malagarie-Cazenave S, Olea N, Vara D, Cuevas C, Diaz-Laviada I: Spisulosine (ES-285) induces prostate tumor PC-3 and LNCaP cell death by de novo synthesis of ceramide and PKCzeta activation. *Eur J Pharmacol* 584:237-245, 2008
10. Penno A, Reilly MM, Houlden H, Laura M, Rentsch K, Niederkofler V, Stoeckli ET, Nicholson G, Eichler F, Brown RH, Jr., von Eckardstein A, Hornemann T: Hereditary sensory neuropathy type 1 is caused by the accumulation of two neurotoxic sphingolipids. *J Biol Chem* 285:11178-11187, 2010
11. Asfari M, Janjic D, Meda P, Li G, Halban PA, Wollheim CB: Establishment of 2-mercaptoethanol-dependent differentiated insulin-secreting cell lines. *Endocrinology* 130:167-178, 1992
12. Hohmeier HE, Mulder H, Chen G, Henkel-Rieger R, Prentki M, Newgard CB: Isolation of INS-1-derived cell lines with robust ATP-sensitive K+ channel-dependent and -independent glucose-stimulated insulin secretion. *Diabetes* 49:424-430, 2000

32. Michaloglou C, Vredeveld LC, Soengas MS, Denoyelle C, Kuilman T, van der Horst CM, Majoor DM, Shay JW, Mooi WJ, Peeper DS: BRAFE600-associated senescence-like cell cycle arrest of human naevi. *Nature* 436:720-724, 2005
33. Braig M, Lee S, Loddenkemper C, Rudolph C, Peters AH, Schlegelberger B, Stein H, Dorken B, Jenuwein T, Schmitt CA: Oncogene-induced senescence as an initial barrier in lymphoma development. *Nature* 436:660-665, 2005
34. Collado M, Serrano M: Senescence in tumours: evidence from mice and humans. *Nat Rev Cancer* 10:51-57, 2010
35. Ruvolo PP: Intracellular signal transduction pathways activated by ceramide and its metabolites. *Pharmacol Res* 47:383-392, 2003
36. Spallarossa P, Altieri P, Barisione C, Passalacqua M, Aloi C, Fugazza G, Frassoni F, Podesta M, Canepa M, Ghigliotti G, Brunelli C: p38 MAPK and JNK antagonistically control senescence and cytoplasmic p16INK4A expression in doxorubicin-treated endothelial progenitor cells. *PLoS One* 5:e15583, 2010
37. Lupi R, Dotta F, Marselli L, Del Guerra S, Masini M, Santangelo C, Patane G, Boggi U, Piro S, Anello M, Bergamini E, Mosca F, Di Mario U, Del Prato S, Marchetti P: Prolonged exposure to free fatty acids has cytostatic and pro-apoptotic effects on human pancreatic islets: evidence that beta-cell death is caspase mediated, partially dependent on ceramide pathway, and Bcl-2 regulated. *Diabetes* 51:1437-1442, 2002
38. Baldwin AC, Green CD, Olson LK, Moxley MA, Corbett JA: A role for aberrant protein palmitoylation in FFA-induced ER stress and beta-cell death. *Am J Physiol Endocrinol Metab* 302:E1390-1398, 2012
39. Butler AE, Janson J, Bonner-Weir S, Ritzel R, Rizza RA, Butler PC: Beta-cell deficit and increased beta-cell apoptosis in humans with type 2 diabetes. *Diabetes* 52:102-110, 2003

Figure legends

Figure 1. Deoxysphingolipids decrease the replication of Ins-1 cells. A. Metabolic activity tested by MTT assay of Ins-1 cells treated at 50% (low density, L) and 90% (high density, H) confluence with sphinganine (SA) and 1-deoxysphinganine (dSA) at the indicated concentrations and incubated for 24 h. B. Enumeration of live cells treated with the indicated dSA concentrations for 24 h. Note that the number of cells treated with 1 μM dSA is comparable to the initial seeding density. C. Bright field images showing cell rounding up upon 24 h dSA treatment. D. Quantification of trypan blue positive cells after treatment with the indicated concentrations of dSA for 24 h. Data are expressed as percentage of total cell number. E. Quantification of LDH released in the medium after 24 h dSA treatment. Data are normalized to the number of cells. F. MTT assay of Ins-1cells treated with dSA for the indicated time and assessed 24 h after adding the lipid. Results are average ± SEM (n=3), *$p<0.05$. Scale bars: 50 μm.

Figure 2. 1-deoxysphinganine triggers senescence in Ins-1 cells. A. Quantification of β-galactosidase activity following incubation for 24 h with 1 μM sphinganine (SA), 0.5 and 1 μM 1-deoxysphinganine (dSA), or BSA as control (cntl). Values are normalized to the number of live cells. B. Immunofluorescence imaging showing nuclear expression of p21 following incubation for 24 h with 1 μM SA, 1 μM dSA, or BSA as control (cntl). Nuclei are stained with DAPI (blue). Lower panels show nuclear localization of p21. C. Western blot and densitometric quantification of p21/GAPDH levels following incubation for 24 h with 1 μM SA, 1 μM dSA or BSA as control. D. Immunostaining of p21 (upper panels) or live imaging (lower panel) of Ins-1 cells infected with p21 (Adp21) and GFP (AdGFP) adenoviruses at multiplicity of infection

(MOI) of 50. E. Enumeration of live Ins-1 cells 24 h after Adp21 or AdGFP infection. Note how Adp21 decreased the replication of Ins-1 cells in a dose response manner without inducing cell death. F. Quantification of β-galactosidase activity 24 h after Adp21 or AdGFP infection. Note how senescence is induced only in presence of Adp21. Results are average ± SEM (n=3), *p<0.05. Scale bars: 50 μm.

Figure 3. 1-deoxysphinganine triggers apoptosis and necrosis in Ins-1 cells. A. Left panel. Quantification of cleaved caspase 3 (CC-3) and p21 positive cells after 24 h incubation with 5 μM sphinganine, 1 and 5 μM 1-deoxysphinganine (dSA) or BSA as control. Right panel. Immunofluorescence imaging showing cytosolic expression of cleaved caspase 3 (CC-3). Note the pyknotic nuclei in CC-3 positive cells (arrows). Nuclei are stained with DAPI (blue). Results are average ± SEM (n=3), *p<0.05. Scale bars: 50 μm. B. FACS analyses of Ins-1 cells after 24 h incubation with 1 and 5 μM dSA or BSA as control and staining with PI and annexin V. C. Quantification of cells PI/ annexin V negative (live cells), PI positive (necrotic cells), annexin V positive (apoptotic cells) and double positive. Total population consisted of 20'000 cells. Note the increased lethality of cells treated with 5 μM 1-dSA.

Figure 4. 1-deoxy-dihydroceramide contributes to 1-deoxysphinganine-induced cytotoxicity in Ins-1 cells. A. MTT assay of Ins-1cells incubated for 72 h with sphinganine (SA), sphingosine (SO), 1-deoxysphinganine (dSA), deoxy-methylsphinganine (dmethSA), deoxy-dihydroceramides (1-deoxy-dh-Cer m18:0,24:1 and m18:0,16:0). B. Mass spectrometry quantification shows the increased formation of 1-deoxy-dh-Cer with different acyl chain length upon 24 h treatment with 3 μM 1 dSA. SA, SO and BSA incubation were used as control. C. RNA expression levels of different ceramide synthase (CerS) isoforms following lipid incubation as in B. Transcript levels were normalized using GAPDH RNA as a reference. D. Enumeration

of live cells following incubation for 24 h with dSA in presence or absence of 5 μM U-18666A or 35 μM fumonisin B1 (FB1). Results are average ± SEM (n=3), *p<0.05.

Figure 5. 1-deoxysphinganine increases the phosphorylation of selected kinases in Ins-1 cells. A. Western blot of phosphorylated and total levels of JNK, p38 and AKT following incubation for 24 h with 1 μM sphinganine (SA), 1 μM 1-deoxysphinganine (dSA) or BSA as control. B. Densitometric quantification of protein phosphorylation/total protein/actin levels. Data are expressed as percentage of control (cntl). C. Densitometric quantification of total protein/actin levels. Data are expressed as percentage of control (cntl). D. Enumeration of live cells treated with the indicated dSA concentrations for 24 h in presence of 10 μM of inhibitors of p38 MAPK (Birb796, Birb), JNK (SP600125, SP) or a combination of Birb796 and SP600125 (B/SP). Cells were pre-treated for 1 hour with the indicated inhibitors before addition of 1-deoxySA. E. Quantification of β-galactosidase activity following incubation for 24 h with 1 μM dSA in presence of 10 μM of inhibitors of p38 MAPK (Birb796, Birb), JNK (SP600125, SP) or a combination of Birb796 and SP600125 (B/SP). Values are normalized to the number of live cells. Results are average ± SEM (n=3), *p<0.05.

Figure 6. 1-deoxysphinganine incubation induced actin cytoskeleton rearrangements. A. Ins-1 cells treated with 5 μM 1-deoxysphinganine (dSA), sphinganine (SA) or BSA as control for 5 h and stained with phalloidin (green, left panels) or anti-tubulin antibody (red, right panels). Nuclei are stained with DAPI (blue). Note the actin staining in punctated structures following dSA treatment (arrows in left panel). In the right panels, arrows indicate tubulin midbody in recently divided cells and arrowhead the mitotic spindle. Scale bars: 50 μm. B. Rac1 activity following 5 h treatment with 5 μM dSA, 5 μM SA or BSA as control. NC, negative control. Constitutively active Rac1 (RCCA) was used as a positive control. C. Western blotting quantification of Rac1

and RhoA expression upon 24 h treatment with 1 μM dSA, 1 μM SA or BSA as control. Results are average ± SEM (n=3), *p<0.05. D. Confocal images of Ins-1 cells treated with 5 μM dSA or BSA as a control for 5 h and stained with phalloidin (green) or anti-insulin antibody (red). Nuclei are stained with DAPI (blue). Signal intensities representing the voxel space of the reconstructed image stacks are depicted as scatterplots showing partial signal overlap of actin and insulin in cntl and dSA-treated samples. Robust overlap of actin and β-catenin signals (dots accumulated in the mid-diagonal of the plot) and limited overlap of actin and DAPI (dots preferentially distributed along the axes) were used as a control. Nuclei are stained with DAPI (blue). Scale bars: 10 μm.

Figure 7. 1-deoxysphinganine treatment is cytotoxic for rat primary islets. Dissociated islets were plated on ECM plates and treated for 24 h with 5 μM sphinganine (SA), 5 μM 1-deoxysphinganine (dSA), and BSA as control. A. Quantification of vacuolized cells following lipid treatment. Data are expressed as percentage of total cell number. Right panels: bright field images of treated cells showing cell vacuolization (arrows and inset) upon dSA treatment. B. Metabolic activity tested by MTT assay. Data are expressed as percentage of BSA-treated control cells. C. Enumeration of live cells following lipid treatment. D. Quantification of insulin secretion stimulated with 3.3 mM (Low I), 16.7 mM (High) and 3.3 mM (Low II) glucose following incubation for 24 h with the lipids. Secreted insulin was normalized to the cell number. E. Filamentous actin (phalloidin, green) and insulin (red) co-staining of treated islets. Nuclei are stained with DAPI (blue). Results are average ± SEM (n=3), *p<0.05. Scale bars: 50 μm.

Figure 8. A. Mass spectrometry quantification of 1-deoxysphinganine (dSA) serum levels of 60 week old wild type (WT) and ob/ob mice. Results are average ± SEM (n=5), *p<0.05. B. Enumeration of live Ins-1 cells treated with the indicated dSA concentrations for 24 h in presence (Gluc) or absence (Cntl) of 30 mM glucose. Results are average ± SEM (n=3), *p<0.05.

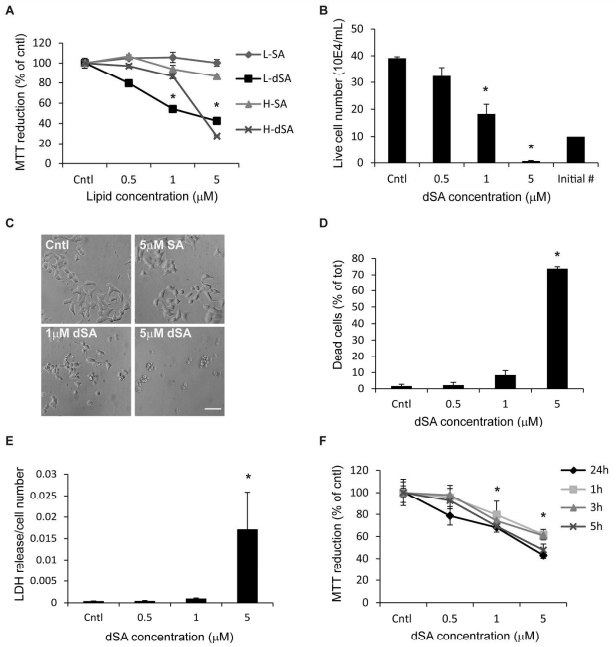

Fig. 1

203x211mm (300 x 300 DPI)

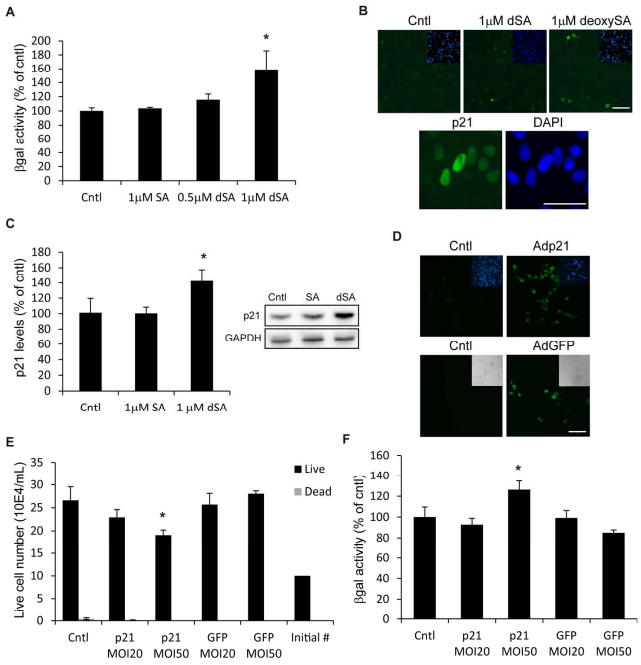

Fig. 2

203x222mm (300 x 300 DPI)

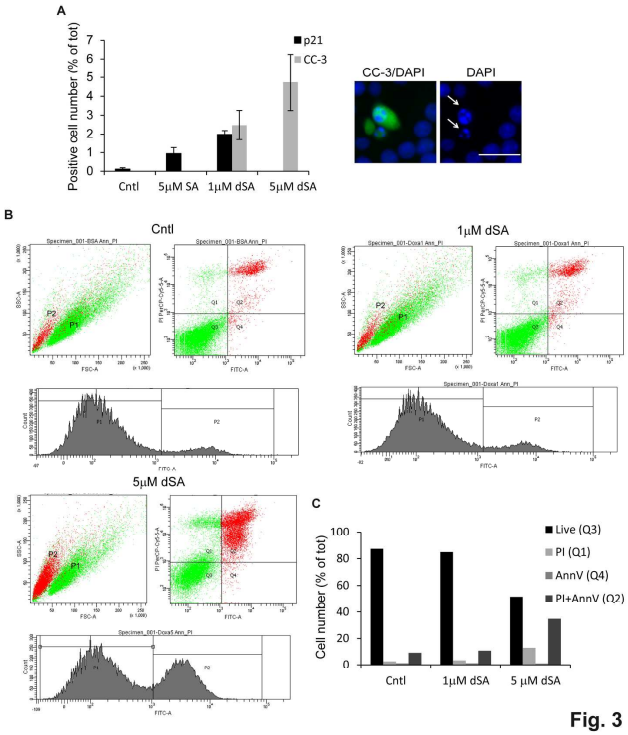

Fig. 3

203x218mm (300 x 300 DPI)

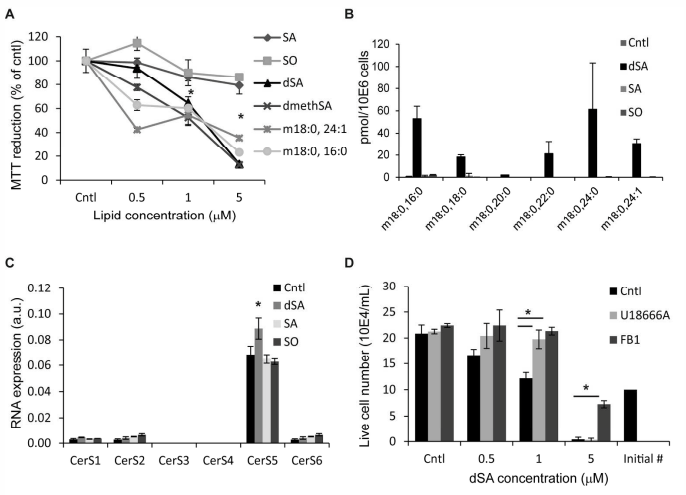

Fig. 4

204x231mm (300 x 300 DPI)

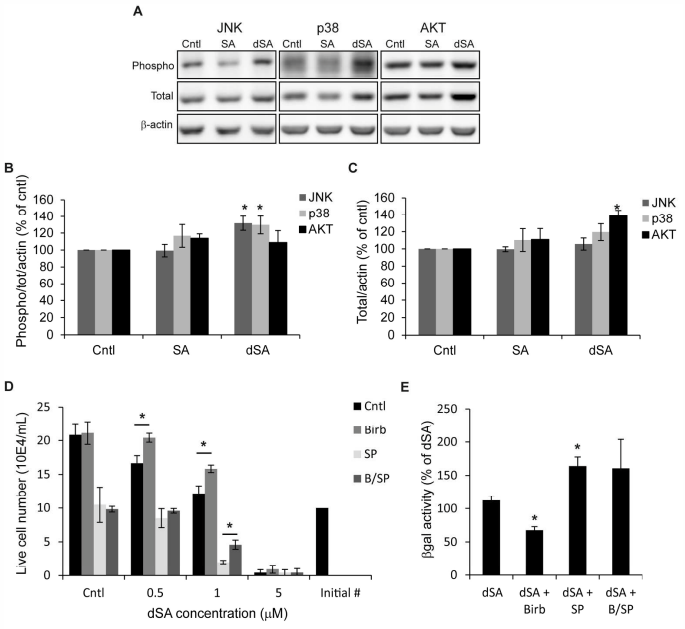

Fig. 5

203x231mm (300 x 300 DPI)

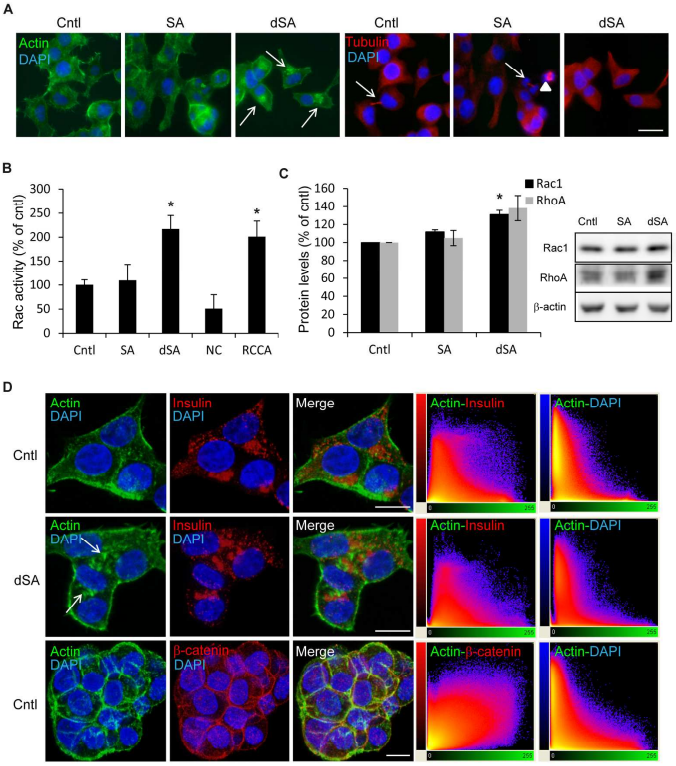

Fig. 6

208x246mm (300 x 300 DPI)

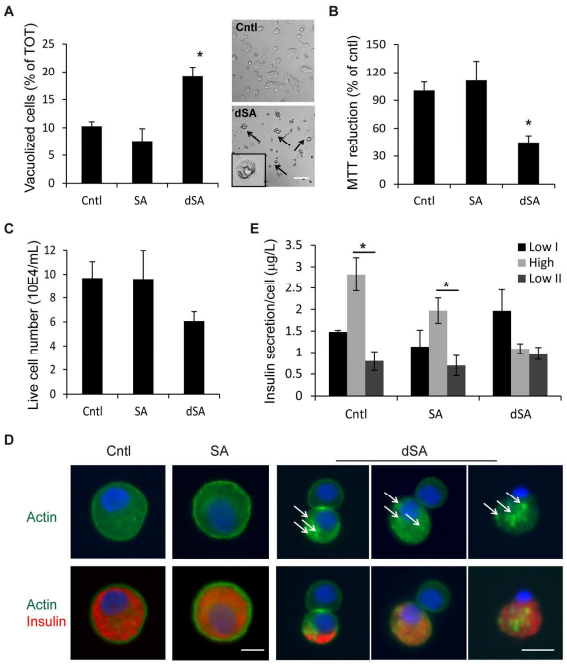

Fig. 7

197x223mm (300 x 300 DPI)

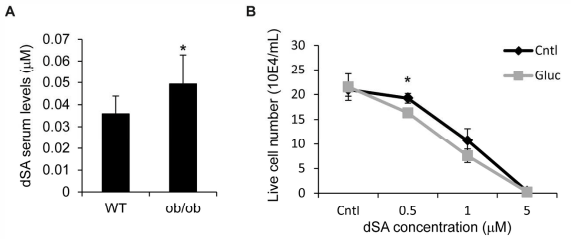

Fig. 8

201x240mm (300 x 300 DPI)

Supplementary Online Material

List of antibodies

Primary antibodies used for immunostaining were: Alexa Fluor 594 phalloidin (Life Technologies), anti-α–tubulin (Cell Signaling), anti-Rac1 (Abcam), anti-cleaved caspase-3 (Cell Signaling), anti-p21 (Abcam), anti-insulin (Dako), anti-glucagon (Sigma), fluorescein-conjugated Annexin V (BD Pharmingen). Fluorophore-conjugated secondary antibodies were from Alexafluor. Nuclei were visualized with 4′, 6-diamidino-2-phenylindole (DAPI).

Primary antibodies used for western blotting were: anti-p21 (Abcam), anti-GAPDH (Santa Cruz), anti-RhoA (Santa Cruz), anti-Rac1 (BD Biosciences), anti-phospho JNK and anti-JNK (R&D System), anti-phospho p38MAPK and anti-p38MAPK, anti-phospho AKT and anti-AKT (all from Cell Signaling) and anti-β-actin (Sigma). Secondary HRP-conjugated antibodies were from Jackson ImmunoResearch.

Ceramide synthase primers for qPCR

Rat CerS1: rat CerS1_LC_F: AGTGCCTGGAAGCTTCTGTT,

rat CerS1_LC_R: GACCTCCAGCCGTAGAAGAC

Rat CerS2: rat CerS2_LC_F: TTGAGGAAAGTTTGGGAAGG,

rat CerS2_LC_R: AAACCAGGAGAAGCAGAGGA

Rat CerS3: rat CerS3_LC_F: TGCCACACCTCTAGCCAATG,

rat CerS3_LC_R: CCTGGCGCTCTGTCAAGTTA

Rat CerS4: rat CerS4_LC_F: TCACTCTGCCCTTTGACATC,

rat CerS4_LC_R: TGACGCTGTAGGAGAAGACG

Rat CerS5: rat CerS5_LC_F: CACACAGCTGGCCTTCTACT,

rat CerS5_LC_R: ACTCGCACCATGTTGTTGAT

Rat CerS6: CerS6_F: GGGATCTTAGCCTGGTTCTGG,

CerS6_R: GCCTCCTCCGTGTTCTTCAG

Rat(Mouse)GAPDH: rat GAPDH_LC_F: GGTCGGTGTGAACGGATTTG,

rat GAPDH_LC_R: TTGCCGTGGGTAGAGTCATA

Figure legends

Figure S1. A. Comparison of Ins-1 metabolic activity by MTT and WST-1 reduction following 24 h incubation with 1-deoxysphinganine (dSA) at the indicated concentrations. BSA incubation was used as a control. Results are average ± SEM (n=3). B. Expression profile of genes involved in different cell death pathways following 1 μM dSA compared to 1 μM sphinganine incubation by Rat Cell Death Pathway Finder PCR Array (SABiosciences). 1 μM 1-deoxysphinganine treatment moderately up-regulated genes involved in necrosis, autophagy and apoptosis (Olr1583, Ctss, Esr1, Casp1, Fas), while anti-apoptotic genes (Bcl2a1d, Tnfrsf11b) were down-regulated. C. Analysis of extracted RNA integrity by Agilent 2100 Bioanalyzer. Examples of electrophoresis runs and assigned RNA integrity number (RIN) are shown. D. List of genes present in the array.

Figure S2. Analysis of MTT reduction /cell number following 24 h of 1-deoxysphinganine (dSA) treatment (A) or Adp21 and AdGFP infection (B). Data are expressed as percentage of control. Results are average ± SEM (n=5), *$p<0.05$.

Figure S3. 1-deoxysphinganine triggers apoptosis in Ins-1 cells. A. Co-staining with cleaved caspase 3 (CC-3, red) and p21 (green) showing the mutually exclusive expression of the proteins upon incubation for 24 h with 5 μM sphinganine, 1 and 5 μM 1-deoxysphinganine or BSA as control. Nuclei are stained with DAPI (blue). Scale bars: 50 μm. B. FACS based quantification of

dead cells following 24 h incubation with 1 and 5 μM dSA or BSA as control as determined by FSC and SSC parameters shown in Fig. 3.

Figure S4. Cell cycle analysis by quantification of DNA content in Ins-1 cells after 24 h incubation with 1 and 5 μM 1-deoxysphinganine (dSA) or BSA as control. The amount of cells in different cell cycle phases is plotted in the lower panel. Total population consisted of 20'000 cells. Note the decreased amount of cells in G2/M phase and accumulation in G0/G1 phase following 5 μM 1-deoxysphinganine treatment.

Figure S5. A. Mass spectrometry quantification of ceramides in Ins-1 cells treated for 24 h with 3 μM of sphinganine (SA), sphingosine (SO), 1-deoxysphinganine (dSA) and BSA as control. B. MTT assay following incubation for 24 h with SA or dSA in presence or absence of 5 μM U-18666A (U). C. Bright field images of Ins-1 cells showing reduced toxicity following 5 μM dSA treatment in presence of FB1. Results are average ± SEM (n=3), *$p<0.05$. Scale bars: 50 μm.

Figure S6. A. Ins-1 cells were treated with 10 μM of inhibitors of JNK (SP600125, SP), p38 MAPK (Birb796, Birb) or 35μM ceramide synthase inhibitor FB1 for 1 h, followed by 5 h treatment with 5 μM 1-deoxysphinganine (dSA), sphinganine (SA) or BSA and phalloidin staining. Nuclei are stained with DAPI (blue). Scale bars: 50 μm. B. FACS-based quantification of actin and insulin cellular content following 5 h treatment with 5 μM dSA, SA or BSA.

Figure S7. Dissociated islets were plated on ECM plates and treated for 24 h with 5 μM sphinganine (C18SA), 1-deoxysphinganine (dSA), and BSA as control. A. Quantification of β-galactosidase activity normalized by the cell number. B. Quantification of cellular insulin content. Cells were lysed and total insulin level was normalized by the cell number. C. Enumeration of insulin-expressing cells. Data are expressed as percentage of total cell number.

D. Quantification of insulin secretion stimulated with 3.3 mM (Low I), 16.7 mM (High) and 3.3 mM (Low II) glucose following incubation for 24 h with the lipids. Secreted insulin was normalized by the total insulin content. Results are average ± SEM (n=3), *p<0.05.

Figure S8. A. Weight and blood parameters of WT and ob/ob mice. B. Histological morphology (HE staining) of paraffin embedded liver and pancreas sections from WT and ob/ob mice. Note the accumulation of lipid deposit and steatotic phenotype in the latter. Staining of insulin/glucagon, replicating (Ki67), senescent (p21) and apoptotic cells (TUNEL) in islets of 60 week old wild type (WT) and ob/ob mice. Nuclei are stained with DAPI (blue). Scale bars: 50 μM. D. Mass spectrometry quantification of serum levels of total sphingoid bases after hydrolyzing the head group and N-linked fatty acid. Results are average ± SEM (n=5), *p<0.05. E. MTT assay of Ins-1 cells incubated for 24 h with 1-deoxysphinganine in presence (Gluc) or absence (Cntl) of 30 mM glucose. Results are average ± SEM (n=3), *p<0.05.

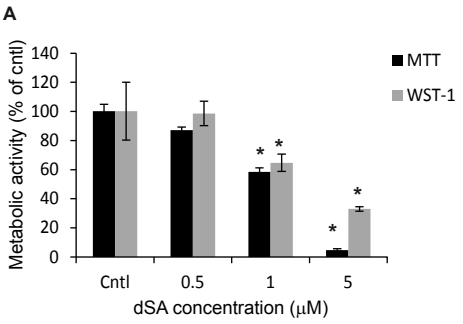

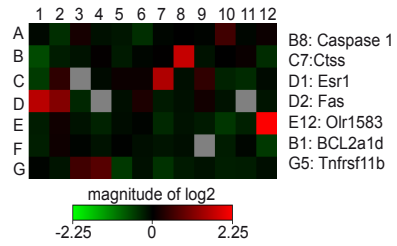

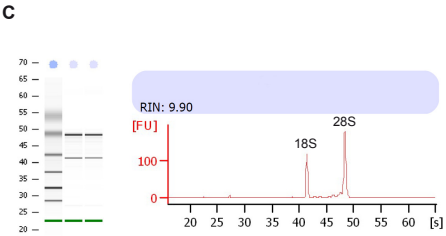

D

Well	Gene symbol
A01	Abl1
A02	Akt1
A03	Apaf1
A04	App
A05	Atg12
A06	Atg16l1
A07	Atg3
A08	Atg5
A09	Atg7
A10	Atp6v1g2
A11	Bax
A12	Bcl2
B01	Bcl2a1d
B02	Bcl2l1
B03	Bcl2l11
B04	Becn1
B05	Birc2
B06	Birc3
B07	Bmf
B08	Casp1
B09	Casp2
B10	Casp3
B11	Casp6
B12	Casp7
C01	Casp9
C02	Cd40
C03	Cd40lg
C04	Cflar
C05	Commd4
C06	Ctsb
C07	Ctss
C08	Cyld
C09	Defb1
C10	Dffa
C11	Dpysl4
C12	Eif5b
D01	Esr1
D02	Fas
D03	Faslg
D04	Foxi1
D05	Gaa
D06	Gadd45a
D07	Galnt5
D08	Grb2
D09	Hspbap1
D10	Htt
D11	Ifng
D12	Igf1

Well	Gene symbol
E01	Igf1r
E02	Ins2
E03	Irgm
E04	Jph3
E05	Kcnip1
E06	Mag
E07	Map1lc3a
E08	Mapk8
E09	Mcl1
E10	Nfkb1
E11	Nol3
E12	Olr1583
F01	Parp1
F02	Parp2
F03	Pik3c3
F04	Pvr
F05	Rab25
F06	RGD1311517
F07	RGD1562639
F08	Rps6kb1
F09	S100a7a
F10	Snca
F11	Spata2
F12	Sqstm1
G01	Sycp2
G02	Tmem57
G03	Tnf
G04	Tnfrsf10b
G05	Tnfrsf11b
G06	Tnfrsf1a
G07	Tp53
G08	Traf2
G09	Txnl4b
G10	Ulk1
G11	Uvrag
G12	Xiap
H01	Rplp1
H02	Hprt1
H03	Rpl13a
H04	Ldha
H05	Actb

Fig. S1

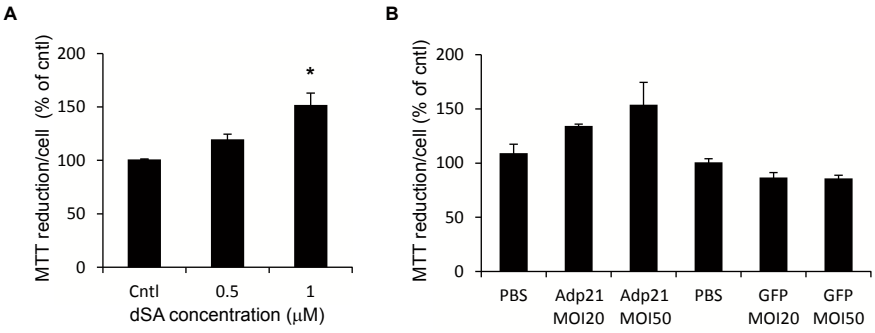
A
MTT reduction/cell (% of cntl)
200
150
100
50
0
*
Cntl
0.5
1
dSA concentration (μM)
B
MTT reduction/cell (% of cntl)
200
150
100
50
0
PBS
Adp21 MOI20
Adp21 MOI50
PBS
GFP MOI20
GFP MOI50

Fig. S2

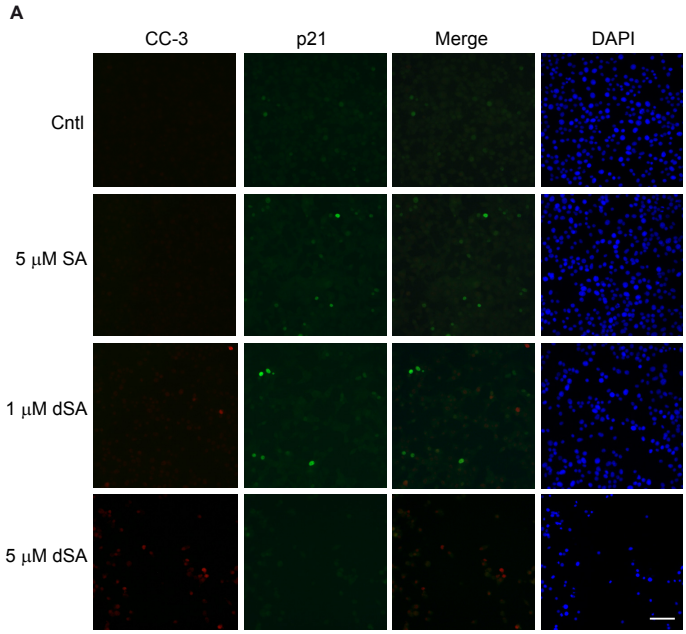
A
CC-3
p21
Merge
DAPI
Cntl
5 μM SA
1 μM dSA
5 μM dSA
B
Cell number (% of tot)
100
80
60
40
20
0
Live (P1)
Dead (P2)
Cntl
1μM dSA
5 μM dSA

Fig. S3

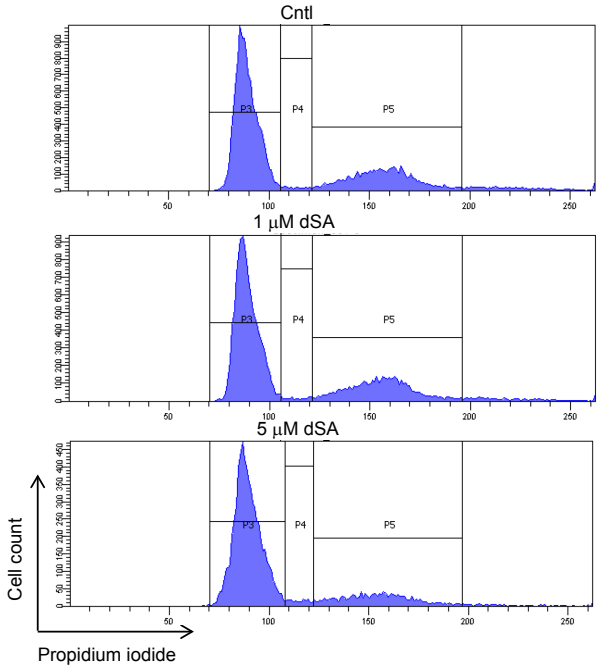
Cntl
P3
P4
P5
1 μM dSA
5 μM dSA
Cell count
Propidium iodide

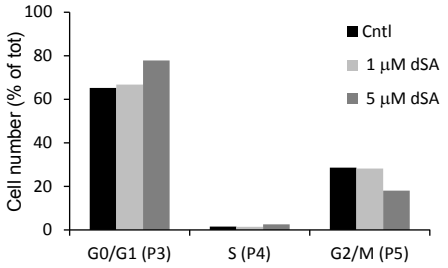
Cell number (% of tot)
Cntl
1 μM dSA
5 μM dSA
G0/G1 (P3)
S (P4)
G2/M (P5)

Fig. S4

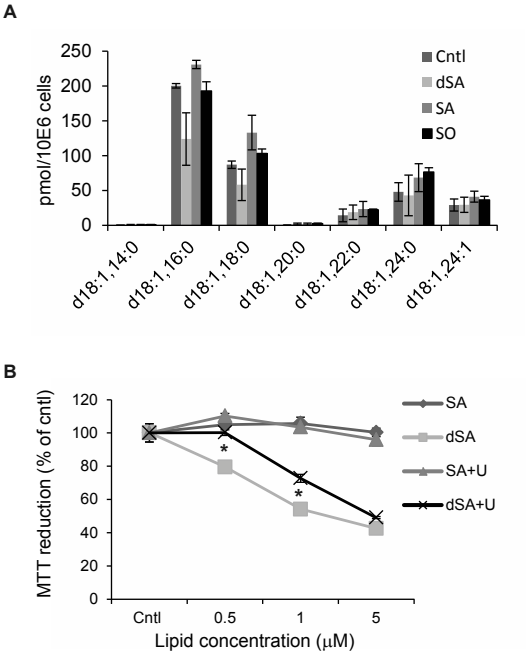
A
250
200
150
100
50
0
pmol/10E6 cells
Cntl
dSA
SA
SO
d18:1,14:0
d18:1,16:0
d18:1,18:0
d18:1,20:0
d18:1,22:0
d18:1,24:0
d18:1,24:1
B
120
100
80
60
40
20
0
MTT reduction (% of cntl)
SA
dSA
SA+U
dSA+U
*
*
Cntl
0.5
1
5
Lipid concentration (μM)
C
Cntl
FB1
Cntl
dSA

Fig. S5

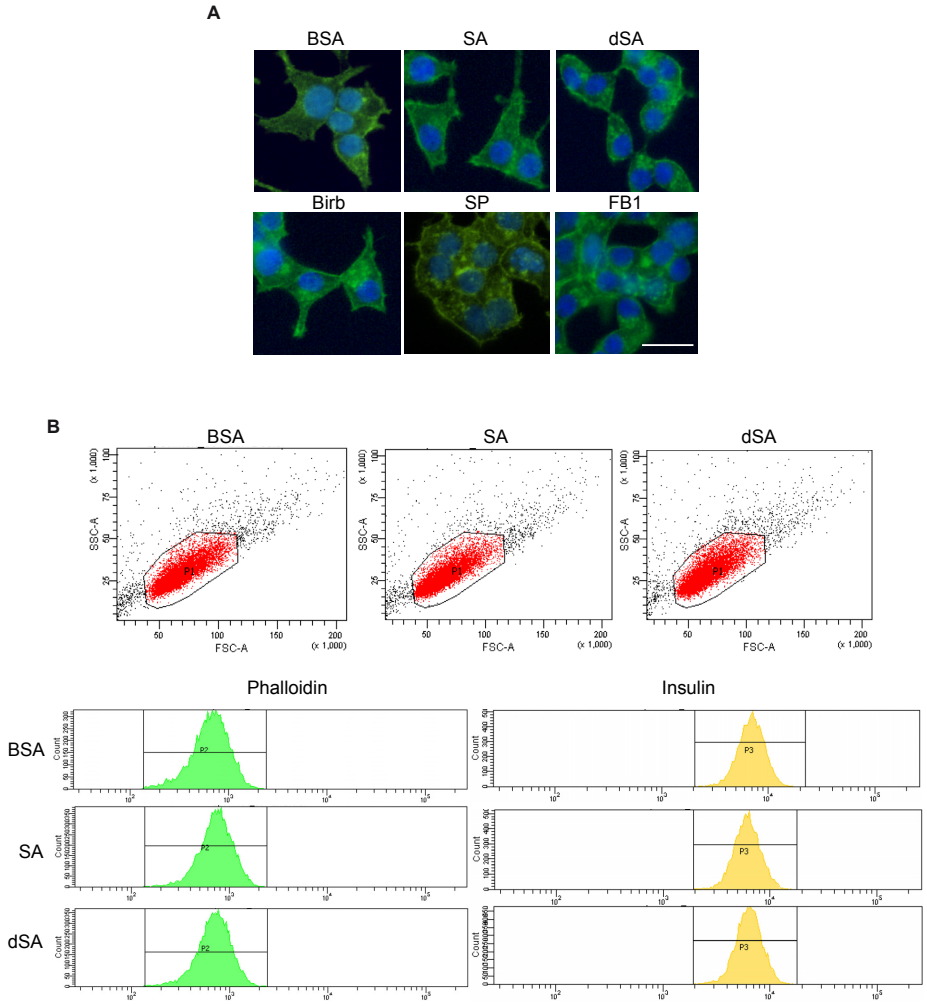
A
BSA
SA
dSA
Birb
SP
FB1
B
BSA
SA
dSA
SSC-A
FSC-A
Phalloidin
Insulin
BSA
SA
dSA

Fig. S6

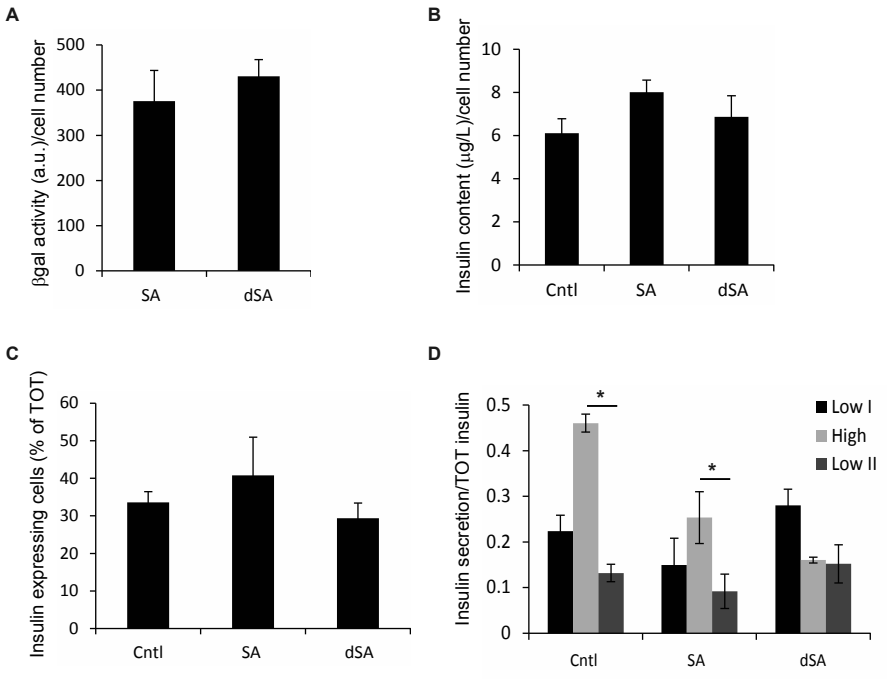
A
βgal activity (a.u.)/cell number
500
400
300
200
100
0
SA
dSA
B
Insulin content (µg/L)/cell number
10
8
6
4
2
0
Cntl
SA
dSA
C
Insulin expressing cells (% of TOT)
60
50
40
30
20
10
0
Cntl
SA
dSA
D
Insulin secretion/TOT insulin
0.5
0.4
0.3
0.2
0.1
0
*
*
Low I
High
Low II
Cntl
SA
dSA

Fig. S7

A

	Weight (G)	Glucose (mmol/L)	TG (mmol/L)	HDL (mmol/L)	Chol (mmol/L)	ALT (U/L)
WT	41.3+/-1.77	10.9+/-0.61	0.89+/-0.09	2.02+/-0.127	2.36+/-0.139	10.88+/-0.61
ob/ob	82.3+/-1.43	14.92+/-1.23	0.94+/-0.14	4.81+/-0.57	5.77+/-0.59	102.87+/-24.3
P value	3.01E-10	0.008098	0.765418	0.000128	2.83E-05	0.001008

TG, triacylglycerol; HDL, high density lipoprotein; Chol, cholesterol; ALT, alanine aminotransferase. Values are expressed as means ± SEM (N=7)

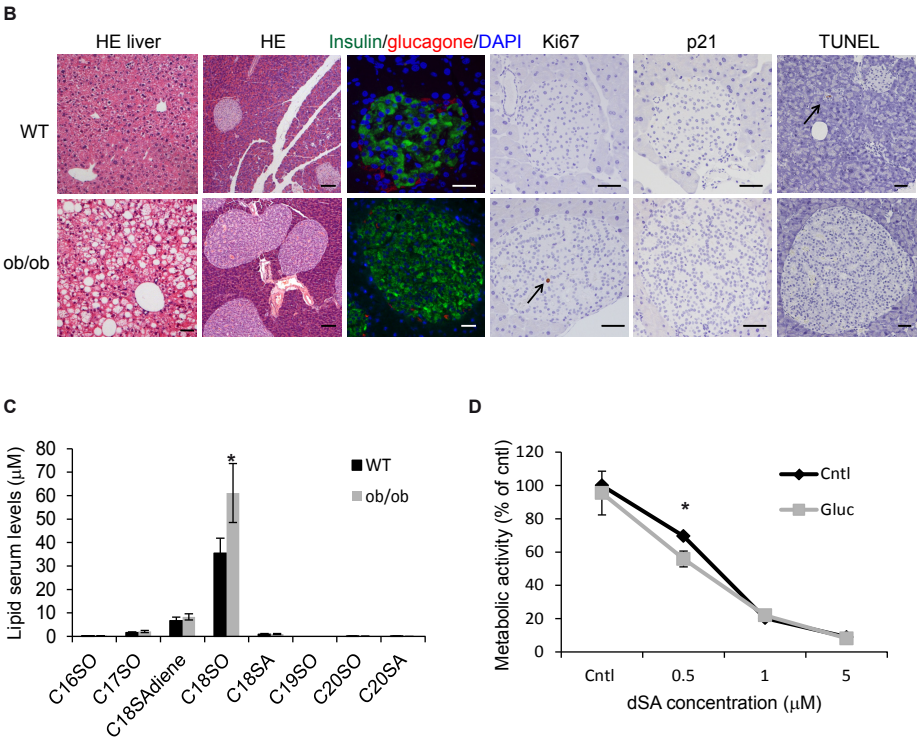

Fig. S8

7. Acknowledgements

I would like to thank Prof. Gassmann for giving me the opportunity to do my PhD in his laboratory. Also I thank my supervisor Dr. Ogunshola for her support during the last years.

A special thank I would like to send to Prof. Fritschy who was a very supportive member of my thesis committee and gave me valuable advice. Also Prof. Agnes Görlach I thank for joining the thesis committee and for supporting me during the last year.

In addition I express my thanks to Professors of the Zirkulationskreis for carefully reading my PhD thesis and to Heidi Preisig from the imMed PhD program for always having an open ear for the students matters.

I thank all the members of the Gassmann group for scientific exchange and technical advice. Especially I want to mention Sarbrina Engelhardt and Shalmali Patkar and thank them for the nice atmosphere and laughter in and outside the lab. Thanks Daniela Nizzari for going all the way with me, from the beginning to the end and even further.

In addition I thank my friends for mentally supporting me in scientific as well as in other issues.

Der grösste Dank geht an meine Familie, die mir in jeder Lebenslage den Rücken stärkt und an Carmen Nauer für ihre endlose Geduld und die bedingungslose Unterstützung.

8. Curriculum vitae

Tanja Güntert

Date of birth:	04.08.1983
Nationality:	German
Work address:	Winterthurerstrasse 260, 8057 Zurich, Switzerland
Home address:	Kornhausstrasse 15, 8037 Zurich, Switzerland
Tel work:	+41 (44) 635 88 05
Work email:	guentert@vetphys.uzh.ch
Personal email:	tanja.guentert83@gmail.com

Education

Since Nov. 2009

PhD studies at the institute of Veterinary Physiology in the group of Prof. Max Gassmann, University of Zurich, Switzerland, Supervision: Dr. Ogunshola
Thesis: *Role of Rac1 in the Neuronal Response to Hypoxia and Deoxy-Sphingolipid-Induced Neurotoxicity*

2008 – 2009

Diploma thesis at the laboratory of Prof. Christof R. Hauck, Cell Biology, University of Konstanz, Germany
Grade 1 (1-5, 1=best)
Thesis: *"Comparative, molecular analysis of CEACAM3 of humans and other primates concerning bacterial interaction and CEACAM-mediated activation of c-Jun N-terminal kinase"*

2003 – 2009

Student of Biology, University of Konstanz, Germany

2000 – 2003

High School for Economics (Abitur), Waldshut, Germany
Grade: 1.9 (1-6, 1=best)

Manuscripts

2014

Güntert T, Max Gassmann, Ogunshola OO. *Rac1 plays a crucial role in the neuronal adaptationnto hypoxia for neuronal adaptation to hypoxia.* In peer review, Journal of Cellular Physiology.

Güntert T, Othman A, Sonda, S, Zuellig RA, Horneman T, Wei Y, Ogunshola OO. *Deoxy-sphingolipid-induced neurotoxicity involves cytoskeleton deregulation and NMDAR signaling.* Submitted to Brain.

2013

Zuellig RA, Hornemann T, Othman A, Hehl AB, Bode H, **Güntert T**, Ogunshola OO, Saponara E, Grabliauskaite K, Jang JH, Ungethuem U, Wei Y, von Eckardstein A, Graf R, Sonda S. *Deoxysphingolipids, a novel biomarker for type 2 diabetes, are cytotoxic for insulin-producing cells.* Diabetes, 2013. (Epub ahead of print).

Posters

6th Symposium of the Zurich Center for Integrative Human Physiology, 27th August, 2010 in Zurich, Switzerland. *Influence of cytoskeleton alterations on hypoxic response and cell survival of primary neurons.* Güntert T, Gassmann M, Ogunshola OO.

Oxygen 2011, HypoxiaNet meeting, January 8-12, 2011 in Davos, Switzerland. *Influence of Rho GTPases on the hypoxic response and cell survival of primary neurons.* Güntert T, Gassmann M, Ogunshola OO.

USGEB meeting 2011, January 27-28, 2011 in Zürich Switzerland. *Influence of Rho GTPases on the hypoxic response and cell survival of primary neurons.* Güntert T, Gassmann M, Ogunshola OO.

7th Symposium of the Zurich Center for Integrative Human Physiology, 26th August, 2011 in Zurich, Switzerland. *Influence of Rho GTPases on the hypoxic response of primary neurons.* Güntert T, Gassmann M, Ogunshola OO.

NCCR Neuro Concluding Symposium & ZNZ Symposium, June 14-15, 2012 in Zürich Switzerland. *Rac1 drives the neuronal response to hypoxia.* Güntert T, Gassmann M, Ogunshola OO.

8th Symposium of the Zurich Center for Integrative Human Physiology, 24th August, 2012 in Zurich, Switzerland*. Rac1 drives the neuronal response to hypoxia.* Güntert T, Gassmann M, Ogunshola OO.

9th Symposium of the Zurich Center for Integrative Human Physiology, 28th August, 2013 in Zurich, Switzerland. *Rac1 – A driving force of neuronal adaptation to hypoxia.* Güntert T, Gassmann M, Ogunshola OO.

Courses

- Introduction to Neuroscience I
- Project management for research
- Introduction to descriptive and analytic statistics
- Scientific writing
- Good Clinical Practice (GCP)
- Intellectual property
- Mouse physiology and pathophysiology
- Inorganic foundation of life